

UCSF

UC San Francisco Electronic Theses and Dissertations

Title

Regulation of Cardiac Progenitors

Permalink

<https://escholarship.org/uc/item/0z2534ns>

Author

Cheng, Paul

Publication Date

2012

Peer reviewed|Thesis/dissertation

Regulation of Cardiac Progenitors

by

Paul Cheng

DISSERTATION

Submitted in partial satisfaction of the requirements for the degree of

DOCTOR OF PHILOSOPHY

in

Bioengineering

in the

GRADUATE DIVISION

of the

UNIVERSITY OF CALIFORNIA, SAN FRANCISCO

AND

UNIVERSITY OF CALIFORNIA, BERKELEY

Dedication and Acknowledgements

I would like to use this opportunity to thank all those who made these work possible, including (but not limited to): Dr. Deepak Srivastava for establishing a highly collaborative and pleasant lab environment, as well as endless support and mentorship; my dissertation committee members for providing vital guidance; Dr. Chulan Kwon for helping me enter and navigate the field of developmental biology and advising me on all the projects; all members of Srivastava lab and Gladstone Institute of Cardiovascular Disease for thoughtful discussions and suggestions; my family for their support and encouragement; Dr. Stephanie Chang for spending every weekend in lab with me and for her endless proofreading, as well as agreeing to marry me; Mr. Shu Niu for sanity-preserving golf outings; Dr. Li Qian, Dr. David Hassel, Dr. Linda Van Laake, Dr. Peter Andersen, Dr. Vishal Nigam, and Dr. Bogac Kaynak for close collaboration and co-authoring various projects. Our numerous collaborators who have generously provided valuable reagents that made our work possible are also separately acknowledged in each chapter.

Chapters 4¹ and 5² have been previously published and the references are included below.

1. Kwon C, Qian L, Cheng P, Nigam V, Arnold J, Srivastava D. A regulatory pathway involving Notch1/beta-catenin/Isl1 determines cardiac progenitor cell fate. *Nat Cell Biol.* 2009;11(8):951-7. PMID: 2748816.

2. Kwon C, Cheng P, King IN, Andersen P, Shenje L, Nigam V, et al. Notch post-translationally regulates beta-catenin protein in stem and progenitor cells. *Nat Cell Biol.* 2011;13(10):1244-51. PMID: 3187850.

Abstract

Heart failure is one of the leading causes of morbidity and mortality in the United States today. Medical advances have significantly improved a patient's prognosis, but remain limited due to our failure to improve cardiac output and contractility. Cardiac cell therapy has the potential to address these functional deficits. While ESC/iPSCs-derived cardiomyocytes are ideal candidates for cell therapy, development of an efficient method for the generation of cardiac progenitors or cardiomyocytes is paramount.

Through a series of in vitro and in vivo experiments, we addressed multiple signals and pathways that are involved in the induction and expansion of cardiac progenitors. We identified a large number of factors that affect the efficiency of cardiac differentiation, and determined the timing and roles that certain Wnt and TGF- β family members play in the specification of cardiac progenitors in vitro. In addition, we uncovered a previously unrecognized role of fibronectin in the induction of cardiac mesoderm in vitro and in vivo. We showed that fibronectin acts as a morphogen by modulating Wnt signaling through an integrin-dependent mechanism. Lastly, we discovered an intricate balance between Notch and Wnt signaling that controls the proliferation and differentiation decision of cardiac progenitors through direct transcriptional control of numerous pro-differentiation cues. Expanding on the Notch-Wnt interaction, we demonstrated the generalizability of this interaction to numerous stem cells and cancer cells, elucidating detailed mechanisms behind this novel post-translational control of beta-catenin by the Notch receptor.

Table of Contents

Chapter 1: Cardiac Therapy - The Next Frontier

1.1 : Cell Therapy Using Cells of Cardiac Origin	3
1.2 : Cell Therapy Using Non-Cardiac Cells	5
1.3 : Generating Cardiac Progenitors - A Quick Overview	8

Chapter 2: Directed Differentiation of ESC/iPSCs to Cardiac Progenitors – Methods and Personal Experiences

2.1 : Introduction	10
2.2 : Results	11
2.3: Discussion	26
2.4 : Materials and Methods	29
2.5 : Figure Legends	32
2.6 : Figures	33

Chapter 3: Fibronectin Mediates Mesendodermal Cell Fate Decisions

3.1 : Introduction	35
3.2 : Results	36
3.3: Discussion	44
3.4 : Materials and Methods	48
3.5 : Figure Legends	54
3.6 : Figures	60

**Chapter 4: A Regulatory Pathway Involving Notch1/ β -Catenin/Isl1
Determines Cardiac Progenitor Cell Fate**

4.1 : Introduction	68
4.2 : Results and Discussion	69
4.3 : Materials and Methods	77
4.4 : Figure Legends	82
4.5 : Figures	87

**Chapter 5: Notch Post-Translationally Regulates β -Catenin Protein
in Stem and Progenitor Cells**

5.1 : Introduction	96
5.2 : Results	98
5.3: Discussion	108
5.4 : Materials and Methods	110
5.5 : Figure Legends	114
5.6 : Figures	121

Chapter 6: Conclusions and Future Directions 131

References 135

Appendix

Serum-Free Differentiation Protocol 145

List of Figures

Chapter 2

Figure 2-1: Induction Kinetics of Mesoderm	33
---	----

Chapter 3

Figure 3-1: Primitive Endoderm-like (End2) Cells Promote the Emergence of Mesoderm in Embryonic Stem Cells Through a Short-Range Signal	60
Figure 3-2: End2-Induced Mesoderm is Biased Toward Precardiac Mesoderm	61
Figure 3-3: Fibronectin Promotes End2-Mediated Induction of Mesoderm and Precardiac Mesoderm in vitro and in vivo	62
Figure 3-4: Fibronectin Augments Mesoderm Induction Through Integrin-Dependent Activation of Wnt/ β -Catenin Signaling	63
Figure 3-S1	64
Figure 3-S2	65
Figure 3-S3	66

Chapter 4

Figure 4-1: Notch1 Loss-of-function Causes CPC Expansion and Increases Free β -Catenin Levels	87
Figure 4-2: Identification of Genes Affected by Stabilized β -Catenin in Cardiac Progenitors.	88
Figure 4-3: <i>Isl1</i> Loss-of-function Results in Expansion of CPCs and Suppression of Their Myocardial and Smooth Muscle Lineages	89
Figure 4-4: Increased Levels of <i>Isl1</i> Promote Myocardial Differentiation	90
Figure 4-5: <i>Isl1</i> Targets <i>Myocd</i> and β -Catenin Regulates <i>Bhlhb2</i> to Repress <i>Smyd1</i>	91
Figure 4-S1	92
Figure 4-S2	93
Figure 4-S3	94

Chapter 5

Figure 5-1: Notch Negatively Regulates Active β -Catenin in Stem Cells Independently of RBP-J	121
Figure 5-2: Notch1 Negatively Regulates Active β -Catenin in ESCs and Physically Interacts with β -Catenin	122
Figure 5-3: Membrane-Bound Notch1 Negatively Regulates Active β -Catenin Levels through Numb and Numb-like in Stem Cells	123
Figure 5-4: γ -Secretase Inhibitors (GSIs) Suppress Expansion of Human Colon Cancer Cells by Blocking Notch Cleavage	124
Figure 5-5: Model for Post-Translational Regulation of β -Catenin Protein by Notch	125
Figure 5-S1	126
Figure 5-S2	126
Figure 5-S3	127
Figure 5-S4	128
Figure 5-S5	129
Figure 5-S6	129
Figure 5-S7	130

1. Cardiac Cell Therapy - The Next Frontier

Rationale and Target Population for Cardiac Cell Therapy

Cardiovascular disease has been the focus of medical research for the past several decades due to its high incidence and morbidity. Unfortunately, despite numerous medical advances, cardiovascular disease remains the leading cause of morbidity and mortality in the United States today¹. In fact, the morbidity and mortality associated with acute myocardial infarctions and their sequelae are still higher than those caused by cancer, HIV, and accidents combined². A significant number of cardiac conditions, particularly those associated with insufficient cardiac output including heart failure and various cardiomyopathies, still hold very grim prognoses^{3,4}. Patients with heart failure usually suffer a downward spiraling course of disease with a median survival of approximately five years characterized by an extremely poor quality of life due to frequent hospital visits, dietary restrictions, and exercise intolerance⁵. Alarming, the prevalence of heart failure is rapidly rising in this country⁶. Current medical management has limited efficacy, and does little to address the underlying pump failure that is critically linked to an improved quality of life. Engineers, however, have been fixing pumps for thousands of years. For that reason, heart failure may prove to be a problem for the engineers.

One approach to address heart failure is through cardiac tissue engineering and cell therapy. Cardiac cell therapy is based on the thought that heart failure is mostly a problem of insufficient cardiomyocyte output relative to pump demand. In the case of

myocardial infarctions, cardiomyocytes are lost through ischemia and infarction. The intrinsic output of individual cardiomyocytes is reduced in certain cardiomyopathies⁷. In dilated cardiomyopathy, the increased diameter of the heart demands higher wall tension for the same pressure, as governed by Pascal's principle. In all these cases, the strategic addition of healthy cardiomyocytes should improve the imbalance between output and demand to improve cardiac function.

While the potential benefits of cardiac cell therapy are clear, it is less clear exactly which cells should be used to replace lost myocardium. After an acute myocardial infarction, up to a billion cardiomyocytes can be lost to apoptosis and necrosis secondary to ischemia⁸. In the case of cardiomyopathies, the number of cardiomyocytes lost over time can be even greater⁹. Healthy adult cardiomyocytes are difficult to obtain and are thought to be post-mitotic. Interestingly, genetic lineage tracing experiments in infarcted mouse hearts demonstrated an emergence of a population of newly formed cardiomyocytes¹⁰, raising the possibility that endogenous myocardial regeneration can be augmented and used as therapy.

The scientific community's long-held belief that the heart is a post-mitotic organ—that a person dies with the same cardiomyocytes he or she had as a child-- has recently been challenged by a flurry of studies. Mitotically active cardiomyocytes can be observed in the adult heart¹¹, and carbon-dating of cardiomyocyte DNA showed a roughly 1% turnover of the adult myocardium, with up to 40% of adult cardiomyocytes generated post-natally¹². These studies have re-ignited the field of cardiac regeneration with the hope that the mammalian heart may be coaxed into regeneration after an acute insult, as seen in the hearts of zebrafish and newts. Although the rate of endogenous

regeneration is still a hotly debated issue, the general consensus of the field is that the rate of natural regeneration is still many orders of magnitude below what is necessary to replace the cardiomyocytes lost in a timely manner¹³. Thus, identifying a proper population of cells that can be utilized to replace lost cardiomyocytes is among the most important questions for cell therapy at this time.

Embryonic stem cells (ESCs) have the ability to grow indefinitely and can differentiate into cardiomyocytes. We believe that ESC-derived cardiomyocytes may be the most ideal choice of cells. However, many hurdles remain to be resolved before ESC-derived cardiomyocytes can be used for such purposes. Other groups have pursued cell therapy with other potential candidates, and lessons learned from these valuable studies are summarized below.

1.1. Cell Therapy Using Cells of Cardiac Origin

Efforts made to propagate and expand populations of fully differentiated cardiomyocytes in vitro have mostly failed. Although embryonic or neonatal cardiomyocytes can temporarily expand in vitro, they quickly reach senescence and lose their ability to divide. Thus, a less differentiated population must be used to obtain the large number of cells needed for cell therapy. Since the heart can undergo modest regeneration, substantial efforts have been placed on identifying the cells responsible for this regenerative effort. While the holy grail of identifying a true cardiac stem cell has yet to be realized, many groups have identified via different means populations of cells that can be expanded in vitro and maintain their ability to differentiate down the cardiac

lineage. Various animal studies have demonstrated the efficacy of these cells in improving the function of a failing heart.

One of these populations is the cardiosphere cells. Cardiosphere cells are identified through a classical method of adult-stem-cell discovery, whereby whole digested tissue is plated at a low density, and colony-forming stem/progenitor cells are identified phenotypically. Several days after plating out cells obtained from large open-heart biopsies, clumps of cells will form containing cardiomyocytes and other cells of cardiac lineage¹⁴. These clumps, called cardiospheres, are then used as a conglomerate for cell therapy. Injection of cardiospheres into rodent and pig models of myocardial infarction and heart failure resulted in modest improvements in cardiac function^{15,16}.

Other populations of cells are identified through markers adopted from the best-characterized adult stem cell system – hematopoietic stem cells. Different research groups used surface markers such as c-Kit¹³ (receptor for stem cell factor), Sca-1¹⁷ (stem cell antigen-1), the ability to exclude hoechst dye¹⁸ (so called “side population”), or a combination of these characteristics, to identify a population of cells that can be expanded in vitro and that maintain their ability to form cells of different cardiac lineages in vitro and in vivo. Like cardiosphere cells, injection of these cells after myocardial infarction resulted in differentiation of these cells into different cardiac lineages with modest functional benefits¹³.

Initial studies from these putative cardiac stem cells sparked a large number of studies in vitro and in vivo. Unfortunately, these results have been less promising. The functional improvements seen after cell therapy are very modest, can disappear over time, and sometimes even lead to no detectable improvements. More concerning is that

subsequent studies have questioned the true identities and lineage plasticity of these cells¹⁹. The populations identified through these methods are mixtures, and the putative stem cells are only a small subpopulation²⁰. Expansion and selection of these cells must be accomplished for these cells to be useful for cell replacement therapy. Whether or not these cells can truly self-renew and maintain their ability to form cardiomyocytes remains to be seen. Until then, their use in cell therapy mostly remains a theoretical possibility.

1.2. Cell Therapy Using Non-Cardiac Cells

While some researchers in the field labor to isolate and expand cardiac stem cells, others have attempted to accomplish the feat of cell therapy with non-cardiac cells. The earliest attempts involved the use of skeletal myoblasts. Although cardiac and skeletal muscles are different, skeletal muscles probably share more characteristics with cardiac muscle than any other cells. Furthermore, unlike cardiac muscle, adult skeletal muscles constantly renew²¹, and the population responsible for regeneration is well-characterized. In addition, the skeletal muscle mass in an adult far outweighs that of the heart, providing a potential source of autologous cells for therapy. Studies in animal models showed injected skeletal myoblasts to be resistant to ischemia and improve cardiac function^{22,23}. The results were so promising that this intervention was quickly advanced to human subjects^{23,24}. A series of studies, including a randomized, double-blinded trial, showed a definite but modest improvement in ejection fraction^{24,25}. However, patients treated with myoblasts appeared to have a significantly increased risk of arrhythmias^{26,27}, resulting in early termination of the trial.

Another approach to cell therapy involving non-cardiac derived cells utilized cells derived from bone marrow. The rationale behind these therapies stems from observations of donor chromosomes in cardiomyocytes in patients with bone marrow transplants²⁸, suggesting the theoretical potential for bone-marrow derived cells to trans-differentiate into cardiomyocytes. The largest advantage of these cells is that they are easily obtainable and can be characterized and purified extensively through surface markers. The exact cells used by different investigators differ subtly, ranging from bone-marrow derived mono-nuclear cells to surface-marker purified circulating progenitor cells²⁹. Due to the ease of isolation, the number of studies using bone marrow-derived cells in humans has exploded in the past decade. Injection of these cells resulted in modest improvements in various outcome-measures in human trials³⁰⁻³³, similar to skeletal myoblasts. Subsequent studies using various adult-derived stem cells such as mesenchymal stem cells or adipose-derived stem cells were performed and showed similar results.

Unfortunately, the flurry of successful trials was immediately followed by a series of studies that put the same results in question^{34,35}. Subsequently published studies, including double-blinded trials, demonstrated no functional benefits from therapy³². A meta-analysis of all published studies shows that the treatment is safe but suggests that clinical improvement after treatment is very modest at best³⁶. Thorough analysis of the differentiation potential of bone-marrow derived cells in vivo suggests that they do not differentiate into cardiomyocytes, and that the initial observations in transplanted patients may have resulted from cell fusion³⁴. Further studies in animal models showed that injection of cell lysates are equally efficacious as live cells³⁷, suggesting that functional improvement may be mostly paracrine in nature. While these studies essentially eliminate

the possibility of using bone marrow-derived cells for cell therapy, they introduced new avenues for potential therapeutic studies to combat the sequelae of myocardial infarctions.

Although adult-derived cell allografts can sidestep the problem of immune rejection, studies in the past decade have largely eliminated them as viable options, mainly due to their inability to expand and form functional cardiomyocytes. An alternative approach involving the use of embryonic stem cell-derived cardiomyocytes does not have these problems, but this technology is still in its infancy. Embryonic stem cells (ESCs) satisfy the strictest definition of stem cells and can self-renew almost indefinitely while maintaining their ability to form cardiomyocytes. Furthermore, the advent of induced pluripotent stem cells (iPSCs) technology offers the opportunity for patient-derived allografts, or at the very least a bank of HLA-matched iPSCs³⁸. Proof-of-principle experiments have demonstrated the ability of ESC-derived cardiomyocytes to engraft in infarcted mouse hearts. However, generation of a large number of cardiomyocytes remains a major hurdle.

1.3 Generating Cardiac Progenitors – A Quick Overview:

Most of our current understanding of directed differentiation of ESCs into cardiomyocytes stems from *in vivo* developmental studies, because ESC differentiation follows stereotyped stages that mirror events during development.

Cardiomyocytes are mostly a mesodermal derivative with the exception of cells involved in the separation of outflow tracks that have some neural crest contributions³⁹. Across all vertebrate model organisms, the cells that are fated to form the heart can be identified spatially as soon as the embryo begins to gastrulate⁴⁰. Transplant experiments suggest that fate determination of these cells occurs soon after gastrulation⁴⁰. In vertebrates, gastrulating mesodermal cells express the T-box transcription factor Brachyury (or its homologs)⁴¹. The subset of mesodermal cells that is fated to form the cardiovascular system also begins to express bHLH transcription factor *Mesp1*^{42,43}. These *Mesp1*-expressing cells are induced bilaterally in the gastrula and then migrate anteriorly and meet in the midline at the beginning of the segmentation stage⁴⁴. As they migrate towards midline, some cells start to express cardiac markers, such as *Nkx2.5* or *Islet1*⁴⁵. These cells are thought to be able to give rise to all lineages in the heart including cardiomyocytes, endothelial cells, and smooth muscle cells^{46,47}.

The specification of mesodermal cells is thought to be governed by a three-dimensional gradient of Nodal, Wnt, and BMP signals⁴⁸. Fgf signaling has been implicated to be critical in this process as well⁴⁹. While knockout studies have shown that these signals are necessary for the induction of cardiac lineage, paradoxical results have

surfaced when these signals are activated or deleted at different times^{50,51}, suggesting a multiphasic role for these signals in cardiac progenitor biology.

To make a large number of cardiomyocytes, we must first generate a well-characterized pool of cardiac progenitors. Thus, we embarked on a series of in vitro and in vivo studies aimed at gaining a better understanding of the signals controlling induction and maintenance of cardiac progenitors.

2. Directed Differentiation of ESC/iPSCs to Cardiac Progenitors – Methods and Personal Experiences

Introduction

Pluripotent stem cells, such as embryonic stem cells, have the ability to differentiate into every cell in the adult animal, including cardiomyocytes. A combination of near-infinite self-renewal and lineage plasticity makes these cells an attractive cell source for commercially scalable cardiac tissue engineering. Furthermore, recently discovered induced pluripotent stem cell (iPSC) technology allows for direct conversion of any cell type into embryonic stem cells⁵². This technology holds endless potential in disease modeling and drug screening. From the cell-therapy point of view, iPSC technology may potentially solve the problem of immune rejection, a difficult problem that has plagued organ transplantation for decades. Overcoming immune rejection can be achieved through either isogenic personalized therapies or the creation of an iPSC bank with exhaustive combinations of all major HLA subtypes in a population⁵³. While the potential for pluripotent cell-derived therapies is endless, various hurdles still remain before any clinical translation can occur. The ability to make infinite amounts of any cells from the body, for example, remains mostly theoretical, since our ability to direct differentiation of these cells remains fairly primitive. Given the complicated nature of development in vivo, it is not surprising that we have not yet been able to recapitulate its entirety in vitro. There is an excess of variables that one can manipulate in a cardiac differentiation. The inductive conditions can vary wildly from cell line to cell line, further complicating the

optimization process. Factors that affect differentiation are rarely covered in methods papers, making optimization of a new cell line extremely difficult. At times, the finicky nature of differentiation can oblige one to approach it more like an art rather than an exact science. These unpredictable variations, particularly between cell lines, significantly diminish the power and efficiency of ESC research.

In the past few years, much of my research effort has been spent on reducing the noise of differentiation through identifying factors that have significant effects on differentiation efficiency. While the findings from these efforts are not included in any papers, they are the foundation behind all of our more polished stories. Although most of the information presented may be more anecdotal rather than quantitative, I believe that these experiences and personal observations will be useful for anyone who wishes to differentiate mESCs into cardiomyocytes. Lessons that we have learned from our experiences in differentiation, along with methods that we found to improve cardiac differentiation, are presented in the section below.

Results

Serum-Dependent Differentiations

The simplest method of cardiac differentiation involves the formation of embryoid bodies (EBs) in serum-containing media in ultra-low attachment dishes. In this method of differentiation, progenies from all three germ layers are formed, as evidenced by the ability to detect expression of characteristic genes/markers in these EBs via either immune-florescence (IF) or quantitative-reverse-transcription real-time polymerase chain

reaction (qRT-PCR). In this rudimentary method, the main determinant of differentiation is the content of the serum in the media, presumably from growth factors contained in the serum. Unfortunately, due to the highly heterogeneous nature of serum and high variation from batch to batch, meaningful data from our studies in optimizing serum-containing differentiation were restricted to mostly growth factor-independent parameters.

Embryoid Body Size

One of the factors consistently found to make a large difference in the extent of cardiac differentiation is the size of the embryoid bodies. Embryoid bodies can range from tens of cells up to hundreds or thousands, which are formed freely in suspension. One can control the number of cells within an individual EB via the hanging-drop method. Using the hanging-drop method, EBs can form with as few as 10 cells, and there does not appear to be an upper limit. Interestingly, embryoid bodies tend to pull themselves into near-perfect spheres, a characteristic not seen in aggregate of other cells, and the mechanism may contain interesting biological underpinnings. The formation of embryoid bodies occurs within the first 12 hours of aggregation. Embryoid body formation in suspension appears to be characteristic of ESCs, as other adherent cell types fail to clump in suspension. However, when other cell types are mixed with ESCs in suspension culture, they become readily incorporated into the EBs that are formed. The ability to form EBs is retained roughly until the end of gastrulation (roughly day 5 in EB). Cells lose their ability to form spherical suspensions after *Mesp1*/Brachyury can no

longer be detected. This process occurs independently of integrins, since blockade of integrins with antibodies does not inhibit the formation of embryoid bodies.

The optimal size of EBs for cardiac differentiation appears to be between 300-750 cells per EB. EBs with too few cells (<30) can survive in suspension, but their growth appears to be disproportionately stunted, and they rarely ever differentiate into beating embryoid bodies. On the other hand, embryoid bodies that are too large result in poor induction of mesodermal genes. Larger EBs tend to more efficiently differentiate down the neuro-ectodermal lineage. Intriguingly this finding very well reflects the relative positions of the different germ layers in vivo, where mesendodermal cells that gastrulate through the primitive streak are near the surface of the embryo, whereas primitive ectoderm cells are more interior. Increasing the EB size increases the volume-to-surface-area ratio, and this is correlated with the change in ratio of neuroectoderm to mesendoderm progenies that are formed. An interpretation of these observations is that either the outermost layer, similar to that of primitive endoderm, is instructive in the induction of mesendoderm in its neighbors, or that the position of cells within a packed sphere, similar to the determination of animal vs vegetal pole in the xenopus, may be sufficient to determine cell fate. This observation, however, remains an interesting hypothesis and beyond the scope of this study.

Replating

Embryoid bodies can efficiently differentiate down the cardiac lineage in suspension. This efficiency can be improved by allowing the EBs to attach and spread on gelatin-coated dishes. The critical window for re-plating is approximately day 6-9 of differentiation. Earlier plating results in poor differentiation, whereas later plating results in little improvement.

Replating density does not appear to be a major factor in differentiation efficiency in terms of the fraction of EBs with beating foci. However, lower density plating allows for overgrowth of non-cardiac cells, which will artificially decrease the relative fraction of resultant cells that are cardiomyocytes.

Media Change

Excessive media change is detrimental to the induction of the cardiac lineage. This is particularly important between the period from day 3 to the onset of contraction. Media changes at a higher frequency result in very poor differentiation, and addition of media conditioned by older EBs appears to improve cardiac differentiation. Excessive media changes potentially result in either the removal of factors important for differentiation in serum or non-cell-autonomous factors that are secreted by cells induced in EBs necessary for differentiation. The fact that this is observed with serum-free media as well as different batches of serum favors the latter hypothesis. The true cause for these observations merits further investigative studies.

Efficiency of Cardiac Differentiation

In normal embryoid body differentiation, the initial contraction can be observed as early as day 7 of differentiation. By day 9-10, contractile foci can be observed in 15-33% of embryoid bodies depending on the cell line and serum. Using the hanging-drop method with 500 cells per EB, contraction can be routinely observed in 80% or more of the embryoid bodies. It is important to note, however, that even though contractions are observed in the majority of the EBs, the EBs are still incredibly heterogeneous. In fact, only a very small fraction of cells within the EBs are truly of cardiac lineage. Using a Nkx2.5-GFP reporter line, we observed an average of 10% of GFP⁺ cells within hanging-drop derived EBs. The reporter, however, can be positive not only in cardiomyocytes and their progenitors, but also within certain population of cells in the foregut endoderm. If a more stringent method of quantifying cardiac differentiation were used, such as cardiac troponin T (cTnT) staining, the percentage of cardiomyocytes in normal embryoid bodies is roughly 1-2% and around 3-5% for hanging-drops.

Serum-Free Methods

Although serum-based differentiations are very robust, the yield leaves something to be desired. Furthermore, the variability created by serum batches causes identification of factors that influence differentiation to be very difficult. The trend in the field, therefore, has been to switch over to a completely defined medium. The remaining section will focus on differentiation with serum-free methods. The main method of serum-free differentiation is based on a protocol initially devised from the lab of Gordon

Keller. The detailed backbone of this protocol is included in the appendix. The serum-free differentiation protocol is very powerful. With some optimization, I was able to create >70% pure cardiomyocytes in every (>10) mESCs/iPSC lines tested. This section will focus mainly on factors that influence the success and consistency of the protocol at critical time points.

Day 0: Starting Cells

The serum-free differentiation protocol follows a strict timeline and cytokine concentrations. Slight variations in the starting population can result in complete failure of cardiac differentiation. Thus, the quality of the undifferentiated mESC is absolutely critical for the success of the protocol. One common cause for failed differentiation is sub-optimal Leukemia Inhibitory Factor (LIF) concentration, resulting in cells that are subtly differentiated from the start. The resultant cells will still express a high level of pluripotent markers; however, akin to epiblast-derived stem cells, these cells will start to spontaneously differentiate into different germ layers earlier than true ES cells. The accelerated spontaneous differentiation throws off the induction timing, resulting in poor cardiac differentiation. The best way to assay if the cells are flawed is by adding activin and wnt at the initial stage of differentiation and assay for induction of *Sox17* and *Brachyury* at day 2. Good ES cells should not respond to a cytokine at this stage, whereas differentiated ones will respond readily and express these germ-layer markers.

When a mESC line is passaged extensively, the population can drift slightly due to the selective pressure of the artificial culturing environment. The result, unfortunately,

is that the optimal cytokine concentration for the differentiation can drift after several passages. For the best reproducibility, it is best that a large number of vials are frozen down from each cell-line of interest from a large expansion. Differentiation can then be initiated from the first passage of each frozen vial, ensuring homogeneity from one passage to the next.

Day 2: Induction

The induction step is arguably the most important step in the serum-free differentiation. At the start of the second day, one should first carefully observe the EBs formed. One should expect to see a large number of small spherical EBs. Cell boundaries on the surface of these EBs should be blurred, as tight cadherin-junctions form between interlocking cells on the surface, similar to those covering a developing embryo. There may be some single cells attached to the surface of the spherical EBs, which is normal. There is also usually a large number of floating single cells that are not detrimental to the differentiation. It is best to gather all the EBs in the middle of the well and harvest only the EBs, as floating cells do not respond to cytokines. The number of cell harvested should be somewhere between 2-3 fold that of D0.

The cytokine concentration is essential for induction. Generally, each cell line has an optimal pair of concentrations of ActivinA and BMP that can efficiently generate cardiomyocytes with particular sensitivity to BMP concentration. Optimization based on a matrix of different ActivinA and BMP concentrations usually shows that at any fixed ActivinA concentration, there is a strict lower-bound for BMP concentration below which

no cardiac differentiation can be observed. Optimal differentiation, based on percentage yield of cTnT positive cells, is usually achieved by BMP concentrations just above the lower bound of BMP. Increasing the BMP concentrations above the optimal level results in a gradual decline in differentiation efficiency. The total dynamic range where one can see cardiac differentiation is fairly small at roughly 30-50% of the optimal BMP concentration, which must be taken into account when one tries to optimize differentiation of a new cell line. One important point is that the activity of the commercially available BMP can vary dramatically from lot to lot. It is therefore advisable to suspend and aliquot a large batch of a very small volume of BMP to ensure consistency from one differentiation to the next. The cells appear to be less sensitive to variation in Activin concentration, though the lower-boundary of BMP concentration generally increases with increasing Activin concentration. Differentiated mESCs at this stage secrete endogenous nodal. Sometimes, the secreted nodal is too high and instead of adding activin, an inhibitor may be needed for differentiation.

The optimal length of induction can vary from cell line to cell line. From our experience, it can vary from 32 hours to 60 hours depending on the ES cell line. There is unfortunately no a priori method to our knowledge that can help us determine the optimal time. Luckily, the optimal window can be as long as 12-18 hours, reducing the amount of optimization needed. Delay in entering to the next stage will result in more *Mesp1*⁺ cardiac progenitors, and timing of the initiation of beating will be delayed by roughly the same amount of time, suggesting that induction media is sufficient to drive temporary amplification of these progenitors. Prolonged exposure, however, results in loss of the cells' ability to differentiate down the cardiac lineage.

Day 4: Replating

In a manner similar to day 2, visual observation alone is often sufficient for predicting differentiation success. Prior to re-plating, the embryoid bodies should be numerous, but relatively small. Their surfaces should again be very smooth, and there should be very few cells attached to the surface. There may again be floating cells, which are viable when re-plated, but do not differentiate down the cardiac lineage. Thus, only aggregated healthy EBs should be gathered to proceed to the next step. There should once again be a 2-4 fold increase in cell number. Deviations from any of the above observations are strong predictors for poor cardiac differentiation.

Cells at this stage should express high levels of *Brachyury* and *Mesp1*. It has been proposed that the quality of the differentiation can be assayed via cell-surface markers Flk1, PDGFra, and CXCR4. Based on our experience, these markers are very good surrogate markers for cardiac progenitor differentiation. The absence of these surface markers guarantees that the differentiation will be poor. However, high levels of these markers do not necessarily translate into satisfactory cardiac differentiations. In fact, even sorting out the double positive cells alone does not result in improved yield of cardiomyocytes (as assayed by % cTnT positive cells). This may be secondary to the stress that cells experience during sorting, cancelling out any improvement from a purified population, or may suggest the presence of an alternative, non-double positive population that is critical for cardiac differentiation.

The wash step prior to re-plating is critical. Addition of a small amount of BMP (i.e. leftover from the inductive step) is highly inhibitive against cardiac differentiation. Stem Pro can vary from lot to lot, which is usually not a problem, but when an adverse

event occurs, it can be catastrophic. We recommend lot testing. StemPro is very expensive, but is only necessary for the first 3 days of re-plating, after which cells can be placed into any media without affecting final differentiation. Fgfs and VEGF are required, but increasing the concentrations does not negatively affect differentiation. Wnt inhibition is critical for the last step of cardiac differentiation in vivo. However, it seems that sufficient Wnt inhibition is supplied either endogenously or via StemPro. Addition of Dkk1 at replating is usually not necessary.

Cell density at re-plating is not absolutely critical, but it is important to seed enough cells to completely cover the bottom of the well. Low density (i.e <75K cells per 96-well dish) results in poor differentiation, but doubling or tripling the recommended number does not adversely affect differentiation.

Cells can be plated onto either gelatin-coated or fibronectin-coated plates. In fact, these cells appear to secrete plenty of extracellular matrices, enough that they can be seeded directly onto tissue-culture-treated plates in StemPro. Cells seeded without matrices consistently start to contract 8-12 hours earlier than those seeded onto gelatin, though this does not affect the percentage of cardiomyocytes in the final culture. An alternative method is to place cells in ultra-low attachment plates. Under these conditions, cells will aggregate to form embryoid bodies and proceed to differentiate down the cardiac lineage. A tissue-patch can be created by plating these cells in very high density in an ultra-low-attachment dish. Cells at this stage can also be seeded onto other matrices, such as synthetic scaffolds or decellularized matrices. As long as the density is sufficiently high and the media remain constant, the cells will differentiate successfully.

Injection of cells at this stage into an infarcted mouse heart, unfortunately, resulted in no engraftment or differentiation.

Replated cells divide rapidly in the supplemented StemPro. If the cells are truly cardiac progenitors, they will start to pile on top of one another, forming thick streaks of cells that can be observed under the microscope. The earliest cardiac differentiation, signaled by initiation of contractile foci, invariably starts in the middle of dense bundles. This observation suggests the presence of an important density-associated cue in the final steps of differentiation. This may also explain why contraction can only be seen in densely populated edges of the well (due to meniscus formation) when cells are plated at lower densities.

A good differentiation is abnormally metabolically active even prior to the onset of contractions. Even with the same number of cells, the media will become markedly more acidic compared to those that lead on to poor differentiation. A yellow-colored well at day 5.5 is highly predictive of the onset of cellular contractions. Depending on the cell line, the onset of contractions can be seen as early as day 6, but may start as late as day 9. Using the same cell line and induction, it appears that the time between re-plating and the onset of contractions is very stereotyped. Induction with higher levels of BMP may sometimes lead to the later onset of contractions. A non-contracting well at day 10 typically does not improve further.

This serum-free differentiation protocol has been tested on a large number of ES and iPS lines, and has been successful in all of the lines tested. This protocol can be used not only for the generation of cardiac progenitors for tissue engineering, but also as a model for studying cardiac development.

Cardiac differentiation in vitro is thought to follow the same progression as those seen in developing embryos in vivo. This assumption is evidenced by the ability to sequentially detect developmental genes that are consistent with their induction kinetics in vivo. Furthermore, levels of progenitor gene expression accurately predict the efficacy of differentiation. Thus, in order to improve and better understand cardiac differentiation, we first focused on directing the differentiation of embryoid bodies into mesoderm and pre-cardiac mesoderm, and determining how differentiation can be influenced via developmentally important cues.

Kinetics of Mesoderm Induction

To better understand how we can influence the induction of mesoderm and precardiac mesoderm, we first wished to characterize the kinetics of mesoderm induction and determine the window in which mesoderm induction and specification can be best influenced in our system. Based on our experiences with serum-free differentiation, we knew that cardiac mesoderm could be efficiently induced via a cocktail that activates nodal, wnt, and BMP signaling. Analysis of the induction kinetics, using a Brachyury-GFP reporter mESC line, revealed that a protein of the primitive streak/mesoderm gene *Brachyury (Bry)* is first detected ten hours after the addition of the cytokine. Within an 8-hour window 12 hours after induction, nearly 100% of the cells within the EBs become positive for Brachyury-GFP (Fig 1a). Gene expression, as analyzed by qRT-PCR at 2 hour intervals, showed that specification of these cells into precardiac mesoderm, as indicated by the expression of *Mesp1*, appears to be induced simultaneously with the

expression of *Bry*. The expression of *Bry*, as assayed by qRT-PCR, peaks around day 3 and then starts to decline. *Mesp1* mRNA, however, continues to accumulate for another day (Fig 1b). The window in which the cocktail of nodal, wnt, and BMP can efficiently induce mesoderm appears to be 12-24 hours and is centered on day 2 of differentiation. When the cocktail is added to cells past day 2.5, a significant population of cells does not respond to the cytokine. On the other hand, addition of cytokines too early results in non-synchronized kinetics, as some cells turn on GFP faster than others. These results suggest that there is a stochastic induction of mesendodermal progenitors that are responsive to the inductive signal. Cells maintain the ability to respond to the cytokines for a period of less than 24 hours. In the absence of a proper inductive signal, these cells will lose their ability to become mesoderm. It is also interesting to note that the cells appear to be highly proliferative in this induction stage, with a doubling time of roughly 18 hours.

Role of Nodal / BMP / Wnt in the Induction and Patterning of Mesoderm

In vivo, mesendodermal progenitors are thought to be multipotent. Their cell fates are determined during gastrulation. In the mouse, the relative positions on the primitive streak where these progenitors gastrulate are thought to predict their resultant fates. The same spatial-fate correlation is conserved in all vertebrate model organisms. This patterning is thought to be achieved by overlapping signaling gradients of Nodal, Wnt, and BMP signaling. While classical developmental studies have confirmed the necessity of these signals, the exact mechanism of how these signals determine cell fate remains to be elucidated. On day 2 of our serum-free differentiation, the cells exhibit characteristics

consistent with mesendodermal progenitors whose fate can be instructed by varying combinations of these developmentally critical cytokines. The flexibility and controlled environment of our serum-free conditions offer an opportunity to study the mechanisms of cytokine-concentration-dependent lineage induction and determination.

As mesendodermal progenitors gastrulate through the streak and become specified, T-box gene *Brachyury* is one of the earliest genes expressed. The first question we asked is whether any of these signals are sufficient to induce Bry⁺ cells. To do this, we added each of the cytokines at day 2 of serum free differentiation, and assayed for induction of Bry⁺ cells at day 3 and 4. To our surprise, addition of Nodal agonist ActivinA or Wnt alone is sufficient to induce Bry⁺ cells in almost the entire population, whereas the addition of BMP resulted in very little induction at day 3 (Fig1c). Looking slightly later at day 4, the cultures with BMP added have slightly more Bry⁺ cells than background, but still significantly less than those induced by nodal or Wnt (Fig 1c). Also worth noting is that while nodal and Wnt can generate a near-100% induction of Bry⁺ cells, this result is never seen in BMP induction even when the experiment is taken further. These results suggest that BMP either promotes the proliferation of induced Bry⁺ cells, or augments a signal that is produced by spontaneously differentiated cells.

The cytokine-gradient model of lineage determination dictates that cells should have a graded response to the cytokine concentrations. To see if this is true in our model, we induced unspecified mesenedodermal progenitors at day 2 of serum-free differentiation with increasing concentrations of ActivinA or Wnt. To our surprise, a dose-dependent effect on the degree of induction with either cytokines was not observed. Instead, there appeared to be a threshold level above which all cells responded (Fig. 1d). Gene-

expression analysis of induced cells at day 3 revealed that cells induced by the two different conditions are vastly different. ActivinA-induced cells express high levels of endodermal markers *Sox17* and *Foxa2*, whereas Wnt-induced cells express high levels of mesodermal markers *Mesp1* and *Flk1*. The mesoderm/endoderm fate appears to be determined at this point, since the addition of Activin to Wnt-induced cells or vice versa fails to alter marker expression. Surprisingly, increasing cytokine concentrations did not significantly alter expression of different lineage markers.

Next, we wanted to examine whether the crosstalk of these different cytokines alters the inductive response. To do so, we added these cytokines pairwise and examined Bry induction (via FACS) and gene expression (via qPCR) at day 3. The combination of Wnt and Activin resulted in no additional induction of Bry⁺ cells. However, markers for both mesoderm and endoderm are both increased in this condition. Exposure to higher Activin and lower Wnt skewed the population towards more endoderm, whereas higher Wnt and lower Activin skewed the cells towards mesodermal gene expression.

Addition of BMP to Wnt-induction resulted in a slight increase in Bry⁺ cells. This effect was more dramatic on day 4 compared to day 3. EBs in conditions including BMP also appeared larger than those without, which was highly suggestive that BMP may promote proliferation. The cells maintained expression of mesodermal markers. Addition of BMP to Activin-induction produced a similar increase in Bry⁺ cells. EBs in this condition were also much larger than those seen in Activin alone. Interestingly though, addition of BMP to Activin ablates the induction of endodermal genes and strongly promotes a mesodermal program.

Discussion

Directed Differentiation - Future Challenges

Based on the efficiency of cardiomyocyte generation alone, it is clear that the future of cell therapy for treatment of heart failure lies in serum-free methods. The significantly decreased variation between experiments, as well as the flexibility to control dose and duration of all inductive components, allow ESCs to be an even more powerful model for studying developmental events. Many lessons learned from studying serum-dependent systems continue to hold true, and serum-mediated differentiation remains valuable for studying processes, such as cardiomyocyte hypertrophy, in which the necessary conditions for serum replacement has yet to be discovered.

Several interesting questions raised by our serum-dependent differentiation merit further study. For example, our observation that re-plating EBs at an early stage results in improved cardiac differentiation suggests the presence of a mechanical cue in the final steps of cardiac differentiation that will either promote cardiomyocyte differentiation or proliferation. The negative influence of media change was observed in both serum and serum-free conditions, suggesting the existence of unknown soluble factors that are important for the final steps of cardiac differentiation. Identifying both soluble and mechanical cues will be essential for large-scale production of cardiac progenitors.

It is clear from simple visual observation of contractile EBs within a well that the population is highly heterogeneous. This is also reflected by the high amount of variability in the expression of different channel genes as well as chamber-specific isoforms. This problem of variability is slightly improved in the serum-free

differentiations, but a rather large variation still exists. Visualizing calcium transients and contractile frequency from well-to-well often also demonstrates large variations.

Qualitative observations suggest a high degree of variability in forces of contraction.

These variations are probably the result of differences in myocyte composition, as well as spontaneously formed re-entrant type circuits. Alignment of ES-derived cardiomyocytes through synthetic matrices may improve noise reduction.

The serum-free differentiation was able to successfully generate a monolayer of beating cardiomyocytes in every cell line tested. Although cytokine conditions, particularly the optimal amount of Activin and BMP, vary greatly from line to line, and sometimes from passage to passage, this variation is thought to derive from variations in endogenous Nodal / BMP production and sensitivity. For example, in some human ESC lines, endogenous phosphor-smad2/3 is high, and inhibition of nodal is necessary. The extreme sensitivity, particularly to BMP concentrations, can be highly prohibitive for any large-scale production or patient-specific applications.

Furthermore, a highly sought-after application of directed cardiac differentiation is to use iPS cell-derived cardiomyocytes to model diseases. Since different cell lines will need to be induced slightly differently, there remains the possibility that the cells generated from different iPS lines are simply different population of cardiomyocytes. In fact, qualitative differences can be seen between cardiomyocytes generated from the same cell-line at different BMP concentrations. The solution to this problem most likely lies in better characterization of the cardiomyocytes generated. A method for sub-stratifying the cardiomyocytes into distinct lineages is most likely critical for iPS-derived myocytes to reach their full potential.

Mesoderm Induction

Our studies aimed at gaining a better understanding of mesoderm induction and patterning reveal that lineage specification in this context is more complex than previously thought. In vivo studies have shown evolutionarily conserved requirements of Nodal and Wnt signaling in both mesodermal and endodermal tissue. Endogenously secreted nodal and wnt are present in our serum-free cultures, presumably from spontaneously differentiated cells. Indeed, in ours and others' works, inhibition of either nodal or Wnt is sufficient to block induction. Furthermore, Wnt inhibition by dkk cannot be rescued by Nodal stimulation and vice versa. These results suggest that both signals are necessary for the induction of both germ layers. Interestingly, this initial fate decision appears to be particularly sensitive to relative doses of Wnt and Nodal, and the decision appears to be irreversible. Since no cells express markers of both germ layers in vivo, it is highly suggestive that the balance between nodal and wnt in a small window during the inductive stage is the main driving signal behind initial mesendodermal cell fate decisions.

The cells' decision-switch is further complicated by the presence of BMP. While BMP alone appears to be insufficient for endoderm or mesoderm induction, it drastically alters the downstream biology when added along with Nodal or Wnt.

The combinatorial effects of BMP and Nodal are particularly interesting. Both Nodal and BMP are TGF- β family members. While Nodal mainly activates Smad2/3, BMP mainly activates Smad1/5. The activated P-Smads then form a heterodimer with Smad4, which then translocates to the nucleus and drives transcription. From Chromatin Immuno-Precipitation (ChIP) experiments, we saw that several of the important early

mesodermal and endodermal genes are direct targets of SMAD4. Since both pathways signal through SMADs, the fact that a small amount of BMP is sufficient to shut off nodal-induced genes entirely is very surprising. The different branches of TGF- β signaling have been shown to interact through inhibitory SMADs. However, inhibitory SMADs usually modulate relative expression of two expressing pathways. The rapid yet polarizing kinetics of the induction of two non-overlapping endoderm/mesoderm programs cannot be simply explained by inhibitory SMADs and thus suggest the presence of a novel mechanism of transcriptional regulation. Disrupted balance between signaling of different TGF- β family members has been recently implicated in numerous human diseases. A better understanding of how these two well-studied pathways interact and crosstalk will benefit future developmental research and beyond.

Materials and Methods

mESC Maintenance

Mouse ES cells were propagated in an undifferentiated state on gelatin-coated cell culture plastic (Nunc) in GMEM supplemented with 10% FBS, 0.1 mM nonessential amino acids, 2 mM GlutaMAX, 0.1 mM sodium pyruvate (Invitrogen), 0.1 mM 2-mercaptoethanol (Sigma-Aldrich), and 1500 U/ml leukemia inhibitory factor (LIF, Millipore). ES cells were passaged every 2–3 days at with TrypLE Express (Invitrogen) at 1:10 ratio, along with daily medium changes.

Serum-Dependent Differentiation

For embryoid body differentiation, mouse ES cells were differentiated in ultra-low attachment dishes (Invitrogen) in GMEM supplemented with 20% FBS, 0.1 mM nonessential amino acids, 2 mM GlutaMAX, 0.1 mM sodium pyruvate (Invitrogen), 0.1 mM 2-mercaptoethanol (Sigma-Aldrich). Cells are plated at a density of 200,000 cells/ml, 10ml for 10cm dishes and 3ml for 6-well dishes. The media is half-changed every 3 days, and the embryoid bodies are transferred to gelatin coated dishes at day 7-8.

For hanging-drop differentiation, the same media is used. Cells are first suspended at a concentration of 250,000 cells/ml, then 20ul of the mixture is pipetted into each 96-well of a low-attachment V-bottom plate (Nunc). The plates are then inverted and placed into the incubator. The following day, plates are inverted back and 200ul of media is added to each well. Media is half changed at day 3 and 6, and replated onto gelatin coated dishes at day 7.

Serum-Free Differentiation

A detailed protocol of cardiac differentiation is included in the appendix. Briefly: ESCs were dissociated to single cells and plated on ultra-low attachment plastic surface (Corning) in IMDM/Ham-F12 (Cellgro) (3:1) supplemented with 1x N2, B27, penicillin/streptomycin, 2 mM GlutaMAX, 0.05% BSA, 5 ng/ml L-ascorbic acid (Sigma-Aldrich), and α -monothioglycerol (MTG, Sigma-Aldrich) at a final concentration of 75,000 cells/ml for two days. For the induction stage, EBs were collected and dissociated to single cells at 48 hours. Cells were resuspended in the same media supplemented with Activin A, BMP, VEGF, and/or Wnt and replated on ultra-low attachment plastic at a

concentration of 75,000 cells/ml. After the induction stage, cells were plated on gelatin-coated cell-culture plastic (Nunc) in StemPro34 (Invitrogen) supplemented with 10 ng/ml L-ascorbic acid, penicillin/streptomycin, 2 mM GlutaMAX, FGF (20 ng/ml), FGF10 (50 ng/ml) and VEGF (10 ng/ml) (All from R&D Systems).

Quantitative qRT-PCR

RNA was extracted with TRIzol (Invitrogen). Reverse transcriptase–quantitative PCR (qPCR) was performed using the Superscript III first-strand synthesis system (Invitrogen) followed by use of TaqMan probes on the ABI 7900HT (Applied Biosystems) according to the manufacturer's protocols. Optimized primers from TaqMan Gene Expression Array were used. Expression levels were normalized to Gapdh expression. All samples were run at least in triplicate. Real-time PCR data were normalized and standardized with SDS2.2 software.

FACS Analyses and Sorting

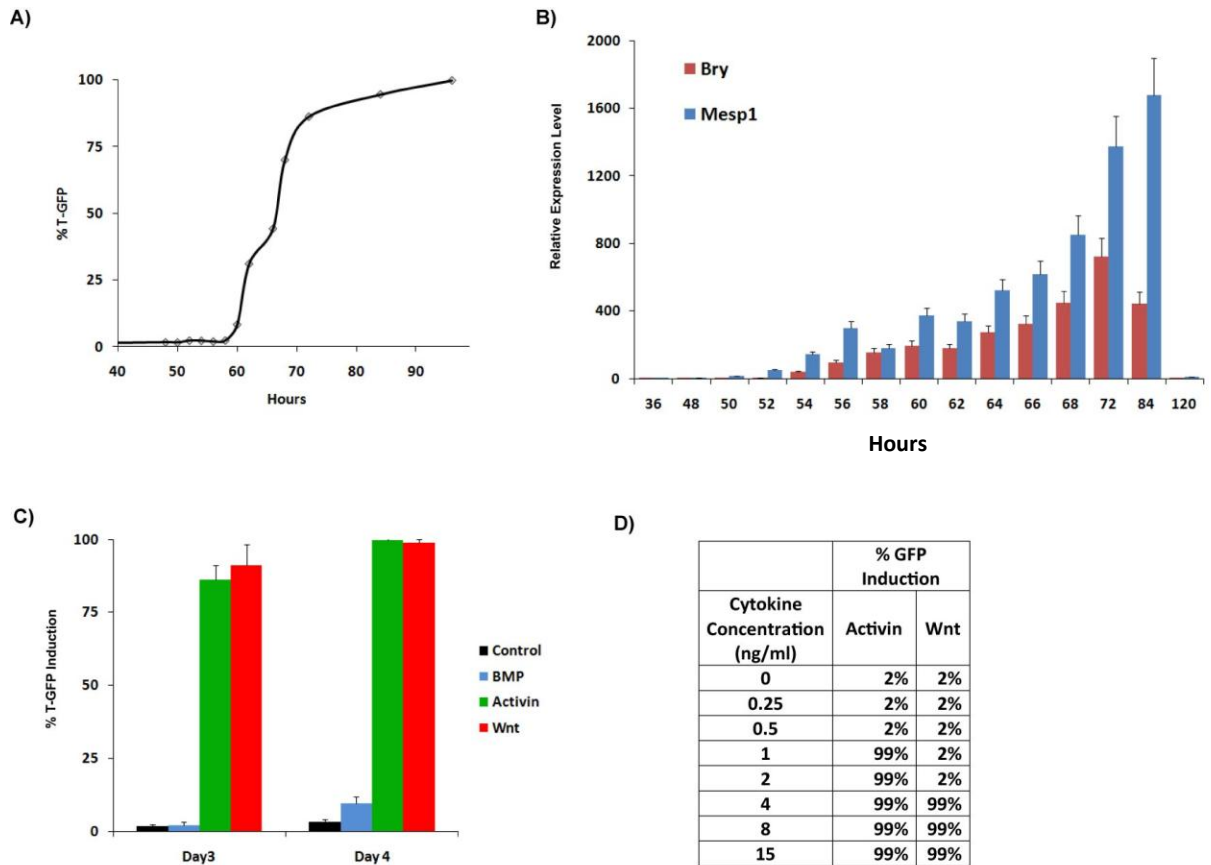
Cells were dissociated and percentages of GFP⁺ cells were analyzed with FACSCalibur (BD Biosciences) and FlowJo software. For FACS, cells were dissociated with trypsin and were resuspended in 0.1% FBS/20 mM Hepes/1 mM EDTA/PBS and sorted on a FACS Aria I or II (BD Biosciences).

2.5 Figure Legends

Figure 1: Induction Kinetics of Mesoderm

A) Number of cells induced as assayed by % of *Bry* (T)-GFP⁺ expression vs time during induction. B) Relative expression of *Bry* and *Mesp1* during serum-free differentiation. C) % of T-GFP⁺ cells induced at day 3 and 4 by nodal, wnt, and BMP. D) % T-GFP⁺ cells induced by increasing doses of Activin A and Wnt.

Figure 1



3. Fibronectin Mediates Mesendodermal Cell Fate Decisions

Abstract

Non-cell-autonomous signals often play critical roles in cell-fate decisions during animal development. Reciprocal signaling between endoderm and mesoderm is vital for embryonic development, yet the key signals and mechanisms remain unclear. Here, we show that early endoderm efficiently promotes the emergence of mesodermal cells in the neighboring population through a short-range signal. The endoderm-mesoderm interaction efficiently promoted precardiac mesoderm formation in embryonic stem cells and involved endodermal production of fibronectin. In vivo, fibronectin deficiency resulted in a dramatic reduction of mesoderm accompanied by endodermal expansion. This event was mediated by regulation of Wnt signaling in mesodermal cells through activation of Integrin $\beta 1$. Our findings highlight the importance of the extracellular matrix in mediating short-range signals and reveal a novel function of primitive endoderm involving fibronectin and its downstream signaling cascades in promoting the emergence of mesoderm.

Introduction

Cells that contribute to the heart arise from distinct pools of mesodermal progenitors during embryonic development and are typically characterized by expression of specific transcription factors⁵⁴. Several lineage-tracing studies have demonstrated the origin and location of distinct populations of precardiac mesodermal cells⁵⁵. The specification, fate, and expansion of cardiac mesodermal progenitors are controlled by diffusible morphogens, such as Wnt, Nodal, BMP, and FGF^{56,57}. Such non-cell-autonomous signals from early endoderm have long been implicated in the formation of cardiac progenitors^{50,58-60}. Furthermore, the function of transcription factors such as Gata4 and Sox17/18 in the endoderm are required for appropriate cell-cell signaling^{61,62}. However, the precise mechanisms by which endoderm-mesoderm communication occurs leading to the specification of precardiac mesoderm remain unclear.

The ability of embryonic stem (ES) cells to spontaneously differentiate into cardiomyocytes offers an opportunity to study non-cell autonomous signals *in vitro*, as co-culturing ES cells with primitive endoderm (PE)-like cells (End2 cells) is known to enhance cardiac differentiation^{63,64}. Conversely, loss of the endodermal HMG-box transcription factor Sox17/18 in ES cell culture suppresses cardiomyogenesis non-cell autonomously, but the suppression can be rescued by co-culturing ES cells with normal endodermal cells⁶².

Here we investigated the mechanism of primitive endoderm-mediated differentiation of the cardiac lineage and found that PE cells promote precardiac mesoderm through a short-range signal involving the extracellular matrix protein

fibronectin1 (Fn1). Fn1 in turn activated β -Catenin signaling through Integrin- β 1, and this signaling event biased cells toward the precardiac mesoderm fate.

Results

Primitive Endoderm Promotes the Emergence of Brachyury⁺ Mesoderm via a Short-Range Signal

Since endoderm has an inductive role for cardiogenesis^{58,63,64}, we investigated the range and nature of this inductive signal. Given the proximity of PE and nascent mesoderm during early development *in vivo*⁶⁵, we hypothesized that the induction of precardiac mesoderm requires close contact with PE. To test this hypothesis, mouse ES (mES) cells were differentiated by aggregation with or without End2 cells, or in End2 cell-conditioned medium. After 8 days of differentiation, 65% of embryoid bodies (EBs) co-cultured with End2 cells had beating foci, compared to 25% or 20% when co-cultured with mES cells alone or in conditioned medium, respectively (Figure 1A).

Correspondingly, the number of cardiomyocytes, marked by the sarcomeric protein cardiac Troponin T (cTnT), was fourfold greater in EBs formed with End2 cells, quantified by fluorescence-activated cell sorting (FACS) (Figure 1B). Furthermore, expression of genes encoding the cardiac transcription factor Nkx2.5, and the cardiac sarcomeric genes α -cardiac actin (*Actc1*) and myosin heavy chain 7 (*Myh7*) was significantly elevated upon co-aggregation with End2 cells (Figure 1C), compared to mES cells cultured alone or in conditioned medium. Increasing the ratio of End2 cells to

mES cells resulted in a dose-dependent increase in expression of *Actc1* and the cardiac transcription factor gene, *Hand2* (Figure S1A).

To test the relationship between cell-cell contact and mesoderm formation in cells exposed to the same medium, we mixed EBs formed from co-culture of mES cells stably expressing GFP (mES^{CAG-GFP}) and End2 cells, with EBs formed from unlabeled mES cells without End2 cells. After 8 days of differentiation in a mixed suspension culture, beating EBs were scored for fluorescence to determine the influence of End2 cells. The percentage of GFP⁺ EBs that was beating was fivefold greater than that of EBs cultured without End2 cells, consistent with the inductive effect of End2 cells being mediated by short-range rather than longer-range diffusible proteins (Figure S1B). End2 cells did not proliferate in EB suspension culture (Figure S1C), and treatment of End2 cells with mitomycin C to arrest cell division before co-culture did not affect their cardiogenic potency (data not shown).

One of the earliest lineage markers of mesodermal precursors is Brachyury (Bry), a T-box transcription factor expressed in the primitive streak/early mesoderm⁶⁶⁻⁶⁸. To determine if End2 cells affect the induction of Bry⁺ cells, we utilized an ES cell line with GFP knocked into the endogenous *Bry* locus (mES^{Bry-GFP})⁶⁹, and aggregated mES^{Bry-GFP} cells with End2 cells (1:1) to form EBs in suspension. EBs co-aggregated with End2 cells showed an increased percentage of Bry⁺ cells compared to control cells (Figure 1D, E). In addition, the co-aggregation resulted in increased induction of Bry⁺ cells in a dose-dependent manner, suggesting an inductive role of End2 at day 3 (Figure 1E-G). No induction was observed when mES^{Bry-GFP} cells were co-aggregated with ectodermal cells, or other mES cells (Figure 1H). To determine if nascent PE has a similar effect, mES^{Bry-}

GFP cells were co-aggregated at 10:1 ratio with nascent PE or extra-embryonic ectoderm (ExE) cells isolated by manual dissection from embryonic day E 6.5 mouse embryos. Similar to End2 cells, the isolated PE cells could induce *Bry*⁺ cells from mES^{*Bry-GFP*} cells, whereas ExE cells had no effect (Figure 1I, J).

Bry transiently marks mesendoderm, and *Bry*⁺ cells can give rise to a variety of different mesoendodermal lineages⁷⁰. By quantitative PCR (qPCR), we found that End2 cell-induced *Bry-GFP*⁺ cells, sorted at day 4 of differentiation, expressed markedly higher levels of *Mesp1*, the earliest marker for cardiovascular progenitors (Figure 2A), and the well-established precardiac mesoderm markers *Flk1* and *Pdgfra*^{42,48} compared to *Bry-GFP*⁺ cells isolated from normal ES cell differentiation (Figure 2B). In contrast, the endodermal HMG-box transcription factor *Sox17* was expressed at significantly lower levels compared to non-induced *Bry-GFP*⁺ cells (Figure 2C). To determine the fate of the End2 cell-induced *Bry-GFP*⁺ cells, FACS-isolated *Bry-GFP*⁺ cells at day 4 were replated and differentiated for 3 additional days in conditions that favor cardiac differentiation. Under these conditions, End2 cell-induced *Bry-GFP*⁺ cells formed a spontaneously contracting sheet of cardiomyocytes (Supplementary Video) with 50% of the cells staining positive for cardiac Troponin T (cTnT) (Figure 2D), compared to <5% in the control *Bry-GFP*⁺ cells, suggesting the endoderm-induced signal favors precardiac mesoderm.

To determine if End2 cells further improve cardiac differentiation after formation of precardiac mesoderm, we assayed if End2 cells affect the progression of precardiac mesoderm to *Nkx2.5*⁺ cardiac progenitors. Using an established combination of Activin A and BMP4^{71,72}, we induced precardiac mesoderm (*Bry*⁺/*Mesp1*⁺) at day 4 of

differentiation in mES^{Nkx2.5-GFP} cells carrying a GFP reporter in the *Nkx2.5* locus⁷³, followed by co-culture with End2 cells. Interestingly, co-culture with End2 cells at this later stage inhibited the progression of Bry⁺/Mesp1⁺-precardiac mesoderm cells into Nkx2.5⁺ progenitors (Figure 2E), suggesting that the inductive signal functions during a narrow window and does not act beyond precardiac mesoderm induction.

Fibronectin Promotes Emergence of *Brachyury*⁺ Mesoderm

Our earlier experiments suggest that the mesoderm-promoting signal from PE may have a short distance of action. We hypothesized that this effect was mediated via extracellular matrix (ECM) components secreted by the PE. To screen for ECM candidates responsible for the observed effect, we used ECM-specific gene-expression arrays to compare End2 cells with mES cells or ectodermal cells. We identified nine ECM genes whose transcripts were highly enriched (>4-fold) in End2 cells (Figure 3A). Of these genes, *Fibronectin1* (*Fn1*), *SPARC*, *collagen Ia1* (*Col1a1*), *collagen IVa1* (*Col4a1*), and *collagen IVa2* (*Col4a2*) were temporally expressed around egg-cylinder and gastrulation stages in mice, according to published EST profiles.

We examined the protein expression of these five genes in E6.5 mouse embryos by immunofluorescent staining and found they were spatially expressed in the PE, but not in the epiblast (Figure 3B). To determine if any of the candidate proteins were involved in inducing Bry⁺ mesoderm, we used siRNAs to knock down each candidate in End2 cells, and then co-cultured these End2 cells with mES^{Bry-GFP} cells. Knockdown efficacies were confirmed via qPCR (Figure S2A). We found that knockdown of Fn1 reduced the

formation of Bry-GFP⁺ cells by 50%, whereas knockdown of *SPARC*, *Colla1*, *Col4a1*, or *Col4a2* had no effect (Figure 3C). Loss of Fn1 did not alter End2 cells' ability to form Cadherin junctions or alter atypical Protein Kinase C (aPKC) localization. Furthermore, in EBs containing End2 cells with reduced fibronectin, we observed no increase in cell death, decrease in mesoderm proliferation, or increase in expression of pluripotent genes, suggesting a more specific defect in the emergence of Bry-GFP⁺ cells (Figure S2B-G). Similarly, blocking Fn1 activity by the addition of antibodies against extracellular Fn1 significantly reduced the appearance of Bry-GFP⁺ cells (Figure S2H). These data suggest that fibronectin plays a critical role during emergence of mesoderm.

To investigate if fibronectin also promoted the formation of Bry⁺ cells *in vivo*, we inactivated fibronectin in zebrafish embryos by injecting a morpholino-modified antisense oligonucleotide directed against *Fn1* and *Fn3* (MO-Fn1/Fn3)⁷⁴, as there are two *fibronectin* genes in zebrafish^{74,75}. As described previously⁷⁴, the fibronectin morphants had severe defects in somite boundary formation (data not shown), confirming the efficacy and specificity of the oligonucleotides. The resulting morphants showed no obvious developmental delays or perturbation in gastrulation. However, both the expression level and domain of the *Bry* orthologue in zebrafish, *no tail* (*ntl*), was markedly decreased at 50% epiboly, a stage equivalent to mid-gastrulation in mouse (Figure 3D). Expression of *Gooseoid* (*Gsc*), another mesodermal gene, was similarly decreased at late gastrulation (90% epiboly). (Figure 3E). At this stage, the decrease in the expression domain of *ntl* was less apparent (Figure S2I).

Given that early mesoderm is derived from mesendodermal progenitors⁷⁶, we tested whether the loss of fibronectin also affects endodermal cells *in vivo*. To accomplish this,

we injected MO-Fn1/Fn3 into transgenic zebrafish embryos expressing GFP under control of the Sox17 promoter, labeling endodermal cell populations⁷⁷. We observed expansion of the Sox17 expression domain at mid gastrulation (50% epiboly), with the Sox17-GFP⁺ domain 3-4 times larger than that of control (Figure 3F,G). Double-labeling of cells with *ntl* revealed the abnormal presence of Sox17-GFP⁺ cells within the expected *ntl* expression domain (Figure 3I). Following these Sox17-GFP⁺ cells revealed that at the 9-somite stage (around 12 hours post fertilization [hpf]), the expanded population of Sox17-GFP⁺ cells in the morphants followed a stereotyped endodermal migration and merge at the midline; however, the increase in number of Sox17-GFP⁺ cells was less dramatic at this point (Figure 3F, H). These results may reflect an expansion of endoderm at the expense of mesoderm and provide in-vivo evidence that fibronectin is involved in normal mesodermal cell fate specification.

Loss of Fibronectin Negatively Affects Precardiac Mesoderm

Loss of fibronectin results in cardiac defects in both mouse and zebrafish, presumably from cell migration abnormalities^{75,78}. To determine if fibronectin was also involved in proper emergence of cardiac progenitors, we performed siRNA knockdown of *Fn1* in End2 cells and co-cultured with mES^{Nkx2.5-GFP} cells. Depleting Fn1 in End2 cells significantly reduced the number of Nkx2.5-GFP⁺ cardiac progenitors by day 5 of differentiation (Figure 3J). We investigated whether the decrease in Nkx2.5⁺ progenitors was due to a general loss of mesoderm or specific loss of precardiac mesoderm. To address this, Bry-GFP⁺ cells were induced by End2 cells treated with control or *Fn1*

siRNA and the percentage of precardiac mesodermal cells, identified by co-expression of the surface markers Flk1 and Pdgfra⁴⁸, was analyzed among the resulting Bry-GFP⁺ cell populations by FACS. The number of Flk1⁺Pdgfra⁺ cells was reduced by 60% (from 25% to 11% of cells) in the Bry-GFP⁺ cell population induced by Fn1-deficient End2 cells (Figure 3K). In agreement with the reduction, the Bry-GFP⁺ cell population isolated from Fn1-deficient End2 cells differentiated poorly into cardiomyocytes under differentiation conditions favoring the cardiac lineage (cTnT⁺ cells) (Figure 3L, M). When sorted Bry-GFP⁺ cells were differentiated in a non-biased manner, we observed a decrease in several mesoderm derivatives, though the cardiac lineage was most adversely affected (Figure S3A). These data show that decreased levels of endodermal fibronectin resulted in fewer mesodermal cells, and a disproportionately smaller fraction of precardiac mesoderm. Similarly, in fibronectin-deficient zebrafish embryos, we observed a significant reduction in cardiac progenitors, as indicated by a decrease in Gata5⁺ cardiac primordia at the 10-somite stage, as well as a reduction of the myosin light chain 7 (myl7)⁺ cardiac domain at the 16-somite stage (Figure 3N, O). These results suggest that fibronectin promotes the emergence of Bry⁺ mesoderm, but also plays a specific role in the formation of precardiac mesoderm.

Fibronectin1/Integrin-β1/β-Catenin Signaling Promotes the Emergence of Mesoderm

Integrins often play a critical role in outside-in signaling mediated by extracellular matrix proteins⁷⁹. Since Integrin-β1 is known to mediate fibronectin signaling⁸⁰, we disrupted

the Fn1/Integrin- β 1 interaction by treating mES cells with Integrin- β 1-specific antibodies⁷⁹. This treatment efficiently inhibited the ability of End2 cells to induce Bry-GFP⁺ mesoderm, similar to that of anti-Fn1 antibodies (Figure 4A). Correspondingly, End2 cells were less effective in inducing Bry-GFP⁺ cells in mES cells expressing dominant negative Integrin- β 1^{79,81} (Figure S3B). These results suggest that Integrin- β 1 activation by fibronectin promotes emergence of mesoderm.

During somitogenesis, Integrin- β 1 activates Wnt/ β -Catenin signaling by phosphorylating and inactivating GSK-3 β resulting in accumulation of the active form of the transcriptional mediator, β -Catenin (active β -Catenin)⁸². We tested if an analogous Integrin- β 1-dependent cascade could affect Wnt/ β -Catenin signaling in mesoendodermal cells and thereby the emergence of Bry⁺ mesodermal cells. Introduction of Integrin- β 1-specific antibodies decreased protein levels of active β -Catenin and β -Catenin/TCF-dependent transcriptional activity (TOP-flash)⁸³ in Wnt3a-treated differentiating mES cells (Figure 4B, C). Similarly, FACS isolated mES^{CAG-GFP} cells co-cultured with End2 cells showed decreased levels of active β -Catenin in the presence of Integrin- β 1 antibodies (Figure 4C). Importantly, knockdown of *Fn1* also decreased End2-cell responsive accumulation of active β -Catenin in sorted mES cells (Figure 4C), suggesting Fn1/Integrin- β 1 signals positively regulate active β -Catenin levels.

Since activated Integrin can negatively regulate GSK3 β activity through Ser9 phosphorylation during somitogenesis⁸², we investigated whether the Fn1/Integrin β 1/ β -Catenin effect in the mesoderm also involved Gsk-3 β . Immunoblotting with an antibody specific for phosphorylated Gsk3 β revealed a decrease in Ser9p-GSK3 β upon cell-non-autonomous loss of fibronectin (Figure 4D). Consistent with the epistatic relationship of

this model, addition of GSK-3 β inhibitor BIO at day 2 of differentiation to mES cells co-cultured with *Fnl*-deficient End2 cells can rescue the *Bry* induction defects caused by *Fnl* knockdown; whereas addition of soluble Wnt3a, which acts upstream of Gsk3 β , increased the absolute number of *Bry*⁺ cells but could not rescue the relative defect in induction (Figure 4E). Lastly, we tested our model in zebrafish and saw that the expression domain of *ntl* was restored *in vivo* when BIO was added to fibronectin morphants at 2.5 hpf (Figure 4F). Together, these results suggest that the PE regulates mesoderm formation through a fibronectin/Integrin- β 1/ β -Catenin signaling cascade.

Discussion

In this study, we demonstrate a previously unrecognized function of PE in the development of mesoderm, involving the extracellular matrix component fibronectin. We found that fibronectin signals through Integrin- β 1 and promotes Wnt/ β -Catenin signaling to promote the mesodermal fate, with a specific bias towards precardiac mesoderm. Loss of fibronectin resulted in impaired mesoderm induction both *in vitro* and *in vivo* and could be rescued by activating β -Catenin signaling. These findings address a fundamental aspect of developmental biology regarding cell-cell interactions during early specification.

Fibronectin regulation of endoderm vs. mesoderm cell fate

In vivo, fibronectin has a critical role during early development^{74,78}. The reported defects upon loss-of-function, such as boundary formation and cell migration, suggest a predominantly structural role of fibronectin during the period of somitogenesis. In zebrafish, for example, disruption of fibronectin-integrin interaction ablates somite boundary formation⁷⁴ and results in cardiac bifida secondary to a migration defect and impaired epithelial organization of the differentiated myocardial progenitors⁷⁵. However, our results suggest that fibronectin also has a morphogenic signaling function that precedes its structural role. Fibronectin-deficient zebrafish morphants showed a significantly reduced expression domain and level of mesodermal markers *ntl* and *gsc* during gastrulation, coupled with an expanded domain of endoderm. Thus, the initial defect in zebrafish fibronectin morphants occurs as early as the initiation of gastrulation, much earlier than previously recognized.

These observations suggest a model for the mesoderm vs. endoderm decision in mesendodermal progenitors. Mesendoderm progenitors are initially defaulted to the endodermal lineage. Stochastic differentiation is thought to drive a sub-population into PE, self-organizing based on cadherin-mediated sorting⁸⁴. Upon secretion of fibronectin, endodermal cells appear to instruct unspecified neighboring cells to adopt the mesodermal fate by promoting Wnt signaling. Whether there is also active inhibition of the endoderm fate in cells receiving the Wnt signal, akin to lateral inhibition, remains to be determined.

Contact-mediated signaling during early specification

Our findings may address an interesting conundrum in evolutionary developmental biology. Morphogenesis during development is thought to be governed by conserved three-dimensional signal gradients. Yet events prior to organogenesis vary widely in both shape and motion from one species to another. While the gastrula differ in their shape, the effect of signal gradients that induce and specify mesoderm, such as Wnt, FGF, Nodal, and BMP is highly conserved^{57,85}.

One unifying explanation of this phenomenon may be the existence of a non-diffusible, yet conserved, regulator of gastrulation that robustly signals independent of the three-dimensional structure and gradient. It is interesting to note that in spite of the different gastrulating motion and architecture across vertebrates, initiation of mesoderm always occurs adjacent to endoderm. The fibronectin matrix between PE and mesoderm is conserved from mammals to sea urchins⁸⁶. Also conserved is the manner in which gastrulating mesoderm migrates through the secreted fibronectin matrix. Such high degree of conservation combined with the novel signaling role uncovered in our study suggest that fibronectin may be a key mediator of gastrulating cells' response to diffusible cues in a localized fashion.

An interesting question raised by this study is the specificity of fibronectin in its signaling role. While Integrin- $\alpha5\beta1$ is thought to be the primary receptor of fibronectin, mice lacking Integrin- $\alpha5$ have less severe developmental defects than mice lacking fibronectin⁸⁷. This is frequently explained by the ability of ECM components to activate multiple integrin dimers. Complete loss of Integrin- $\beta1$ signaling results in embryonic

lethality as early as E6.5⁸⁸. The observation that zebrafish fibronectin morphants initiate gastrulation normally implies that integrins are at least partially activated despite fibronectin knockdown. Redundant mechanisms of integrin activation may explain the partial rescue of *ntl* expression. However, the rescue remains incomplete, as evidenced by the persistence of endoderm expansion and other mesodermal defects, including the decrease in *gsc* expression and disproportional loss of cardiac progenitors *in vitro* and *in vivo*⁷⁵. The integrin-signaling involved in normal gastrulation movement, therefore, appears to be distinct from that of specification and determination of mesoderm. The latter involves fibronectin specifically. The source of this specificity warrants further studies.

ECM-mediated activation of Wnt and Brachyury

We demonstrated that the fibronectin-integrin interaction promoted mesoderm formation at least in part through Wnt signaling. The decrease in mesoderm upon disruption of fibronectin-integrin interaction was rescued by exogenous inhibition of Gsk-3 β activity. These findings are consistent with previous findings in somites where Integrin- β 1 acts upstream of Wnt signaling and activates Wnt signaling through GSK-3 β phosphorylation⁸².

Wnt/ β -Catenin signaling has biphasic roles during cardiac development. Early activation of Wnt/ β -Catenin signaling directly regulates *Bry* expression⁸⁹ and is required for mesoderm formation, while Wnt signaling suppresses initial induction of Nkx2.5⁺ cardiac progenitors, before positively regulating further expansion of cardiac progenitors

^{50,51,90}. This is consistent with the biphasic role of fibronectin observed in our study. Interestingly, Wnt/ β -Catenin signaling has been reported to regulate expression of ECM components, including fibronectin ⁹¹. This suggests a potential positive feedback loop for activation and propagation of Wnt signaling. It will be interesting to determine whether such ECM-mediated spatial localization of signal response is a more commonly used mechanism in cell specification during development and adulthood.

Methods

Cell culture and differentiation

Mouse ES cells were propagated in an undifferentiated state on gelatin-coated cell culture plastic (Nunc) in GMEM supplemented with 10% FBS, 0.1 mM nonessential amino acids, 2 mM GlutaMAX, 0.1 mM sodium pyruvate (Invitrogen), 0.1 mM 2-mercaptoethanol (Sigma-Aldrich), and 1500 U/ml leukemia inhibitory factor (LIF, Millipore). ES cells were passaged every 2–3 days with TrypLE Express (Invitrogen) with daily medium changes.

For co-culture experiments, ES cells and End2 cells were dissociated to single cells and plated on ultra-low attachment plastic surface (Corning) in IMDM/Ham-F12 (Cellgro) (3:1) supplemented with N2, B27, penicillin/streptomycin, 2 mM GlutaMAX, 0.05% BSA, 5 ng/ml L-ascorbic acid (Sigma-Aldrich), and α -monothioglycerol (MTG, Sigma-Aldrich) at final concentration of 75,000 cells/ml.

For cardiac mesoderm induction, cells were propagated as described above (75,000 cells/ml) for 48 h. EBs were collected and dissociated to single cells. Cells were replated on ultra-low attachment plastic surface as described above and induced for 40 h with Activin A (5 ng/ml), BMP4 (0.5 ng/ml) and VEGF (10 ng/ml).

For cardiac differentiation, GFP⁺ cells from co-cultures were plated on gelatin-coated cell-culture plastic (Nunc) in StemPro34 (Invitrogen) supplemented with 10 ng/ml L-ascorbic acid, penicillin/streptomycin, 2 mM GlutaMAX, FGF (20 ng/ml), FGF10 (50 ng/ml) and VEGF (10 ng/ml) (All from R&D Systems). Unbiased differentiation was done by growing EBs in 20% FBS in GMEM supplemented with 2 mM Glutamax and 0.1 mM non-essential amino acid.

For Top/Fop-flash luciferase assays, transfected mESCs were treated with 20 ng/ml Wnt3A, 2 μ M BIO and/or anti-CD29 (BD Biosciences) for 24 h before analysis. Top/Fop-flash luciferase constructs were kindly provided by Randall Moon (University of Washington, WA).

ES^{Bry-GFP} cells were a kind gift from G. Keller (McEwen Centre for Regenerative Medicine, Toronto, Canada). ES^{Nkx2.5-GFP} cells were generated from the mouse E14 ESC cell line, carrying the RP11-88L12/NKX2-5-Emerald GFP as described⁷³. The ES^{GFP} cell line is a variant of the E14 line that expresses GFP under control of the CMV/ β -actin (CAG) promoter. All mES cells used in this study were E14 derivatives. NSCs were obtained from ATCC. End2 cells were a kind gift from Christine Mummery (Leiden University Medical Centre, Leiden, Netherlands).

Isolation of Primitive Endoderm and Extra-Embryonic Ectoderm

Primitive endoderm (PE) and extra-embryonic ectoderm (ExE) were isolated from 20 embryos by micro-dissection of E6.5 embryos. PE and ExE were dissociated into single cells and co-cultured with ES^{Bry-GFP} cells in a 1:10 ratio.

Quantitative qRT-PCR

RNA was extracted with TRIzol (Invitrogen). Reverse transcriptase–quantitative PCR (qPCR) was performed using the Superscript III first-strand synthesis system (Invitrogen) followed by use of TaqMan probes on the ABI 7900HT (Applied Biosystems) according to the manufacturer's protocols. Optimized primers from TaqMan Gene Expression Array were used. Expression levels were normalized to Gapdh expression. All samples were run at least in triplicate. Real-time PCR data were normalized and standardized with SDS2.2 software.

FACS Analyses and Sorting

Cells were dissociated and percentages of GFP⁺ and cTnT⁺ cells were analyzed with FACSCalibur (BD Biosciences) and FlowJo software. For cTnT expression, cells were incubated with anti-cTnT antibody (Neomarkers) followed by incubation with secondary antibody conjugated with Alexa 647 (Invitrogen). For FACS, cells were dissociated as described above. Cells were resuspended in 0.1% FBS/20 mM HEPES/1 mM EDTA/PBS

and sorted on a FACSAria I or II (BD Biosciences). FACS analyses were performed on days indicated in figures.

SiRNA Knockdown Studies, Antibody Targeted Inhibition of Itgb1 and Fibronectin

For knockdown studies, ON-TARGET smartpools of fibronectin siRNA, Collagen 1A1, Collagen 4A1, Collagen 4A2, Sparc siRNA, scrambled siRNA (Dharmacon), or Block-iT Alexa Fluor Red (Invitrogen) were used at a concentration of 75 nM. End2 cells were transfected using LipofectamineRNAiMAX (Invitrogen) 24h before co-culture experiments. For antibody inhibition studies, anti-CD29 (BD Biosciences) or anti-fibronectin (Hybridoma Bank) was added from start of the experiment in the concentrations described.

Embryo Immunostaining

E6.75 embryo cryosections were stained with anti-fibronectin, anti-collagen1, anti-collagen IV or anti-Sparc, followed by incubation with secondary antibodies conjugated with Alexa 488 and 546 (Invitrogen).

Mouse Extracellular Matrix (ECM) PCR Array

The ECM RT² Profiler™ PCR Array (PAMM-013) was obtained from SABiosciences. The following samples were used: 1) ES^{CAG-GFP} cells; 2) ES^{CAG-GFP} cells that had been

differentiated with End2 cell co-culture for 2.5 days and sorted by FACS; 3) NSCs; 4) End2 cells from condition (2) that were negatively sorted by FACS to remove ES cells; and 5) End2 cells. RNA was extracted with TRIzol (Invitrogen). Reverse qPCR was performed using the Superscript III first-strand synthesis system (Invitrogen). The ECM RT² Profiler™ PCR Array was run on the ABI 7900HT (Applied Biosystems) according to the manufacturer's instructions. Data from condition (4) and (5) were compared to conditions (1-3). Results were analyzed and visualized using software provided from the manufacturer with the arrays.

Western Blotting

Cell lysate was resolved by SDS-PAGE and electroblotted onto PVDF membranes. The membranes were incubated with primary antibodies in 5% nonfat milk overnight at 4°C, and secondary antibodies for 1 h at room temperature. The chemiluminescence detection method was used for western blot experiments.

Zebrafish studies

Zebrafish *Danio rerio* care and breeding was carried out as described previously⁹². For *in vivo* knockdown studies in zebrafish, previously described morpholino-modified antisense oligonucleotides against the translational start sites of zebrafish fibronectin 1 (MO-Fn1: 5' - TTTTTTCACAGGTGCGATTGAACAC - 3')⁷⁵ and of zebrafish

fibronectin 3 (MO-fn3: 5' - TACTGACTCACGGGTCATTTTCACC - 3')⁷⁴ individually (6–8 ng) or in combination were injected into one-cell-stage embryos.

Whole-mount in situ hybridization of stage matched zebrafish embryos was carried out as described⁹³. Embryos were all staged before the procedure as described⁹⁴.

Zebrafish *ntl* and *gsc*, expression vectors used as templates for digoxigenin-labeled RNA antisense probe synthesis were kindly provided by D. Stainier (University of California, San Francisco).

Statistical Analyses

The two-tailed Student's *t*-test, type II, was used for data analyses. $P < 0.05$ was considered significant.

ACKNOWLEDGEMENTS

We thank G. Keller for ES^{Bry-GFP} cells; C. Mummery for End2 cells; D. Stainier for transgenic Sox17^{GFP} zebrafish and use of the zebrafish facility; R. Ross for Tacβ1 constructs; K. Tomoda for mouse embryo sections; and members of the Srivastava and Kwon labs for thoughtful discussions. We also thank S. Elmes from the UCSF Flow Core for cell sorting; G. Howard and S. Ordway for editorial assistance; B. Taylor for assistance with manuscript and figure preparation; and B. Bruneau for critical reading of the manuscript.

Figure Legends

Figure 1: Primitive Endoderm-like (End2) Cells Promotes the Emergence of Mesoderm in Embryonic Stem Cells Through a Short-Range Signal

(A, B, C) Co-aggregation of ES cells with End2 cells during embryoid body (EB) differentiation resulted in increases in (A) number of EBs with beating foci, (B) % of cardiac troponin T (cTnT)⁺ cells as well as (C) cardiac gene expression. Improvement in cardiac induction was not observed in EB differentiation with End2 conditioned medium. (D, E) % of Brachyury (Bry)-GFP⁺ mesodermal cells in EBs differentiated with End2 cells or End2 conditioned medium. (F) FACS plot of Bry-GFP⁺ cells at day 3 in EBs differentiated with increasing ratios of End2 cell co-culture, quantified in (G). (H) % of Bry-GFP⁺ cells at day 3 in co-culture of ES cells with End2 cells, neural stem cells (NSCs) or other mES cells (E14 ESC). (I, J) FACS plot and quantification of Bry-GFP⁺ cells at day 3 in co-culture with smaller numbers of dissected nascent PE, End2 cells, or dissected extra-embryonic endoderm (ExE) from E6.5 embryos at 10:1 (mESC : PE/End2/ExE) ratio. *P<0.05, n≥5 for all experiments. Error bars indicate standard error of biological replicates.

Figure 2: End2-Induced Mesoderm is Biased Toward Precardiac Mesoderm

(A) Relative *Mesp1* expression in Bry-GFP⁺ cells isolated from ES^{Bry-GFP} cells at day 4 with or without control or End2 cell co-culture. (B) Relative number of Flk1⁺/PDGFRα⁺

cells among Bry-GFP⁺ cells isolated from control or End2 co-culture. (C) Relative Sox17 expression in Bry-GFP⁺ cells isolated at day 4 from ES^{Bry-GFP} cells with or without End2 cell co-culture. (D) % of cTnT⁺ cells at day 8 from Bry-GFP⁺ or Bry-GFP⁻ cells isolated from control or End2 co-culture conditions. (E) Percentage of GFP⁺ cells derived from ES^{Nkx2.5-GFP} cells differentiated into pre-cardiac mesoderm that was then co-cultured with End2 or control cells as illustrated. *P<0.05, n≥5. Error bars indicate standard error of biological replicates.

Figure 3: Fibronectin Promotes End2-Mediated Induction of Mesoderm and Pre-cardiac Mesoderm *in vitro* and *in vivo*

(A) Volcano plot of ECM expression array comparing End2 vs. control cells. (B) E6.5 transverse embryo sections immunostained for Fn1, Col4, Col1, or SPARC; arrows indicate visceral endoderm and arrowheads indicate epiblast. (C) Bry-GFP⁺ cells induced by co-culturing ES^{Bry-GFP} cells with End2 cells containing siRNA knockdown of Fn1, Col4A2, Col4A1, Col1A1 or SPARC. (D) *ntl* expression by in situ hybridization in zebrafish embryos injected with control or Fn1/Fn3 morpholinos (MO) at mid-gastrulation (50% epiboly, dorsolateral view, animal pole on top). (E) *gsc* expression by in situ hybridization in zebrafish embryos injected with control or FN1/3 MO at late gastrulation (90% epiboly, dorsal view, animal pole on top). (F) GFP expression in transgenic Sox17-GFP zebrafish embryos injected with control or Fn1/Fn3 MO at 50% epiboly (5.5 hpf, dorsal view, animal pole to the top) and 9-somite stage (12 hpf, dorsal

view, anterior to the left). (G) Relative number of Sox17-GFP⁺ cells at 50% epiboly (5.5 hpf) in control or Fn1/Fn3 MO injected zebrafish embryos. (H) Relative number of Sox17-GFP⁺ cells at 9-somite stage (12 hpf) in control or Fn1/Fn3 MO injected zebrafish embryos. (I) Sagittal section of control or MO-Fn1/Fn3 morphant sox17-GFP zebrafish embryos at 50% epiboly (5.5 hpf) after *in situ* hybridization for expression of *ntl* (black); immunofluorescence indicates sox17-GFP⁺ cells in the *ntl* expression domain after Fn knockdown. (J) % of GFP⁺ cells induced in ES^{Nkx2.5-GFP} cells at day 6 by co-culture with control or fibronectin-deficient End2 cells. (K) Relative number of Flk1⁺/PDGFR α ⁺ precardiac mesoderm cells induced at day 4 by control or fibronectin-deficient End2 cells. (L) cTnT staining of day 8 replated Bry-GFP⁺ mesoderm isolated from co-culture of ES^{Bry-GFP} cells with control End2 or Fn1-deficient End2 cells at day 4. (M) % cTnT⁺ cells in (L) quantified by FACS. (N) Dorsal views of *gata5* expression in zebrafish embryos at the 10 somite stage, assayed by *in situ* hybridization, after control or Fn1/Fn3 knockdown. pcm, pre-cardiac mesoderm; lpm, lateral plate mesoderm. (O) Dorsal views of *myl7* expression in zebrafish embryos at 16 somites stage, assayed via *in situ* hybridization, after control or Fn1/Fn3 knockdown. Cardiac progenitors are indicated with arrows. *P<0.05, n \geq 5. Error bars indicate standard error of biological replicates.

Figure 4: Fibronectin Augments Mesoderm Induction Through Integrin-Dependent Activation of Wnt/ β -Catenin Signaling

(A) Percentage of Bry-GFP⁺ cells induced in day 4 embryoid bodies (EBs) cultured with control (IgG) or anti-Integrin- β 1 (Itgb1) antibody. (B) Relative luciferase activity from a β -Catenin/TCF responsive luciferase construct (TOP-Flash), in day 3 EBs with IgG or anti-Itgb1 antibody. White bar indicates luciferase reporter with mutation in the TCF-binding site (FOP-Flash). (C) Western analysis for active β -Catenin in day 3 EBs exposed to Wnt3a or End2 co-culture in the presence or absence of Integrin inhibition with anti-Itgb1 or *Fn1* knockdown. (D) Western analysis for Ser9-phosphorylated GSK3B in GFP⁺ cells sorted from ES^{CAG-GFP} cells co-cultured with control or Fn1-deficient End2 cells at day 3. (E) Relative number of Bry-GFP⁺ mesoderm cells induced by control or Fn1-deficient End2 cells, with or without Wnt3a or the Wnt agonist BIO. (F) In situ hybridization for *ntl* expression in zebrafish embryos deficient in Fn1 and Fn3 (MO-Fn1/Fn3) at mid-gastrulation (dorsolateral view, animal pole to the top). The expression domain was rescued by ectopic activation of Wnt signaling via addition of BIO to egg water at 0.5 μ M at 2.5 hpf. *P<0.05, n \geq 5. Error bars indicate standard error of biological replicates.

Supplementary Figure 1

(A) Relative expression of cardiac genes *actc1* and *hand2* in embryoid bodies (EBs) formed with increasing ratios of End2 cells compared to ES cells (ESCs). (B) % of observed beating foci with (green/red) or without (yellow) End2 cells in a mixed culture of EBs formed with or without End2 cells. (C) Number of mES cells and End2 cells at day 0 and after five days of co-culture.

Supplementary Figure 2

(A) Knockdown efficiency of indicated siRNA molecules assayed by qPCR. (B) End2 cells 48h after transfection with scrambled siRNA or siRNA against Fn1, stained for Fn1 (green) and β -Catenin (red). (C) End2 cells 48hr after transfection with scrambled siRNA or siRNA against Fn1, stained for pan-Cadherin (green) and aPKC (red). (D) Embryoid bodies containing End2 cells transfected with scrambled siRNA or siRNA against Fn1, stained for pan-Cadherin (green) and aPKC (red). (E) FACS analysis of cell-proliferation as assayed by Ki-67 or phosphohistone H3 (PH3) staining among Bry-GFP⁺ cells in EBs aggregated with control or fibronectin-deficient End2 cells. (F) FACS analysis of cell-death as assayed by PI⁺ and AnnexinV staining among Bry-GFP⁺ populations in EBs aggregated with control or fibronectin-deficient End2 cells. (G) Expression of pluripotent genes Oct4 and Nanog in Day 2 EBs with control or Fn1-deficient End2 cells. (H) Percentage of Bry-GFP⁺ cells in day 4 embryoid bodies (EBs) cultured with End2 cells with control (IgG) or anti-Fn1 antibody. (I) Whole-mount in situ hybridization of *ntl* in

control or Fn1/Fn3 knockdown (MO-Fn1/Fn3) zebrafish embryos at 90% epiboly (9 hpf).

* $P < 0.05$, error bar indicate standard error.

Supplementary Figure 3

(A) Expression of various mesodermal markers in cells differentiated from Bry-GFP⁺ cells isolated from EBs with control or fibronectin (Fn1)-deficient End2 cells. (B)

Relative number of Bry-GFP⁺ cells induced by End2 cells in mES^{Bry-GFP} cells with the integrin signaling mutant TAC β 1 or control (lacZ). * $P < 0.05$, n=3 or greater. Error bars indicate standard error.

Figure 1

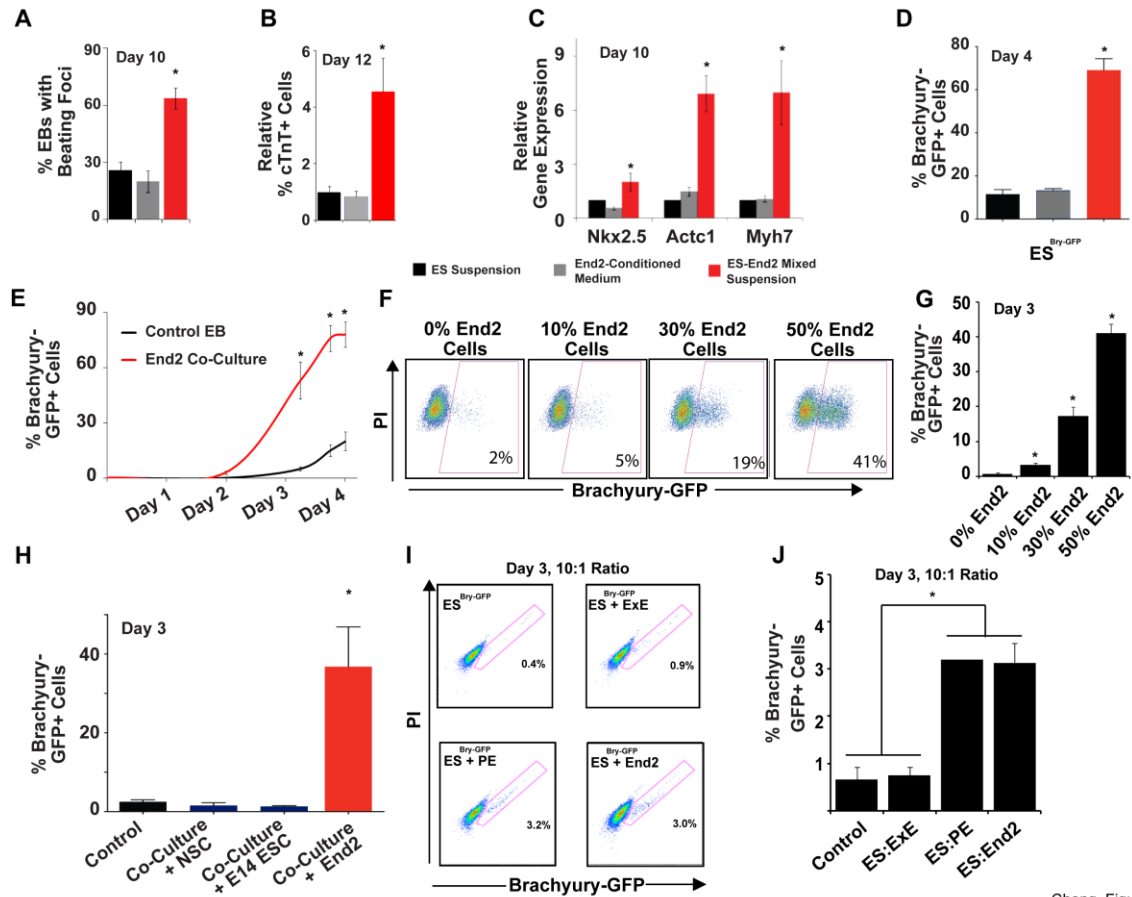
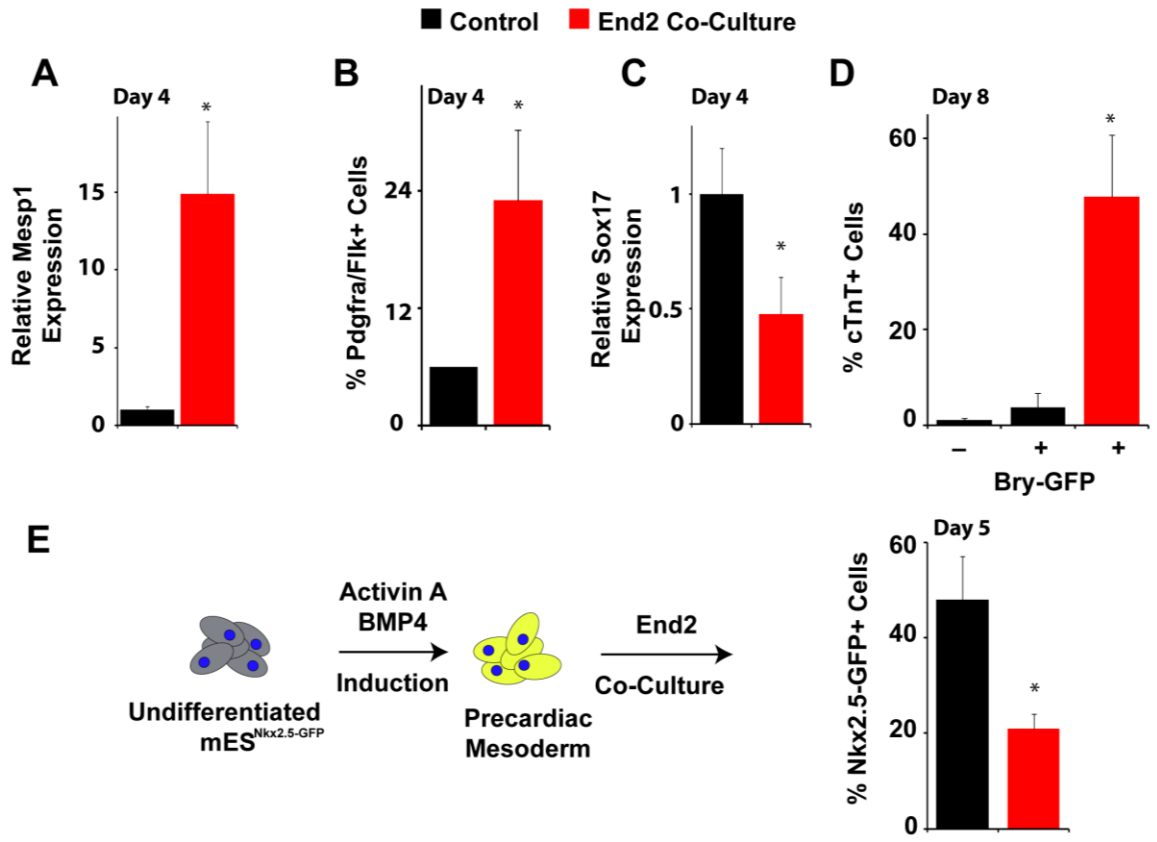


Figure 2



Cheng, Figure 2

Figure 3

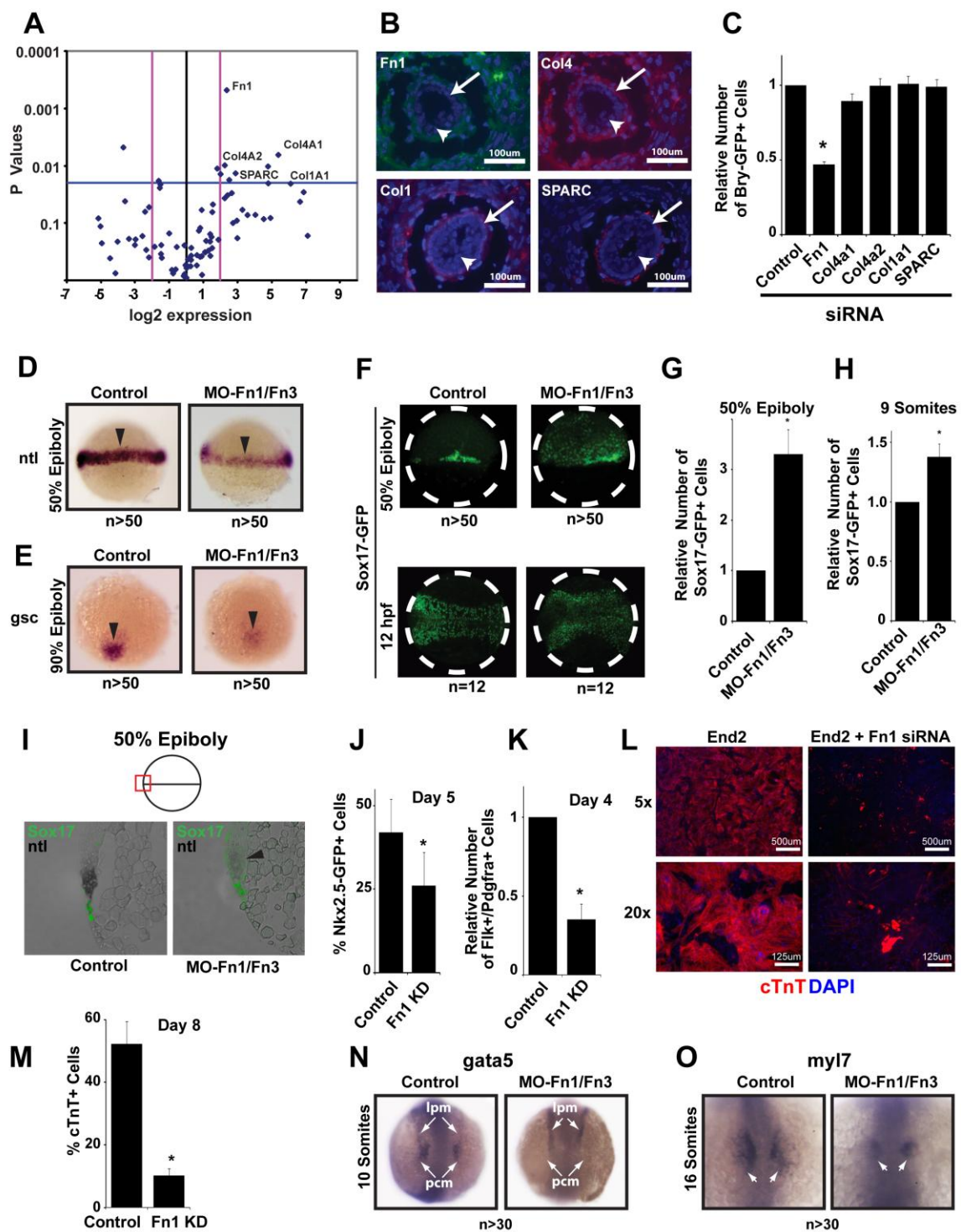


Figure 4

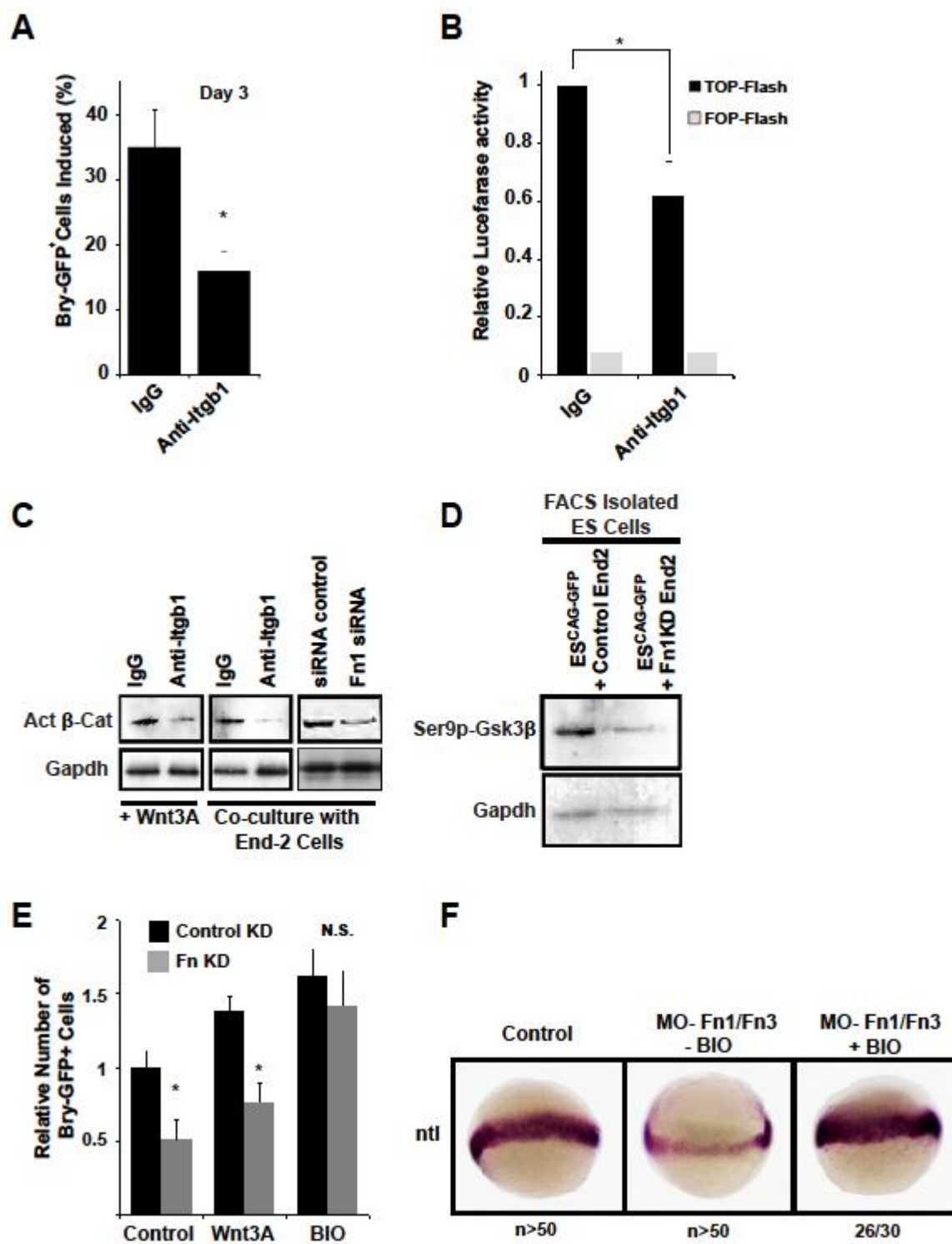


Figure S1

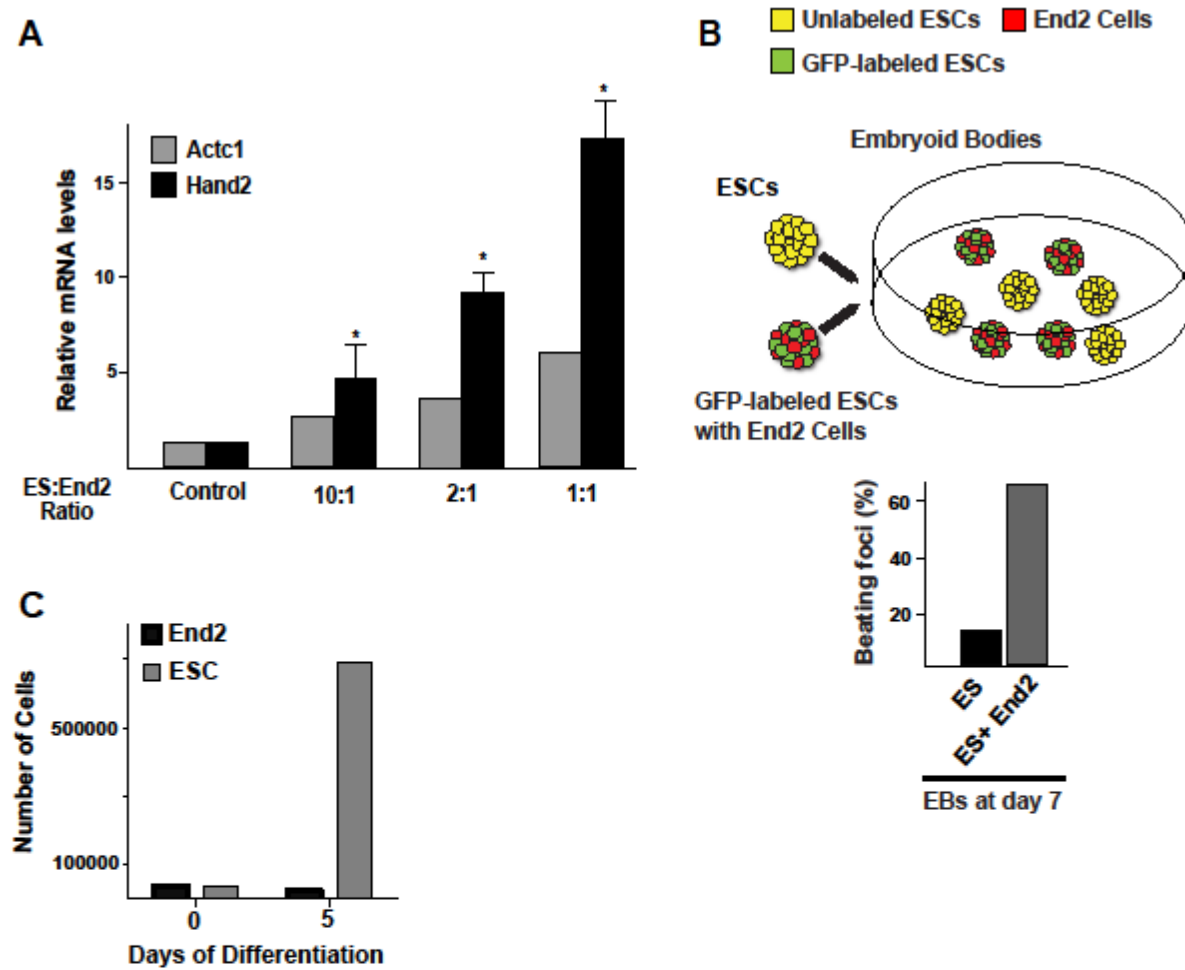


Figure S2

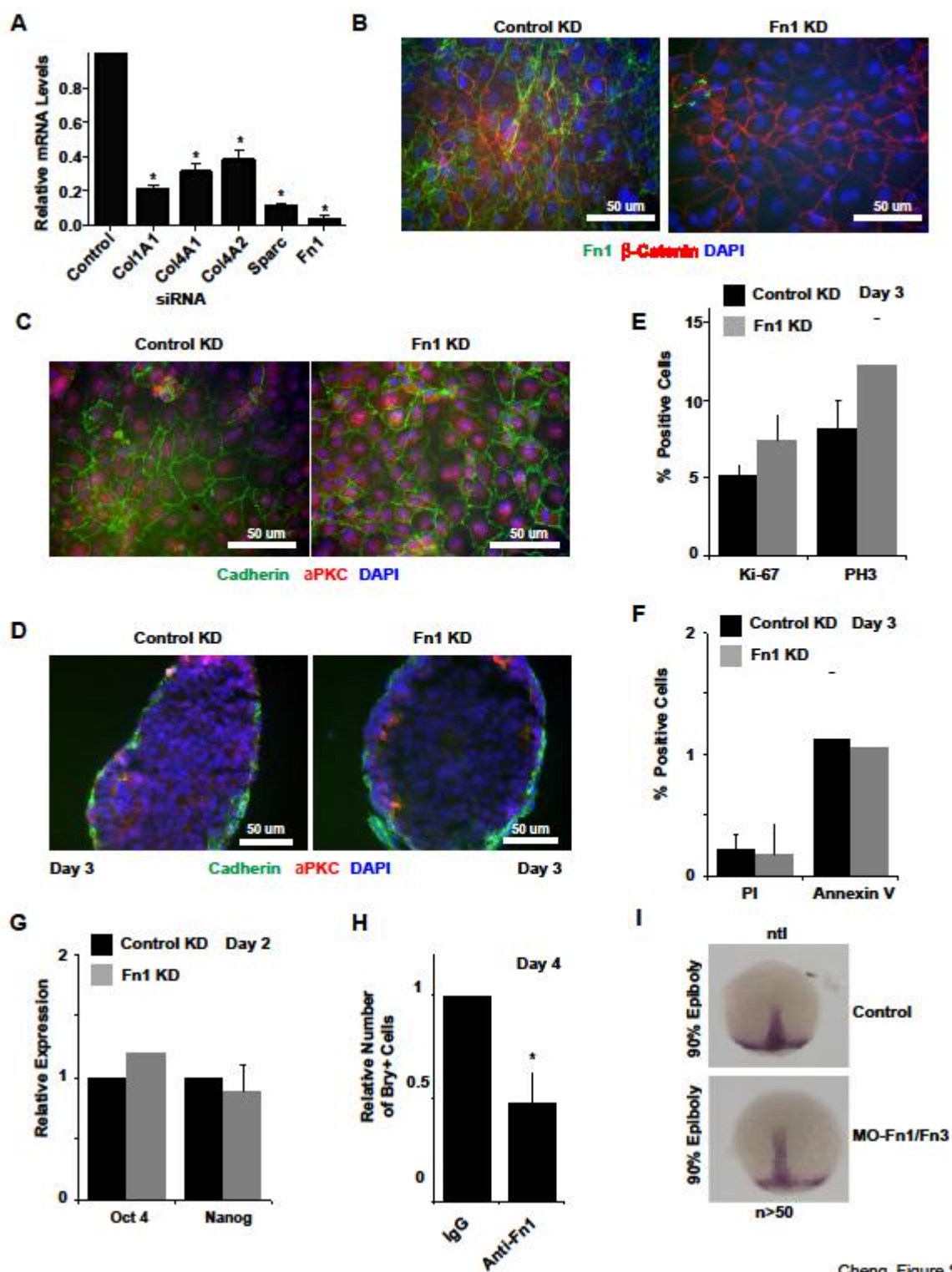
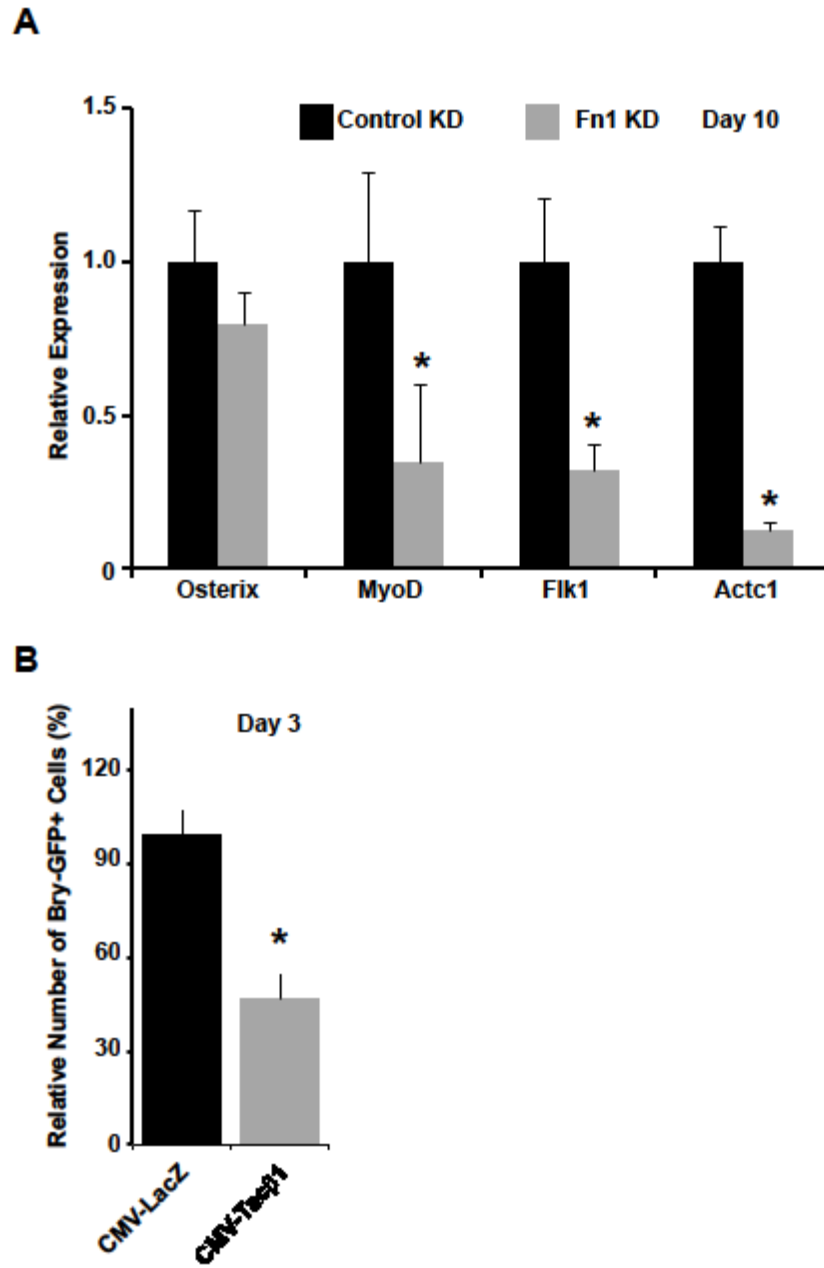


Figure S3



4. A Regulatory Pathway Involving Notch1/ β -Catenin/Is11 Determines Cardiac Progenitor Cell Fate

Abstract

The regulation of multipotent cardiac progenitor cell (CPC) expansion and subsequent differentiation into cardiomyocytes, smooth muscle, or endothelial cells is a fundamental aspect of basic cardiovascular biology and cardiac regenerative medicine. However, the mechanisms governing these decisions remain unclear. Here, we show that Wnt/ β -Catenin signaling, which promotes expansion of CPCs^{51,95,96}, is negatively regulated by Notch1-mediated control of phosphorylated β -Catenin accumulation within CPCs, and that Notch1 activity in CPCs is required for their differentiation. Notch1 positively, and β -Catenin negatively, regulated expression of the cardiac transcription factors, *Isl1*, *Myocd* and *Smyd1*. Surprisingly, disruption of *Isl1*, normally expressed transiently in CPCs prior to their differentiation⁹⁷, resulted in expansion of CPCs in vivo and in an embryonic stem (ES) cell system. Furthermore, *Isl1* was required for CPC differentiation into cardiomyocyte and smooth muscle cells, but not endothelial cells. These findings reveal a regulatory network controlling CPC expansion and cell fate that involve unanticipated functions of β -Catenin, Notch1 and *Isl1* that may be leveraged for regenerative approaches involving CPCs.

Introduction

Heart malformation is the most frequent form of human birth defects and heart disease remains the number one killer of adults in the developed world, largely because of the limited regenerative capacity of the heart. Recent advances have provided insights into potential therapies based on multipotent cardiac progenitor cells (CPCs). Such CPCs can be isolated from early embryos or embryonic stem (ES) cells and cultured to differentiate into numerous cardiac cell types^{46,54,55,71,72,97-100}. For instance, *Nkx2.5*⁺, *Flk1*⁺ or *Isl1*⁺ CPCs purified from embryoid bodies (EBs) can each give rise to cardiomyocyte, endothelial, and smooth muscle lineages^{46,71,98,100}.

Nkx2.5 is an ancient cardiac gene activated in CPCs of early embryos¹⁰¹. *Nkx2.5*⁺ cells and their progeny populate the precardiac mesoderm located dorsal to the cardiac region and the developing heart tube in vivo¹⁰². Isolated *Nkx2.5*⁺ cells spontaneously differentiate into distinct cardiac cell lineages including cardiomyocytes, smooth muscle cells and endothelial cells in vitro^{46,100}. These cardiac cell lineages can also be generated from cells expressing *Flk1*, a marker of the primitive streak in early embryogenesis⁷¹ or *Isl1*, a CPC marker^{98, 45}. All of these CPCs exhibit overlapping expression patterns in precardiac mesodermal cells in vivo⁹⁸ and have similar differentiation potential in vitro^{46,71,98,100}, suggesting that they comprise a similar CPC population. Although these multipotent CPCs hold great potential for cardiac repair, the mechanisms that regulate their self-renewal, expansion, and differentiation remain elusive.

We, and others, recently reported that canonical Wnt signaling is a critical regulator of *Nkx2.5*⁺ and *Isl1*⁺ CPCs and is responsible for their expansion in vivo and in

vitro^{51,95,96}. The inactivation of β -Catenin, the transcriptional mediator of canonical Wnt signaling, in precardiac mesoderm resulted in nearly complete loss of Isl1 cells that contribute to the right ventricle⁵¹. Conversely, stabilization of β -Catenin in the same cells led to an expansion in the number of CPCs⁵¹ in vivo, while Wnt/ β -Catenin signaling promoted the renewal of CPCs isolated from ES cells^{51,96}. Notch signaling reciprocally affects Wnt signals in many contexts¹⁰³ and is thought to inhibit cardiac differentiation^{104,105}, although its function within CPCs in vivo is unknown. Ultimately, these and other early signals must be integrated with a network of transcriptional regulators that influence CPCs.

Results and Discussion

To examine the CPC-autonomous role of Notch1 signaling in vivo, we deleted *Notch1* in precardiac mesodermal progenitors by crossing *Notch1^{flox}* mice¹⁰⁶ with mice containing *Cre recombinase* in the *Isl1* locus (*Isl1^{Cre}*)¹⁰⁷, resulting in Cre-mediated recombination in early CPCs by E7.75. The resulting *Notch1*-null embryos failed to populate the developing right ventricle segment, which is derived from Isl1⁺ CPCs (**Fig. 1a–c, g–i**). Strikingly, the affected Isl1⁺ CPC pool dorsal to the developing heart was expanded with an increased percentage of proliferating cells marked by a phosphohistone H3 (PH3) antibody (**Fig. 1d–f, j–m**). The accumulation and proliferation of CPCs behind the developing heart was similar to the effect of stabilized β -Catenin on CPCs⁵¹, although in the latter CPCs also migrated into the heart.

The striking similarity of Notch1 loss-of-function and β -Catenin gain-of-function mutants in CPCs led us to hypothesize that Notch and β -Catenin signaling intersect during CPC fate or expansion decisions. No significant expression changes of genes involved in the Notch signal transduction pathway were observed in β -Catenin stabilized mice (not shown), suggesting it is unlikely that β -Catenin regulates Notch signaling in CPCs. Using an ES cell line with a bacterial artificial chromosome (BAC) containing green fluorescent protein (GFP) in the *Nkx2.5* locus⁷³, we isolated *Nkx2.5*-GFP⁺ cells by fluorescent-activated cell sorting (FACS). The *Nkx2.5*-GFP⁺ cells expressed high levels of *Isl1* (**Supp. fig. 1a**), consistent with these cells representing CPCs. We knocked down (KD) Notch1 levels with *Notch1* siRNAs in *Nkx2.5*-GFP⁺ CPCs cultured in a monolayer. Endogenous levels of Notch1 were considerably reduced by the siRNA transfection, determined by Western blot analysis (**Fig. 1n**). Consistent with the in vivo data, *Notch1* KD resulted in an increased number of CPCs (**Fig. 1o**). *Notch1* KD did not affect the levels of total β -Catenin in CPCs (**Fig. 1n**). However, the levels of dephosphorylated (free) β -Catenin, a form required to mediate Wnt/ β -Catenin signaling, were considerably higher in the *Notch1*-KD CPCs (**Fig. 1n**). Consistent with this, *Notch1*-KD CPCs showed significantly increased levels of Topflash activity, a luciferase-based reporter system for Wnt/ β -Catenin signaling (**Fig. 1p**). Increased levels of nuclear β -Catenin were also observed in the cardiac mesoderm of the Notch1 mutant embryo (**Supp. fig. 1b**). These findings suggest that Notch1 normally represses CPC expansion and negatively regulates the active form of β -Catenin.

To search for genes responsible for CPC expansion in an unbiased manner, we performed gene expression analyses of β -Catenin-stabilized CPCs in vivo. For this

analysis, we generated *Rosa^{YFP}; Isl1^{Cre}; β -Catenin(ex3)loxP^{loxP}* embryos that express *YFP* in descendants of *Isl1*⁺ progenitors in the cardiac region with stabilized β -Catenin (**Fig. 2a**). *YFP*⁺ cells from embryonic (E) day 9.0 embryos, before cardiac dysfunction, were purified by FACS (**Fig. 2b**) and used for mRNA expression arrays.

Many known targets of canonical Wnt signaling, including components of the Wnt signaling pathway, were upregulated in mutants, supporting the quality of the data set (**Supp. table 1, Supp. fig. 1c**). We found that the expression of genes implicated in cell proliferation and differentiation (e.g., *Ndr1*, *Bhlhb2*, and *Fgfs*) was highly upregulated (4–11 fold) in mutants (**Supp. table 1, Supp. fig. 1c**). Unexpectedly, several genes essential for CPC development, including *Isl1*, *Myocd*, *Shh* and *Smyd1* were significantly downregulated in the mutants and this was validated by quantitative real-time PCR (qPCR) (**Fig. 2c, d**). It was curious that *Isl1* was downregulated upon stabilization of β -Catenin. In agreement with the array analyses, *Isl1* transcripts were barely detectable in CPCs of β -Catenin-stabilized embryos by in situ hybridization (**Fig. 2e, I, Supp. fig. 1d**). *Smyd1* and *Myocd* transcripts were also significantly downregulated in β -Catenin-stabilized embryos, while *Bhlhb2* was upregulated specifically in the *Isl1^{Cre}* domain (**Fig. 2f–h, j–l, Supp. fig. 1d**). Consistent with the opposing functions of Notch1 and β -Catenin described above, *Isl1*, *Myocd*, *Shh* and *Smyd1* were significantly downregulated and *Bhlhb2* was upregulated in *Notch1* mutant embryos (**Fig. 2d, Supp. fig. 1e**).

Isl1 is a homeodomain-containing factor that is transiently expressed in CPCs prior to their migration into the heart tube, but is extinguished as further migration and differentiation proceed⁹⁷. Although *Isl1* is intuitively thought to promote CPC expansion

based on its temporal expression, we investigated whether *Isl1* downregulation mediates the expansion of CPCs observed in embryos with stabilized β -Catenin. To test this possibility, we used the *Isl1*^{Cre} line described above which contains an *IRES-Cre* cassette inserted into the exon encoding the second LIM domain of *Isl1*, resulting in an *Isl1*-null allele¹⁰⁷. The *Isl1*^{Cre} mice were bred with *Rosa*^{YFP} mice to generate *Isl1*^{Cre/Cre}; *Rosa*^{YFP} embryos. We quantified the number of YFP⁺ cells at E8.0 (5 somite stage), before *Isl1*^{Cre} expression is initiated in neural cells, by FACS. Surprisingly, *Isl1*-null embryos had a significantly higher percentage of YFP⁺ cells than control embryos (**Fig. 3a, b**). The results suggest that *Isl1* negatively regulates the number of CPCs in vivo. The significant increase is unlikely from higher *Cre* expression in *Isl1*-null embryos, since heterozygous *Cre* mice mediate recombination as efficiently as homozygous *Cre* mice.

To determine if *Isl1* also negatively regulates expansion of CPCs derived from pluripotent ES cells, we transiently knocked down *Isl1* levels in the *Nkx2.5-GFP* ES cell line by introducing an *Isl1-shRNA* construct, which efficiently reduced *Isl1* transcripts by ~75% (**Supp. fig. 1f**). We then quantified the number of *Nkx2.5-GFP*⁺ CPCs in EBs from embryoid day (ED) 6 as cardiac progenitors begin to emerge and differentiate from primitive mesoderm^{46,98}. The KD of *Isl1* from ED0–3 did not change the number of *Nkx2.5*⁺ progenitors (data not shown). However, the KD of *Isl1* from ED3–6, just after emergence of mesoderm, resulted in an increased cardiac progenitor population at ED6–8 (**Fig. 3c, Supp. fig. 2a**), consistent with our in vivo data.

These findings prompted us to test if *Isl1* downregulation was required for CPC expansion induced by β -Catenin. We transfected *Nkx2.5-GFP*⁺ FACS-purified CPCs from day 5 EBs with a stabilized β -Catenin expression construct¹⁰⁸ with or without an *Isl1*

expression construct. As previously reported, increased CPC expansion was evident two days after transfection with stabilized β -Catenin (**Fig. 3d**). However, co-transfection with *Isl1* restored the number of CPCs to normal levels (**Fig. 3d**). This suggests that the decrease in *Isl1* is necessary for Wnt/ β -Catenin signaling–mediated expansion of CPCs.

Because *Isl1* appeared to be involved in repressing expansion of CPCs, we investigated whether *Isl1* promotes differentiation in the ES cell system. We generated a stable *Isl1*-KD ES cell line by introducing an *Isl1 shRNA* construct into *Nkx2.5-GFP* ES cells and clonally isolating cells with effective (~80%) *Isl1*-KD (**Supp. fig. 1f**). Similar to the transient *Isl1*-KD, the number of *Nkx2.5-GFP*⁺ cardiac progenitors was significantly increased at ED6 (**Supp. fig. 2b**). However, cells differentiated from the *Isl1*-KD ES cells showed severely reduced beating frequencies with compromised expression of cardiac sarcomeric genes (*Myh6*, *Myh7*, *Mlc2a*, *Mlc2v*) from ED9 (**Fig. 3e, f**). To determine the CPC-autonomous role of *Isl1* during cardiac differentiation, we FACS-purified *Nkx2.5-GFP*⁺ CPCs from ED5 EBs and differentiated them by re-aggregating in suspension (**Fig. 3g**). *Nkx2.5-GFP*⁺ CPCs are multipotent and differentiate into myocardial, smooth muscle, and endothelial lineages^{46,100}. Normal levels of endothelial gene expression (*CD31*, *Flk1*) were observed in differentiating *Isl1*-KD CPCs (**Fig. 3h**). However, expression of cardiomyocyte and smooth muscle genes was severely downregulated (**Fig. 3h**). This suggests that *Isl1* not only represses expansion of CPCs, but is also necessary for proper differentiation of CPCs into the myocardial and smooth muscle, but not endothelial, cell lineages.

Given that *Isl1* loss-of-function suppressed cardiomyocyte differentiation, we sought to determine if *Isl1* conversely plays an instructive role in myocardial lineage

formation. *Isl1* expression levels were upregulated from ED4–5 EBs (**Supp. fig. 3a**). To prematurely increase *Isl1* expression levels in a temporally and physiologically relevant way, we transiently transfected an *Isl1* expression construct (30 ng/10⁵ cells) into dissociated ED2 EB cells and re-aggregated them for further differentiation (**Fig. 4a**). This resulted in about a twofold increase in *Isl1* levels at ED6 (**Fig. 4b**). Myocardial differentiation was monitored by sarcomeric gene (e.g., *Myh7*, *Mlc2v*, *Actc1*) expression over the course of EB differentiation. Sarcomeric gene expression levels did not change during the early phase of CPC differentiation (data not shown). However, by ED8, *Isl1*-transfected EBs expressed higher levels of cardiac muscle genes than control EBs (**Fig. 4c**). To determine the effect of excess *Isl1* on the number of cardiomyocytes, we utilized the *Myh7-GFP* ES cell line to quantify cardiomyocytes. We observed a 25% increase in *Myh7*⁺ cells in *Isl1*-overexpressed EBs (**Fig. 4d, Supp. fig. 3b**). This suggests that *Isl1* can promote myocardial differentiation of CPCs in an instructive manner.

In addition to *Isl1*, *Myocd* and *Smyd1* are important genes for cardiogenesis¹⁰⁹⁻¹¹³ that were downregulated in CPCs with increased β -Catenin (**Fig. 2c–g, i–k**). *Myocd* is a potent coactivator for serum response factor regulation of smooth muscle¹¹⁰ and cardiac gene expression³³. *Smyd1* is a muscle-restricted histone methyltransferase essential for cardiomyocyte differentiation in vivo^{109,111}. To determine whether *Isl1* regulates these genes in CPCs, we used *Nkx2.5-GFP*⁺ CPCs purified from the stable *Isl1*-KD ES cell line. *Smyd1* levels did not change, but *Myocd* levels were significantly reduced in the *Isl1*-KD CPCs (**Fig. 5a**). To determine if this is also the case in vivo, we performed in situ hybridization for *Myocd* transcripts in *Isl1*-null embryos. In agreement with in vitro data, *Myocd* levels were severely compromised in *Isl1*-null embryos, while *Smyd1* levels

did not change (**Fig. 5b–i**). This suggests that *Isl1* is required for normal *Myocd* expression.

Through bioinformatic searches, we identified an *Isl1* consensus site in an evolutionarily conserved island (555 bp) located in the first intron of the *Myocd* locus (**Fig. 5j**). We observed robust transactivation of luciferase when the element was linked to luciferase reporter and introduced into ED6–8 EBs (when endogenous *Isl1* is enriched and biologically functional) (**Fig. 5k**). However, the luciferase activity was significantly reduced when the *Isl1* site was mutated (**Fig. 5k**). In addition, excessive *Isl1* further increased luciferase activity with the *Isl1* site intact but not with the site mutated (**Fig. 5k**). Chromatin immunoprecipitation (ChIP) with anti-*Isl1* antibodies in ED8 EBs revealed that the site was associated with *Isl1* protein (**Fig. 5l**). This association was further confirmed by electrophoretic mobility shift analyses that showed the specific binding of *Isl1* to the site (**Fig. 5m**). Together, these data suggest that *Isl1* may directly regulate *Myocd* expression.

Since *Isl1* did not affect *Smyd1* expression, we hypothesized that β -Catenin might activate a transcriptional repressor to downregulate *Smyd1* expression. Among the transcriptional repressors affected by β -Catenin in our array, *Bhlhb2* was the most highly upregulated. *Bhlhb2* is a basic helix-loop-helix (bHLH)-containing DNA-binding repressor that is involved in many biological processes, including proliferation, differentiation and regulation of circadian rhythms¹¹⁴⁻¹¹⁶. qPCR confirmed that *Bhlhb2* was highly upregulated in embryos with stabilized β -Catenin (**Fig. 5n**) consistent with the upregulation by in situ hybridization in the cardiac area and other domains of *Isl1*^{Cre} activity (**Fig. 2h, l**). Overexpression of *Bhlhb2* in *Nkx2.5*-GFP⁺ CPCs mimicked the

Smyd1 repression observed with β -Catenin stabilization (**Fig. 5o**). *Isl1* expression was not affected by *Bhlhb2*, providing an important control (**Fig. 5o**). We identified four conserved Lef/Tcf consensus sites in the 5' and 3' UTRs of *Bhlhb2* (**Fig. 5p**) and tested whether any were directly bound by β -Catenin. ChIP with anti- β -Catenin antibodies in ED8 EBs revealed that two of the four sites (A and D) were indeed associated with β -Catenin (**Fig. 5q**). To determine which site can mediate Wnt/ β -Catenin signaling, conserved elements encompassing the Lef/Tcf sites were individually inserted upstream of luciferase reporter and examined luciferase activity in ED8 EBs. We found that the construct containing site D, but not A, resulted in a significant increase in luciferase activity upon stimulation with β -Catenin or 6-bromoindirubin-3'-oxime (BIO), a Wnt/ β -Catenin signaling activator (**Fig. 5r**). This increase was, however, not observed in cells transfected with a mutant construct (**Fig. 5r**). These data suggest that *Bhlhb2* may be a direct target of the Wnt signal.

Through use of mouse genetics and the embryonic stem cell system, we have shown that Wnt/ β -Catenin signaling functions as a central regulator of CPCs by integrating signals from the Notch pathway and regulating a cascade of downstream transcriptional events involving *Isl1*, *Myocd* and *Smyd1* (**Fig. 5s**). We found that Notch1 activity within CPCs was required for their exit from the expansive state into the differentiated state, providing the first evidence for Notch signaling requirement within multipotent CPCs in vivo. Consistent with Notch1's negative regulation of active β -Catenin, Notch1 loss-of-function and β -Catenin gain-of-function had similar effects on expression of the cardiac transcription factors, *Isl1*, *Myocd*, *Smyd1* and *Bhlhb2*. Our finding that CPCs in vivo and in vitro had greater expansion upon disruption of *Isl1* and

that *Isl1* could promote differentiation suggests that despite its very transient expression, *Isl1* triggers the further development of CPCs into cardiac cells rather than promoting its renewal state. Strikingly, *Isl1* downregulation induced by β -Catenin was necessary for Wnt/ β -Catenin-induced expansion of CPCs. These findings reveal a regulatory network controlling CPC expansion and cell fate that involve unanticipated functions of β -Catenin, Notch1 and *Isl1* that may be leveraged for regenerative approaches involving CPCs.

Methods

Mouse Genetics and CPC and ES Cell Culture

The control (*Rosa*^{YFP/+}; *Isl1*^{Cre/+}) or mutant (*Rosa*^{YFP/+}; *Isl1*^{Cre/+}; β -Catenin(*ex3*)*loxP*^{loxP/+}) embryos were obtained by crossing *Rosa*^{YFP/+}; β -Catenin(*ex3*)*loxP*^{loxP/+} with *Isl1*^{Cre/+} mice^{107,117}. YFP⁺ cells from the resulting embryos were purified by FACS and used for gene expression analyses. To quantify embryonic CPCs, *Rosa*^{YFP/+}; *Isl1*^{Cre/+} were crossed with *Isl1*^{Cre/+} mice, and YFP⁺ cells from the resulting embryos were counted by FACS. To generate *Isl1*^{Cre/+}; *Notch1*^{loxP/loxP}, *Isl1*^{Cre/+}; *Notch1*^{loxP/+} mice were crossed with *Notch1*^{loxP/loxP} mice¹⁰⁶. Genotyping was done as described⁵¹. To identify *Isl1*-het (*Isl1*^{Cre/+}) or null (*Isl1*^{Cre/Cre}) embryos, DNA was isolated from individual embryos, and qPCR was done using SYBR Green (Applied Biosystems) with control *Isl1* and *Cre* primers shown in Supp. table 2. ES cells and purified Nkx2.5-GFP⁺ CPCs were propagated undifferentiated or differentiated as previously described⁵¹. For CPC

differentiation, the FACS-purified GFP⁺ cells were re-aggregated in suspension (10⁵ cells per well) in ultra-low-attachment 24-well plates (Corning).

Flow Cytometry and Gene Expression Analysis

A Becton Dickinson FACS Diva flow cytometer and cell sorter were used for quantifying and purifying Nkx2.5-GFP⁺ or Myh7-GFP⁺ cells. For the microarray analysis and qPCR, total RNA was amplified with the WT-Ovation Pico RNA Amplification System, fragmented and labeled with the FL-Ovation cDNA Biotin Module V2 (Nugen). The hybridization, staining and scanning of the Affymetrix GeneChips were performed in the Gladstone Genomics Core Lab. Raw data generated from at least three independent experiments were further analyzed by the group of Dr. Ru-Fang Yeh at the Center for Informatics and Molecular Biostatistics, UCSF. To quantify gene expression in *Notch1* mutant embryos, total RNA was isolated from hearts and pharyngeal arches from E10.0 embryos. qPCR was performed with the ABI Prism system (7900HT, Applied Biosystems). TaqMan primers used in this study are listed in Supp. table 2. All samples were run at least in triplicate. Real-time PCR data were normalized and standardized with SDS2.2 software.

Constructs, siRNA, Transfection, EMSA and Luciferase Assays

For *Isl1*-KD experiments, an *Isl1 shRNA* construct set (RMM4534-NM_021459, Open Biosystems) was used to transiently transfect EBs and to generate stable KD ES cell

lines. For *Isl1* or *Bhlhb2* overexpression studies, their full-length cDNAs (Open Biosystems) were amplified and cloned into the *pEF-DEST51* vector (*pDEST51-Isl1* or *Bhlhb2*) through the *pENTR* vector (*pENTR-Isl1* or *Bhlhb2*) using the Gateway system (Invitrogen). *pEF-lacZ* (Invitrogen) was used as a control. For *Notch1*-KD studies, Block-iT Alexa Fluor Red (46-5318, Invitrogen) or *Notch1 siRNA* (M-041110-00-0005, Dharmacon) was used at concentration of 50 or 100 nM. *Myocd-luc* was generated by cloning their corresponding regions into the *pGL3* luciferase vector (Promega). *Myocd-luc^{mt}* was generated using QuikChange Site-Directed Mutagenesis Kit (Stratagene). For *Bhlhb2D-luc* and *Bhlhb2D-luc^{mt}* generation, oligonucleotides containing the Tcf/Lef site were cloned into the *pGL3* vector. All the oligonucleotide sets are listed in Supp. table 2. Stabilized β -Catenin and Top/Fop-flash luciferase constructs were kindly provided by Dr. A. Barth (Stanford University) and the laboratory of Dr. R. Moon (University of Washington), respectively. ES cells, EBs or CPCs were transfected with indicated constructs or siRNA using Lipofectamine 2000 (Invitrogen) after generating single-cell suspension with Accutase (Chemicon). EMSAs and luciferase assays were performed as described previously^{118,119}. For EMSAs, the pCITE-ISL1¹²⁰ construct containing the truncated *Isl1* cDNA with the homeodomain was kindly provided by Dr. B. Black (University of California, San Francisco) and used to generate Isl1 protein. All EMSA probes are listed in Supp. table 2. For luciferase assays, Renilla was used as an internal normalization control.

In Situ Hybridization, Immunostaining and Western Analysis

Whole-mount in situ hybridization was performed as described with designated antisense probes^{97,109,112}. *Bhlhb2* antisense riboprobe was synthesized and purified from *pENTR-Bhlhb2*. To detect proliferating cells in CPCs, embryo sections were stained with anti-Phospho-histone H3 (Upstate) and anti-Isl1 (DSHB). To visualize Isl1 protein in Notch1 mutant embryos, the TSA System (PerkinElmer) was used to amplify Isl1 signals.

Nuclear β -Catenin was detected with anti-PY489 antibody (DSHB). For western blotting, lysates from day 3 CPCs after transfection with indicated siRNAs were analyzed using antibodies against Notch1 (DSHB), Dephospho β -Catenin (Calbiochem), and GAPDH (Santa Cruz Biotechnology).

Chromatin Immunoprecipitation Assays

For chromatin immunoprecipitation (ChIP) assay, EBs were treated with BIO (2.5 μ M) or transfected with *Isl1* or *β -Catenin* constructs¹⁰⁸ (100 ng/ 10^5 cells) from ED 5–7, and harvested at ED 8. Cross-linking of histones to DNA, chromatin extraction, immunoprecipitation and elution were performed using the ChIP Assay Kit (Upstate) with anti-IgG-HRP, Isl1 (Abcam) or β -Catenin (Santa Cruz Biotechnology). PCR primer sets spanning the indicated Lef/Tcf binding sites in the *Bhlhb2* locus are shown in Supp. table 2.

Accession Number

The full microarray data performed in this study are available in NCBI Gene Expression Omnibus (GEO, accession number: GSE15232).

Acknowledgements

We thank R. Kopan (Washington University, St. Louis, MO) and M. M. Taketo (Kyoto University, Kyoto, Japan) for providing *Notch1^{fllox}* and *β-Catenin/loxP(ex3)^{loxP}* mice, respectively. The authors thank G. Howard and S. Ordway for editorial assistance, R.F. Yeh for statistical analyses, K. Cordes for graphical assistance and Srivastava lab members for helpful discussions.

Author Contributions

C.K. designed, performed, supervised in vivo and in vitro work and wrote the manuscript. L.Q. performed flow cytometry and EMSA, and contributed in luciferase assays. P.C. designed and performed *Isl1* gain-of-function studies and contributed in ChIP and luciferase assays. V.N. performed *β-Catenin* western and Top/Fop flash assays. J.A. contributed in ChIP assays. D.S. designed and supervised this work and wrote the manuscript.

Figure Legends

Figure 1: Notch1 loss-of-function causes CPC expansion and increases free β -Catenin levels. **a-f**, Control embryos. **g-l**, *Isl1^{Cre}*, *Notch1^{flox/flox}* embryos (N1-KO). **a, g**, Lateral views of ED10.5 embryos. **b, c, h, i**, Lateral (**b, h**) or frontal (**c, i**) view of embryos focused on cardiac regions showing absence of right ventricle (rv) in mutants. **d, e, j, k**, Transverse sections (H&E) of embryos (**d, j**) with enlargement of boxed areas (**e, k**) showing hyperplasia of precardiac progenitors (asterisk). **f, l**, Phosphohistone3 (Ph3, red) and *Isl1* (green) immunostaining of transverse sections through the precardiac region. To compensate for the severe downregulation of *Isl1* in *Notch1* mutant embryos, *Isl1* signals were amplified with the TSA system. DAPI (blue) was used to counterstain the nuclei. **m**, Percentage of ph3-positive cells in precardiac mesoderm region shown in **e** and **k** (n=4). **n**, Western analyses of FACS-purified CPCs transfected with *control siRNA* (C) or *Notch1 siRNA* (N1-KD) using Notch1, free or total β -Catenin antibodies. Free β -Catenin antibodies detect dephosphorylated β -Catenin, the effector molecule of the Wnt/ β -Catenin signaling pathway. GAPDH antibody was used as a control. **o**, Relative number of cells on the 2nd day after transfecting CPCs with *control* or *Notch1 siRNA*. **p**, Top/Fop flash activity in CPCs transfected with indicated *siRNA*. Top flash is a luciferase reporter with Tcf binding sites to read Wnt/ β -Catenin signaling activity. Fop flash contains mutated Tcf binding sites. Luciferase values were normalized to Renilla activity. *, $P < 0.01$. Error bars indicate standard error. h, heart; pa, pharyngeal arch; ot, outflow tract; lv, left ventricle.

Figure 2: Identification of genes affected by stabilized β -Catenin in cardiac progenitors. **a**, Lateral view of *Rosa^{YFP}; Isl1^{Cre}; β -Catenin(ex3)^{loxP}* embryo at E9.0 showing YFP⁺ cells in precardiac mesoderm (pm). **b**, Histograms of YFP⁺ cell populations from control (*Isl1^{Cre}*, left) and stabilized β -Cat (*Isl1^{Cre}; β -Catenin(ex3)^{loxP}*, right) embryos. **c**, A heatmap of expression arrays showing significantly downregulated cardiac genes (green) in stabilized β -Catenin pm cells. Color bar indicates fold change in log₂ scale. **d**, qPCR data of downregulated genes in FACS-purified cardiac progenitors with stabilized β -Catenin (Top). These genes were similarly affected in pm of Notch1 loss-of-function embryos (Bottom). **e-l**, Whole-mount in situ hybridization of genes indicated from control (top) and stabilized β -Catenin (bottom) embryos at E 9.5. Asterisks indicate precardiac mesoderm. h, heart. *, $P < 0.01$. Error bars indicate standard error.

Figure 3: *Isl1* loss-of-function results in expansion of CPCs and suppression of their myocardial and smooth muscle lineages. **a**, YFP expression in control (*Rosa^{YFP}, Isl1^{Cre/+}*, left) and *Isl1-null* (*Rosa^{YFP}, Isl1^{Cre/Cre}*, right) embryos at the 5-somite stage. Arrows indicate YFP⁺ CPCs. **b**, Quantification of YFP⁺ cells in indicated embryos at somite 5. **c**, Quantification of GFP⁺ cells in ED6 *Nkx2.5-GFP* EBs with or without *Isl1* KD. **d**, Relative number of cells on the 2nd day after transfecting EB-derived CPCs with *lacZ*, *β -catenin*, or *Isl1*. **e**, Relative mRNA expression of indicated genes in control or *Isl1-KD* EBs at ED 9, determined by qPCR. **f**, Number of beating foci per 10⁵ cells in control or *Isl1-KD* EBs at ED12. **g**, Schematic diagram of isolating CPCs from ES cells and their differentiation. **h**, Relative mRNA expression of endothelial (*Flk1*, *CD31*),

cardiomyocyte (*Myh7*, *Mlc2v*) or smooth muscle (*Sma*, *Sm-mhc*) genes during CPC differentiation, determined by qPCR. *, $P < 0.05$. Error bars indicate standard error.

Figure 4: Increased levels of *Isl1* promote myocardial differentiation. **a**, Schematic diagram of differentiation of *Myh7-GFP* ES cells with *Isl1* overexpression. **b, c**, Relative expression levels of *Isl1* on ED6 EBs (**b**), and endothelial (*Flkl1*), cardiac sarcomeric (*Actc1*, *Mlc2v*, *Myh7*) and smooth muscle (*Sma*) genes on day 8 EBs (**c**), determined by qPCR. **d**, FACS analyses on ED 9 EBs to identify % of cells entering myocardial-lineage. *, $P < 0.005$. Error bars indicate standard error.

Figure 5: *Isl1* targets *Myocd* and β -Catenin regulates *Bhlhb2* to repress *Smyd1*. **a**, Relative expression levels of *Myocd* and *Smyd1* in FACS-purified control and *Isl1* knockdown (KD) CPCs, determined by qPCR. **b–i**, Control (**b–e**) and *Isl1-null* (**f–i**) embryos at E 9.5 after in situ hybridization with *Myocd* (**b–d, f–h**), or *Smyd1* (**e, i**) riboprobes. **c, g**, Lateral views focused on heart (h) and pharyngeal arch (pa) regions. **d, h**, Transverse section through the outflow tract. Asterisks indicate pre-cardiac mesoderm. **j**, Location of the conserved island containing *Isl1* binding site (red) in the *Myocd* locus. **k**, Relative luciferase activity determined with luciferase reporters linked to the conserved island with the intact *Isl1* site (*Myocd-luc*) or with a mutant *Isl1* site (*Myocd-luc^{mt}*) in the presence or absence of *Isl1*. **l**, Chromatin immunoprecipitation (ChIP) assay shows specific PCR amplification of the *Isl1* consensus site shown in **j**, representing association with *Isl1* protein. **m**, Electrophoretic mobility shift assay with in-vitro

synthesized *Isl1* protein and radiolabeled probes (Probe) spanning the *Isl1* site shown in **j**. Unlabeled probes were used as competitors. WT, wildtype; MT, mutant. **n**, Relative expression levels of *Bhlhb2* in CPCs with stabilized β -Catenin, determined by qPCR. **o**, Relative expression levels of *Smyd1* and *Isl1* after transfecting FACS-purified CPCs with *Bhlhb2* and differentiating them for 3 days. **p**, The *Bhlhb2* locus showing four conserved Lef/Tcf binding sites. **q**, ChIP assays performed with Lef/Tcf consensus sites shown in **p**. β -Catenin forms complexes with sites A and D as revealed by amplification of those sites. **r**, Relative luciferase activity determined with luciferase reporters containing the intact Lef/Tcf site D (*Bhlhb2D-luc*) or with a mutant Lef/Tcf site D (*Bhlhb2D-luc^{mt}*) in the presence or absence of β -Catenin or BIO (2 μ M). **s**, A molecular cascade involving Notch1/ β -Catenin/ *Isl1* during CPC fate determination. Notch1 functions to negatively regulate accumulation of free β -Catenin, which regulates *Myocd* and *Smyd1* through *Isl1* and *Bhlhb2*, respectively, to determine CPC fates. Relationships indicated may be direct or indirect. Error bars indicate standard error. *, $P < 0.005$.

Supplementary figure 1: **a**, Relative *Isl1* expression levels in GFP⁻ and GFP⁺ cells isolated from Day 5 *Nkx2.5-GFP* EBs, determined by qPCR. **b**, Immunostaining of transverse sections through the pre-cardiac mesoderm and outflow tract (ot) of indicated E 9.5 mouse embryos for nuclear β -Catenin. Higher levels of β -Catenin are observed in precardiac regions (arrowheads) in Notch1 mutants. Numerous Wnts are expressed in the ectodermal cells and form a gradient pattern of active β -Catenin (arrows), providing a positive control. **c**, qPCR data of positively affected genes in cardiac progenitors with

stabilized β -Catenin. **d**, β -Catenin represses *Isl1*, *Myocd* and *Smyd1* but activates *Bhlhb2*. **a–h**, Whole-mount in situ hybridization of genes indicated from control (top) and stabilized β -Catenin (bottom) embryos at E 9.5. **i–p**, Transverse sections of corresponding embryos (**Fig. 2e–l**), focused on precardiac mesoderm (asterisk) and outflow tract (ot) area. h, heart. **e**, Relative *Bhlhb2* expression levels in hearts and precardiac mesoderm from E10.0 control or *Isl1^{Cre}; Notch1^{flox/flox}* embryos (Notch KO), determined by qPCR. **f**, Relative *Isl1* expression levels in EBs 2 days after transfection with an *Isl1* siRNA construct (transient *Isl1-KD*, left) and in ED6 EBs differentiated from control and stable *Isl1-KD* lines (stable *Isl1-KD*, right), determined by qPCR. Error bar indicates standard error. *, $P < 0.01$.

Supplementary figure 2: a, Histograms showing percentages of GFP⁺ cells of ED6, 7, and 8 EBs after transient transfection with an *Isl1* siRNA construct on ED3. **b**, Histograms showing percentages of GFP⁺ cells of ED6 EBs differentiated from control and stable *Isl1-KD* lines.

Supplementary figure 3: a, Relative *Isl1* expression levels in EBs at indicated days of differentiation (ED), determined by qPCR. **b**, Histograms showing percentages of Myh7⁺ cells entering myocardial-lineage in ED9 EBs.

Figure 1

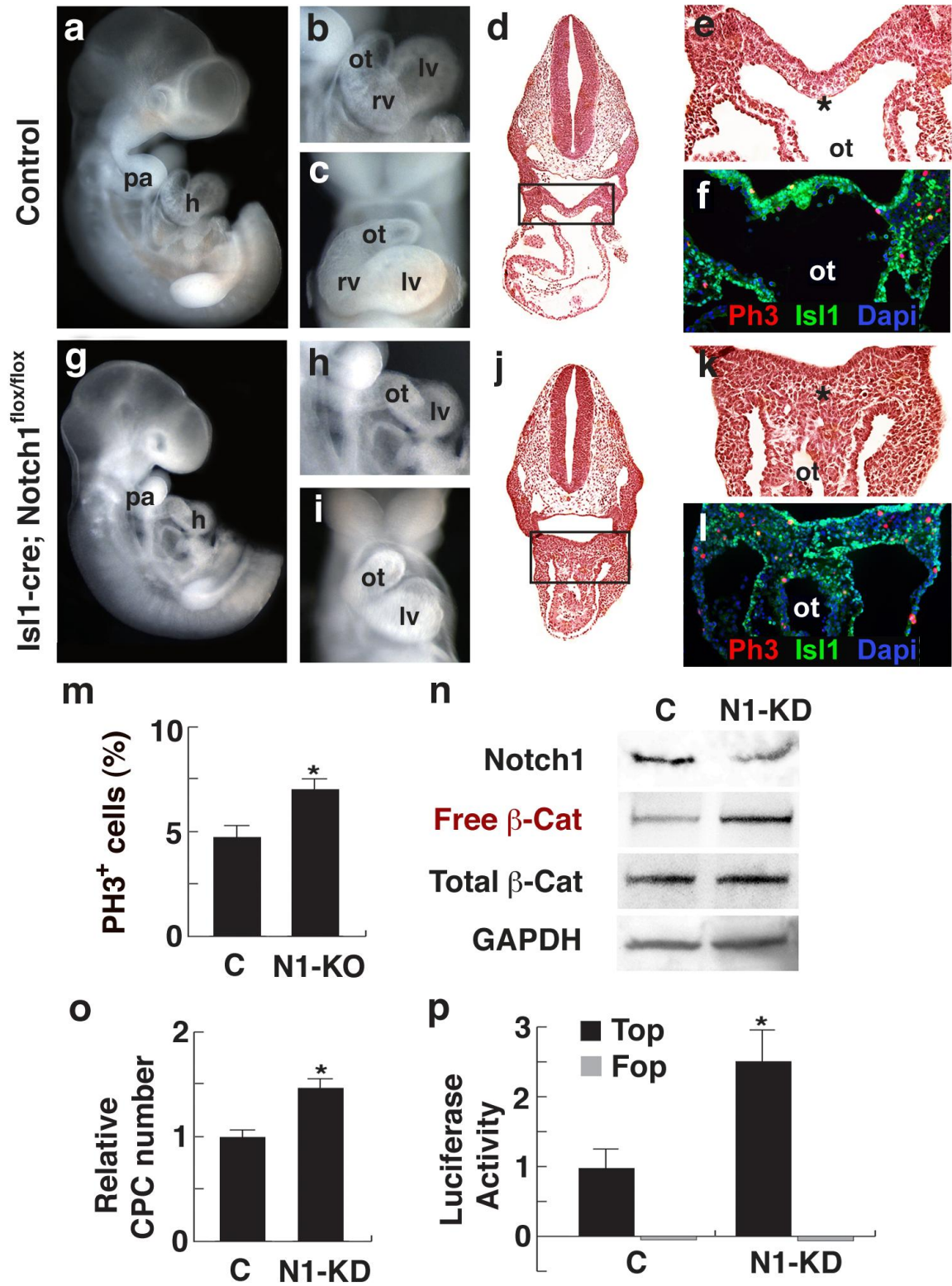


Figure 2

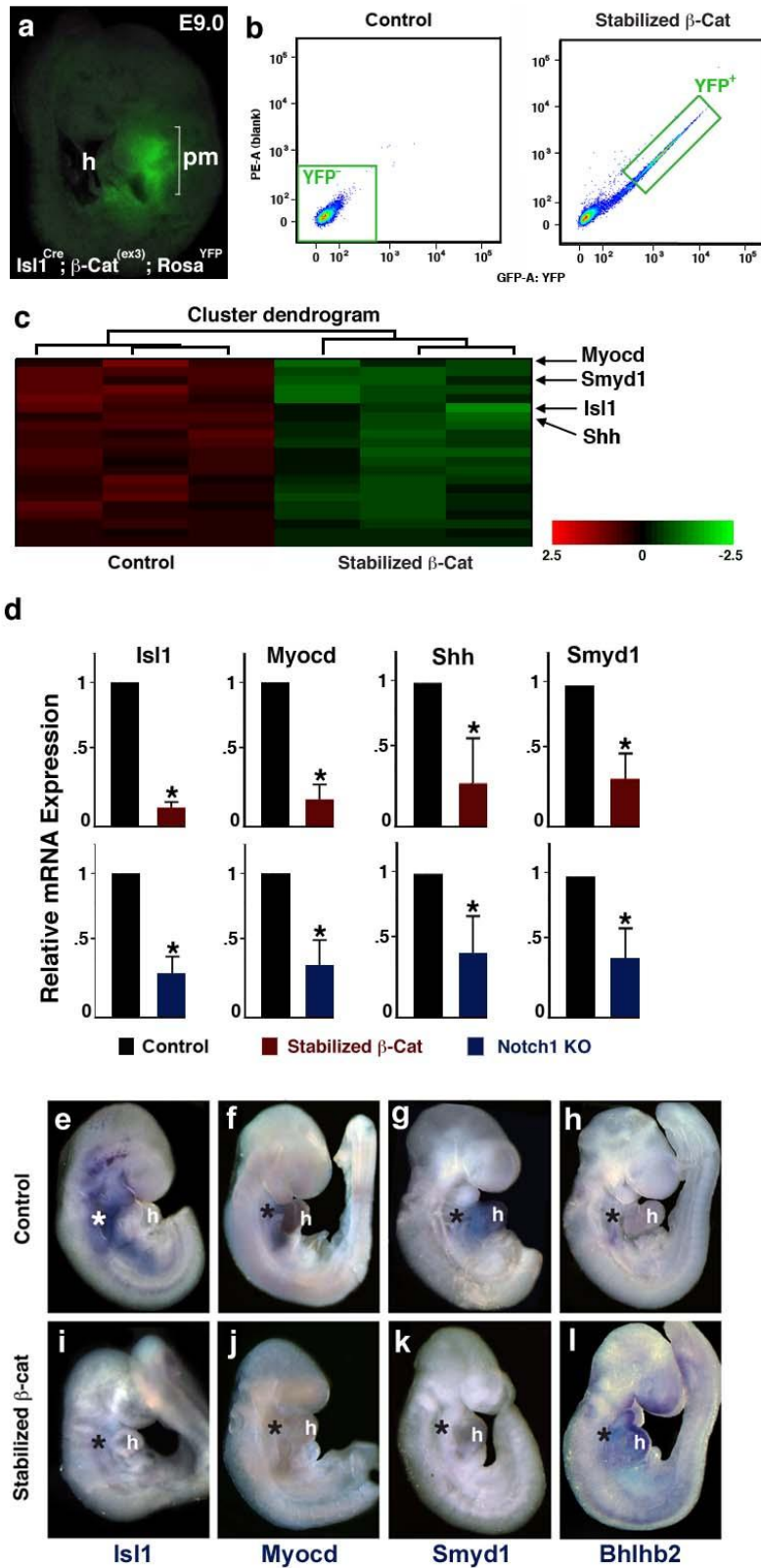


Figure 4

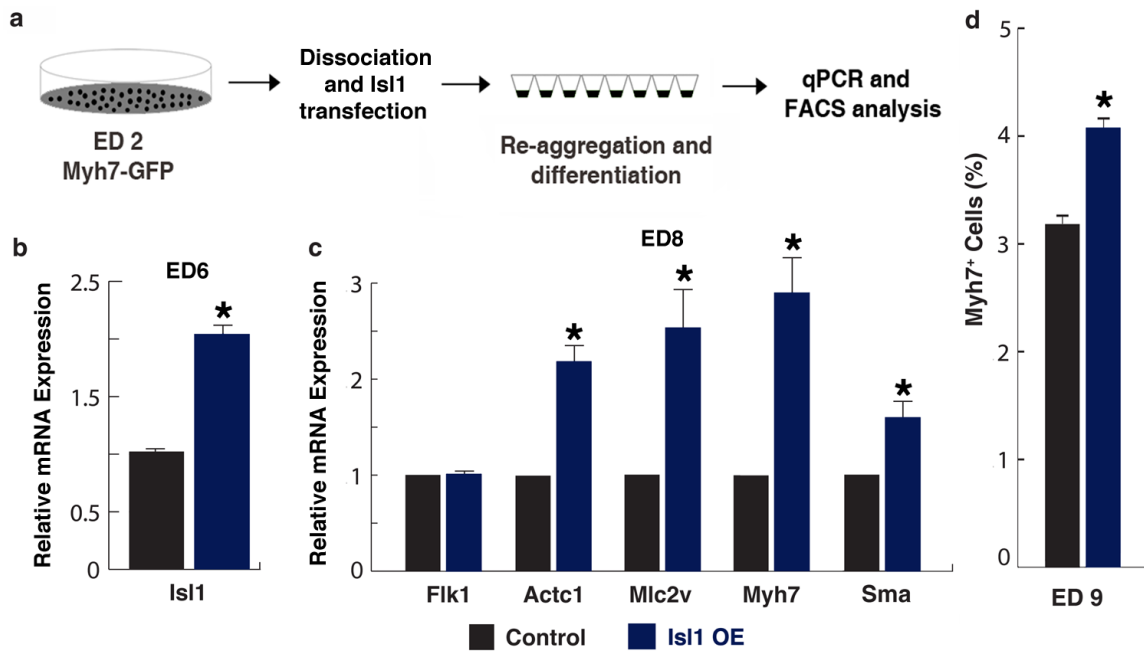


Figure 5

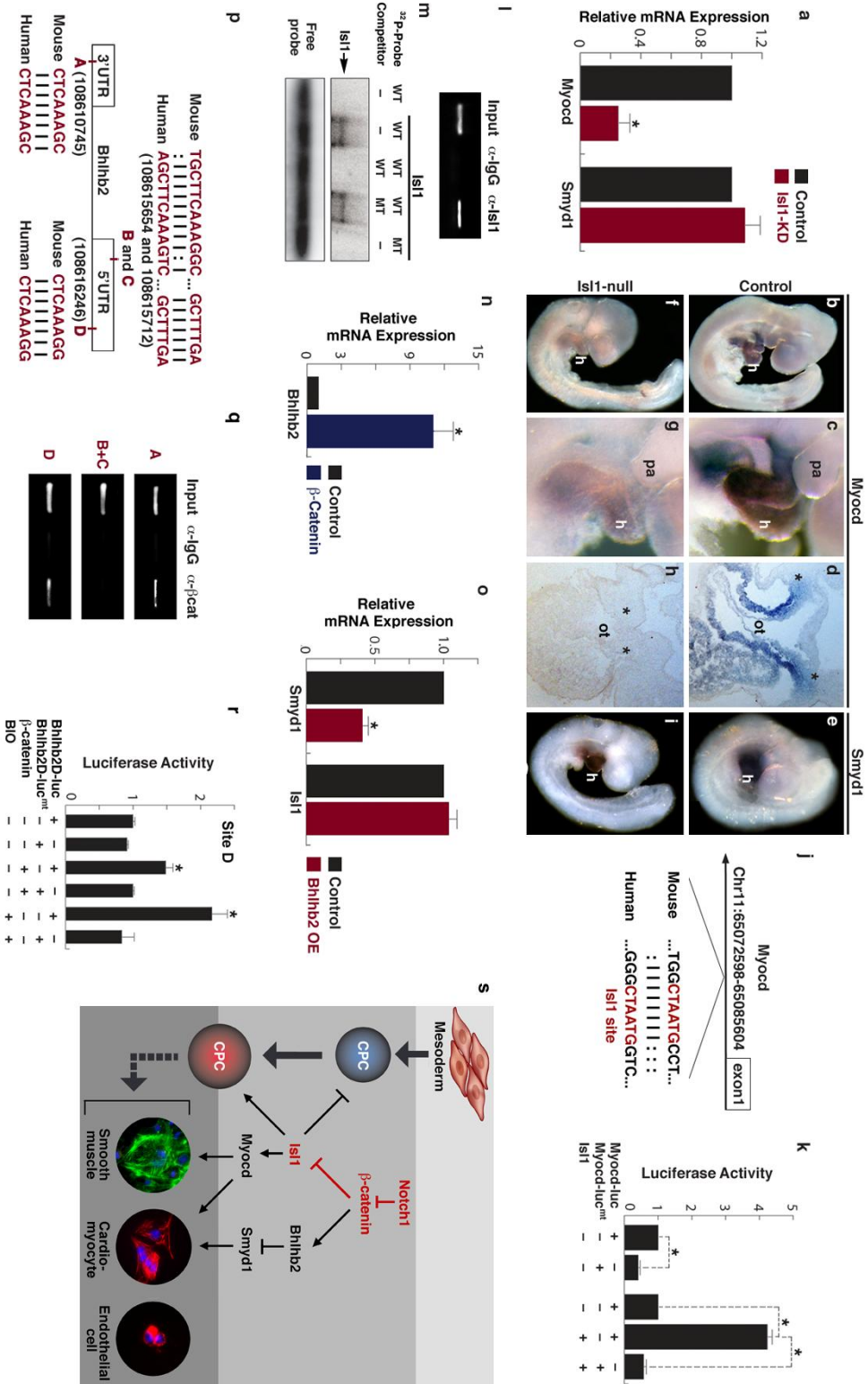


Figure S1

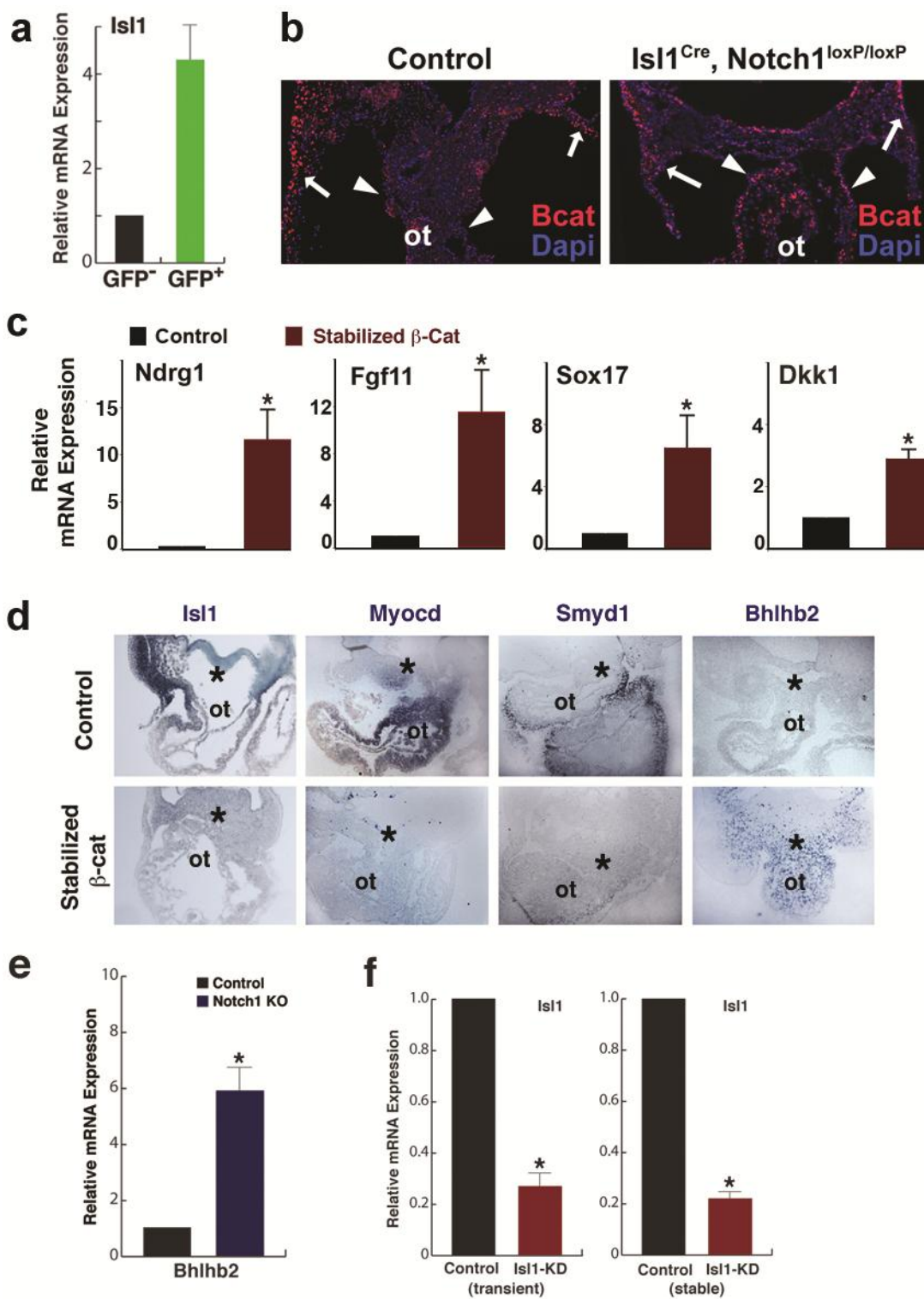


Figure S2

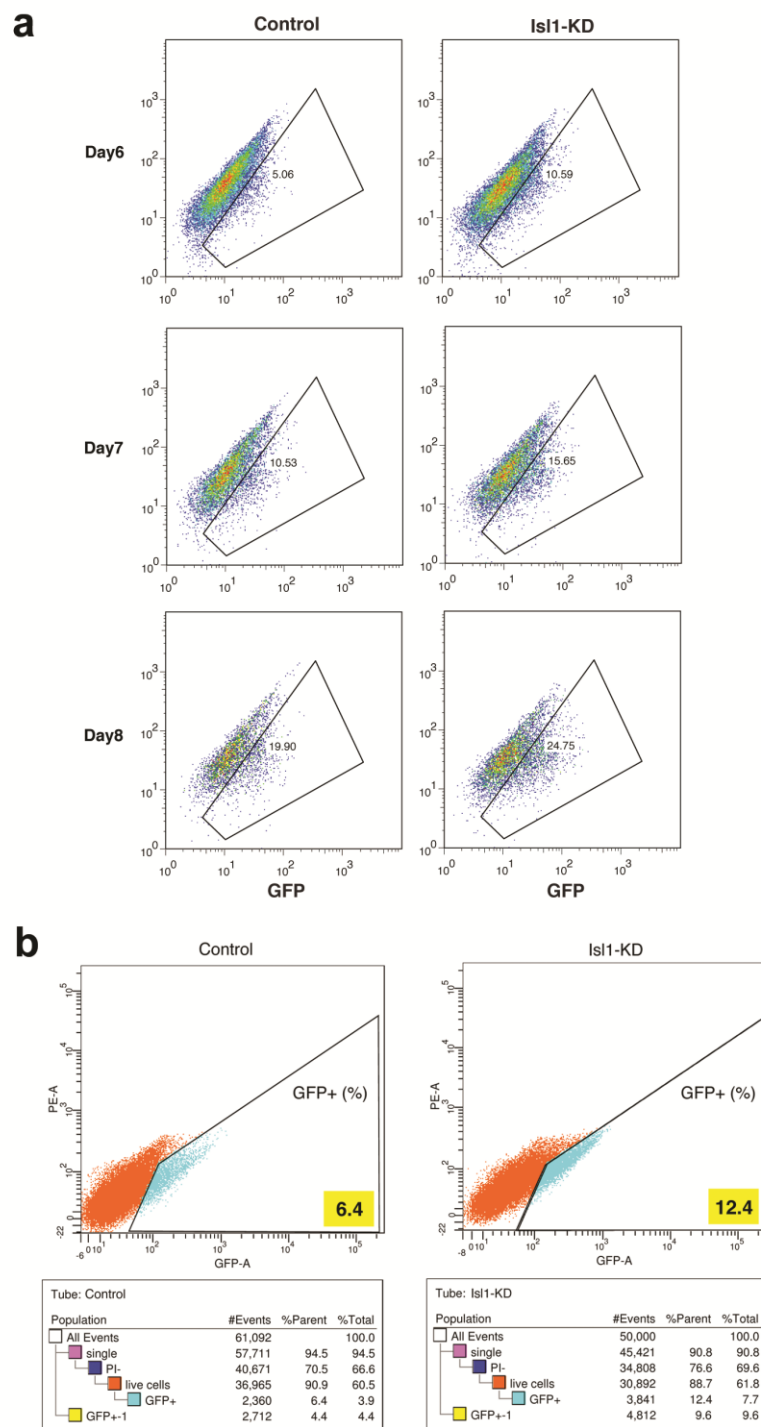
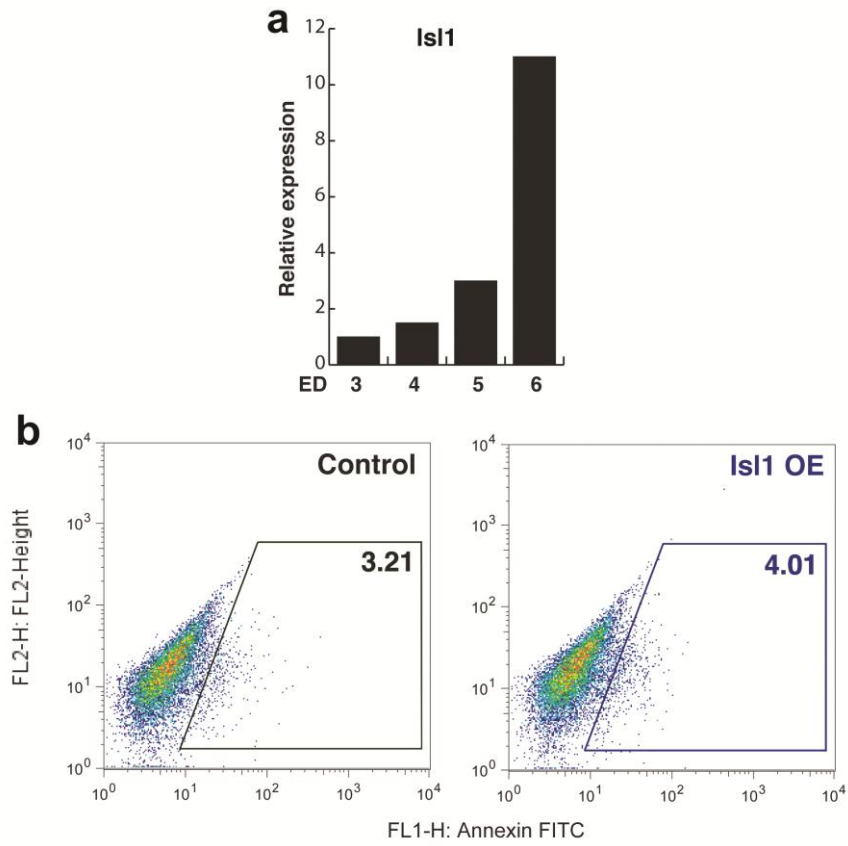


Figure S3



5. Notch Post-Translationally Regulates β -Catenin Protein in Stem and Progenitor Cells

Abstract

Cellular decisions of self-renewal or differentiation arise from integration and reciprocal titration of numerous regulatory networks. Notch and Wnt/ β -Catenin signaling often intersect in stem and progenitor cells and regulate one another transcriptionally. Here, we show that membrane-bound Notch physically associates with unphosphorylated (active) β -Catenin in stem and colon cancer cells and negatively regulates post-translational accumulation of active β -Catenin protein. Notch-dependent regulation of β -Catenin protein did not require ligand-dependent membrane cleavage of Notch or the glycogen synthase kinase-3 β -dependent activity of the β -Catenin destruction complex. It did, however, require the endocytic adaptor protein, Numb, and lysosomal activity. This study reveals a previously unrecognized function of Notch in negatively regulating active β -Catenin protein levels in stem and progenitor cells.

Introduction

Stem cells hold tremendous therapeutic potential due to their unique ability to self-renew and to differentiate into specific cell types. Notch and Wnt/ β -Catenin pathways are evolutionarily conserved signaling cascades that regulate cell proliferation and cell-fate decisions, including the binary decision of stem cell renewal or differentiation¹⁰³. The biological outcome of signaling through each pathway often depends on the context and timing as cells progress through stages of differentiation.

Canonical Wnt signals are mediated by the transcriptional effector, β -Catenin. In the absence of Wnt signaling, β -Catenin is phosphorylated by a destruction complex of glycogen synthase kinase-3 β (GSK3B), adenomatous polyposis coli (APC), and axin¹²¹. Wnt signaling disrupts the destruction complex, allowing the unphosphorylated β -Catenin protein at the serine at residue 37 (Ser37) or threonine at residue 41 (Thr41) to accumulate and function as a co-activator for the transcription factor TCF/LEF¹²¹. Human mutations in APC are associated with colon cancer where excessive accumulation of β -Catenin activity in intestinal stem cells promotes their abnormal proliferation¹²². Thus, quantitative titration of β -Catenin protein is likely important in regulating the proliferative rate of progenitor cells.

The TCF/ β -Catenin complex targets many genes that promote the cell cycle and simultaneously regulate transcription of some members of the Notch signaling pathway, establishing reciprocal interactions between Wnt and Notch signals^{103,123,124}. The canonical Notch signaling pathway is initiated when transmembrane ligands bind to the extracellular domain of transmembrane Notch receptors. This leads to cytoplasmic

cleavage of the Notch intracellular domain (NICD) by γ -secretase and its rapid translocation to the nucleus. In the nucleus, Notch functions as a co-activator for the DNA-binding transcription factor RBP-J to activate Notch target genes, which often promote cellular differentiation¹²⁵.

We recently demonstrated that Notch1 antagonizes Wnt/ β -Catenin signaling by reducing levels of active β -Catenin in cardiac progenitor cells (CPCs)⁹⁰, which represent a multipotent transient amplifying cell population. However, the mechanism of Notch's negative regulation of β -Catenin protein and the breadth of this event in other stem cell types were unknown.

Here, we show that Notch post-translationally regulates β -Catenin protein levels in multiple stem cells in a GSK3 β -independent manner. The negative regulation of β -Catenin protein involved a physical interaction of Notch with β -Catenin. Numb and its homolog Numb-like (Numbl) were necessary for the negative regulation, suggesting that Notch may promote β -Catenin degradation through endocytic trafficking into lysosomes in stem cells. Finally, we present evidence that α - or γ -secretase inhibition, which stabilizes Notch at the membrane, efficiently suppresses accumulation of β -Catenin protein and cell expansion in human colon cancer cells containing APC mutations.

Results

Notch Negatively Regulates Active β -Catenin Protein Levels, Independent of RBP-J, in Multiple Stem Cells

To determine if Notch negatively regulates β -Catenin protein levels in stem cells, we used a *Notch1* siRNA to decrease Notch1 levels in E14 embryonic stem cells (ESCs). We found that reduced Notch1 levels did not noticeably affect the levels of total or N-terminal phosphorylated (Ser37) β -Catenin protein but resulted in an increase in the dephosphorylated, transcriptionally active form of β -Catenin protein (**Fig. 1a**). The active form of β -Catenin normally constitutes a small fraction of total β -Catenin and was detected with antibodies that specifically recognize dephosphorylated β -Catenin at Ser37 and Thr41¹²⁶. In agreement with this finding, knockdown (KD) of Notch1 in ESCs showed significantly more TCF/ β -Catenin-dependent luciferase activity than controls (**Fig. 1b, s1**). Interestingly, knocking down transcripts of all four Notch receptors (*Notch1, 2, 3, 4*) by applying *Notch1–4* siRNAs further increased β -Catenin activity but the degree of increase was mild (**Fig. 1b, s1**). This indicates that Notch1 is the predominant Notch receptor for this event in ESCs, consistent with the high level of Notch1 in ESCs¹⁰⁵. The increase in TCF/ β -Catenin-dependent luciferase activity was also observed in *Notch* siRNA-treated neural stem cells (NSCs) (**Fig. 1c**) and in mouse CPCs lacking Notch1 in vivo and in vitro⁹⁰, suggesting that Notch1 may function to negatively regulate active β -Catenin levels in stem cell populations.

We next sought to determine if the regulation of β -Catenin protein occurs through the canonical Notch signaling pathway involving the transcription factor, RBP-J. We

introduced an *RBP-J*-specific siRNA into ESCs to reduce RBP-J levels. Despite a ~70% KD of *RBP-J* mRNA (**Fig. 1d**), active β -Catenin levels were unchanged (**Fig. 1e**). To determine if RBP-J mediates the Notch regulation of β -Catenin in vivo, we deleted *Notch1* or *RBP-J* in CPCs by inter-crossing *Notch1*^{tm2Rko} 127 or *RBP-J*^{fllox/fllox} mice 128 with mice containing Cre recombinase in the *Isl1* locus (*Isl1*^{Cre}) 107. *Isl1* marks an undifferentiated pool of CPCs 47,97, whose expansion depends on Wnt/ β -Catenin signaling 51,96. Unlike embryos with a *Notch1* deletion, the resulting *RBP-J* mutant embryos showed no expansion of CPCs (**Figs. 1f**). These data suggested that Notch-mediated regulation of active β -Catenin protein in ESCs and CPCs did not involve RBP-J-dependent transcriptional regulation.

Notch Regulates β -Catenin Protein Levels Independent of GSK3 β Activity

RBP-J-independent Notch signaling has been described in vertebrates and invertebrates 129 and is thought to involve Notch-mediated transcription through other DNA-binding proteins. However, quantitative PCR (qPCR) revealed that levels of *β -Catenin* transcripts were not altered in *Notch1* KD ESCs, although *Axin2* and *Cyclin D1*, direct targets of TCF/ β -Catenin 130,131, were significantly upregulated in *Notch1* KD cells (**Fig. 2a**). This raised the possibility that Notch affects β -Catenin protein at the post-translational level. As the key step in the activation of Wnt signaling is the regulation of the amount and localization of β -Catenin by GSK3 β -dependent phosphorylation of its N-terminus in an APC-based destruction complex, we analyzed whether the effects of Notch are mediated by this complex. We first confirmed that a pharmacological GSK3 β

inhibitor, 6-bromoindirubin-3'-oxime (BIO) specifically inhibits GSK3 β activity and inactivates the destruction complex¹³², resulting in the accumulation of active β -Catenin (**Fig. s2**). Overexpression of the Notch1 intracellular domain (N1ICD) in ESCs reduced active and total β -Catenin protein levels, but not mRNA, and decreased its activity in the presence of BIO (**Figs. 2b, c**). The decrease was also evident in ESCs deficient for RBP-J or Mastermind-like (MAML), an essential co-transcriptional regulator for Notch signaling¹³³ (**Fig. 2c**), providing additional evidence that Notch negatively regulates β -Catenin in a transcription-independent fashion. Furthermore, reduced levels of Notch1 increased β -Catenin activity even beyond that seen in BIO-treated ESCs (**Fig. 2d**). This suggested that Notch regulation of β -Catenin protein in vitro is independent of GSK3 β activity.

To determine if Notch could suppress β -Catenin activity in vivo, independent of GSK3 β activity, we expressed a form of β -Catenin that cannot be degraded by the destruction complex, with or without *Notch1*, in the domain of precardiac mesoderm. This was done by crossing *Isl1*^{Cre} mice with *β -Catenin(ex3)^{loxP}*; *Gt(ROSA)26Sor^{tm1(Notch1)Dam}/J* mice. The *β -Catenin(ex3)^{loxP}* allele contains *loxP* sites surrounding exon 3 of *β -Catenin* that encodes amino acids required for GSK3 β -mediated degradation, generating stabilized β -Catenin upon *Cre* expression¹¹⁷, and the *Gt(ROSA)26Sor^{tm1(Notch1)Dam}/J* allele contains a *loxP-stop-loxP* sequence before *Notch1* in the *Rosa* locus, allowing tissue-specific overexpression of Notch1 upon *Cre* expression¹³⁴. Co-expression of stabilized β -Catenin and Notch1 completely rescued the abnormal expansion of precardiac mesoderm induced by activated β -Catenin alone (**Fig. 2e**). Immunochemical analyses revealed that β -Catenin protein levels were increased in the

domains of *Isl1*^{Cre} expression (pharyngeal mesoderm, ectoderm and endoderm) but were reduced close to baseline levels upon Notch1 expression in the same domains (**Fig. 2f**).

These findings provide evidence that Notch can negatively titrate β -Catenin protein levels in vivo, independent of GSK3 β activity, and thereby regulate expansion of progenitor cells.

Notch Physically Associates with Active β -Catenin

Given that Notch expression did not require GSK3 β activity to regulate β -Catenin protein, we examined if Notch modulates active β -Catenin protein levels through a direct physical interaction. We expressed N1ICD in ESCs by transfecting cells with a Myc-tagged N1ICD construct and performed co-immunoprecipitation (Co-IP) assays with anti-Myc antibodies with or without BIO. Comparable introduction of control Myc and Myc-N1ICD constructs into ESCs was confirmed by qPCR (**Fig. s3**). We did not detect an interaction of endogenous β -Catenin with Notch1 in the absence of BIO (**Fig. 2g**). However, when treated with BIO, which greatly increases active β -Catenin levels by inactivating the destruction complex, Notch1 co-precipitated with endogenous β -Catenin (**Fig. 2g**), but not with APC, Axin, Gsk3 β or TrCP (**Fig. s4**). This suggested that Notch might selectively interact with active β -Catenin, whose levels are normally very low in ESCs. To investigate this possibility further, we used a human colon cancer cell line, SW480, which contains high levels of active β -Catenin due to an APC mutation that causes colon cancer¹³⁵. When expressed in SW480 cells, Notch strongly associated with endogenous β -Catenin even without BIO treatment (**Fig. 2g**). Further analysis of the

precipitated β -Catenin confirmed enrichment of active β -Catenin, but not of N-terminal phosphorylated β -Catenin (**Fig. 2h**). These data suggest that Notch physically associates with the active form of β -Catenin, although we cannot exclude the possibility that interaction with the phosphorylated form is below the level of detection.

Next, we mapped the domains of Notch responsible for β -Catenin association by performing Co-IP experiments with a series of truncated Notch mutants that lacked the extracellular domain¹³⁶ (**Fig. 2i**). We found that Notch mutants lacking the RAM domain had limited association with β -Catenin (**Fig. 2j**). To determine if the RAM domain, also required for RBP-J interaction¹³⁷, was necessary for Notch regulation of β -Catenin transcriptional activity, we expressed control and mutant Notch constructs in BIO-treated ESCs with the β -Catenin luciferase reporter. In agreement with the Co-IP result, deleting the RAM domain significantly compromised Notch's ability to repress β -Catenin activity (**Fig. 2k**). Interestingly, Notch without the transactivation or PEST domains also showed reduced repressive activity, implying these domains also contribute to repression (**Fig. 2k**).

Membrane-bound Notch can Antagonize Wnt/ β -Catenin Signaling

The overexpression of N1ICD results in its excessive cytoplasmic accumulation as well as normal nuclear localization (**Fig. s5**). We therefore investigated whether ligand-dependent cleavage of Notch to free the NICD, which is essential for canonical Notch signaling, was necessary for the Notch regulation of active β -Catenin protein, or if membrane-bound Notch was sufficient.

Notch1 intracellular cleavage occurs between amino acids G1743 and V1744 in a highly conserved manner; mutations of V1744 (V1744K or V1744L) block intracellular cleavage, leaving Notch tethered to the membrane¹³⁸ (**Fig. 3a**). We confirmed that the tethered form of Notch (V1744L) remained uncleaved in ESCs and exhibited negligible levels of Notch/RBP-J-dependent luciferase activity (**Fig. 3a, b**). Surprisingly, expression of the tethered forms of Notch in ESCs decreased β -Catenin transcriptional activity comparable to the repression mediated by the well-known Wnt inhibitor, Dkk1 (**Fig. 3c**). The tethered Notch-mediated repression occurred independent of RBP-J (**Fig. s6**). In addition, endogenous active β -Catenin immunoprecipitated with the tethered form of Notch (**Figs. 3d**) in the presence of BIO. In agreement with the Co-IP result, active and total β -Catenin protein levels were considerably lower in cells with the tethered form of Notch (**Fig. 3e**).

Membrane-bound Notch has no transcriptional activity and would conventionally be considered biologically inert. To determine if negative titration of active β -Catenin protein by Notch has biological consequences, we assayed the effects of tethered Notch on Wnt-dependent differentiation of ESC to mesoderm^{139,140}. We expressed tethered Notch (V1744) in early embryoid bodies (before induction of mesodermal cells) derived from ESCs containing GFP in the endogenous mesoderm-specific *Brachyury* (*Bry*) gene⁶⁹. Fluorescence-activated cell sorting revealed that the number of *Bry*⁺ cells was significantly reduced upon expression of tethered Notch. This occurred with or without BIO (**Fig. 3f**). This result indicates that membrane-bound Notch can negatively titrate a cellular response mediated by Wnt/ β -Catenin signaling in stem cells.

To determine if endogenous membrane-bound Notch negatively regulates active β -Catenin protein, we blocked Notch endoproteolysis, which is mediated by the presenilin- γ -secretase complex¹⁴¹. We found that mouse ESCs treated with the γ -secretase inhibitor (GSI), DAPT¹⁴², had a significant reduction of active β -Catenin activity and protein levels in a dose-dependent fashion (**Figs. 3g, h**). This trend was also observed in hESCs, NSCs and bone marrow mesenchymal stem cells (**Figs. 3g, h**) and, importantly, occurred in the absence of any overexpression. The number of Bry⁺ cells was also decreased in embryoid bodies when treated with DAPT (**Fig. 3i**). Similarly, blocking γ -secretase activity, required for ligand-mediated cleavage of the Notch extracellular domain, resulted in a significant reduction of active β -Catenin activity (**Fig. 3j**). To confirm this, we utilized *Notch1*^{lbd/lbd} ESCs where endogenous Notch1 lacks the 11 and 12th EGF repeats required for ligand binding¹⁴³. When stimulated with Wnt3a, we found that *Notch1*^{lbd/lbd} ESCs exhibited significantly lower β -Catenin-dependent luciferase activity than controls (**Fig. 3k**).

Notch-Mediated Degradation of β -Catenin Requires Numb and Lysosomal Activity.

Membrane-bound Notch is regulated by endosomal sorting pathways, leading to recycling or lysosomal degradation^{144,145}. In *Drosophila*, the conserved endocytic adaptor protein Numb, which is present as two orthologues Numb and Numbl in mammals, negatively regulates Notch^{146,147}. As one mechanism, Numb inhibits Notch signaling by trafficking membrane-bound Notch into the lysosome for degradation¹⁴⁸. Surprisingly, we found that endogenous Numb was also co-immunoprecipitated with the

tethered form of Notch (**Fig. 3l**), suggesting Numb may be involved in Notch-mediated degradation of active β -Catenin.

To determine if Numb activity was required for degradation of active β -Catenin complexed with membrane-bound Notch, we knocked down *Numb* and *Numbl* with siRNAs in ESCs in the presence of the tethered form of Notch (V1744L). Tethered Notch was unable to repress β -Catenin transcriptional activity in *Numb* and *Numbl*-deficient ESCs (**Fig. 3m**). In agreement with this finding, knockdown of Numb and Numbl abrogated the ability of tethered Notch to lower active β -Catenin protein levels (**Fig. 3n**). Similarly, Numb and Numbl-deficiency relieved repression of β -Catenin activity observed upon overexpression of N1ICD (**Fig. 3m**).

These data suggested that Numb and Numbl were involved in lysosomal trafficking of the Notch- β -Catenin complex for degradation. In agreement with this, inhibition of lysosomal activity with Bafilomycin A1, a potent and specific inhibitor of vacuolar proton ATPases¹⁴⁹, abrogated the DAPT-induced decrease in active β -Catenin protein in ESCs (**Fig. 3o**). Furthermore, immunocytochemistry revealed that tethered Notch1 and active β -Catenin co-localized with the lysosomal protein, Lamp1 (**Fig. s7**). These findings indicate that the Notch- β -Catenin complex is present in the lysosome and that lysosomal activity is important for the Notch-mediated decrease in active β -Catenin.

Inhibition of Notch Cleavage Decreases Active β -Catenin Levels in Human Colorectal Cancer Cells

Upregulation of active β -Catenin levels is an important oncogenic step in a number of cancers¹²². Extrapolating our results from stem/progenitor cells, we hypothesized that membrane-bound Notch could affect β -Catenin levels in *APC*-mutated human cancer cells containing markedly elevated active β -Catenin protein. We knocked down *Notch 1–4* in SW480 human colorectal cancer cells and found a prominent increase in active β -Catenin protein levels (**Fig. 4a**). This result provided additional evidence for regulation of β -Catenin by Notch, independent of the destruction complex. Conversely, treatment of two human colorectal cancer cell lines, SW480 and HT-29, with DAPT, which chemically prevents NICD cleavage, resulted in a paradoxical dose-dependent decrease in TCF/ β -Catenin-dependent transcriptional activity, β -Catenin protein, and a decrease in cell expansion (**Fig. 4b–d**). Proteasome inhibitors that block the destruction complex-mediated degradation of β -Catenin resulted in increased active β -Catenin levels but failed to prevent the Notch-mediated decrease in β -Catenin protein (**Fig. 4e**). This indicates that Notch regulation of β -Catenin protein is unlikely proteasome-mediated and supports the earlier evidence showing Numb-dependence and potential involvement of the lysosome.

Ibuprofen Lowers β -Catenin Levels through Notch in Human Colon Cancer Cells

Chronic use of non-steroidal-anti-inflammatory drugs (NSAIDs) in humans has frequently been reported to lower the risk of developing primary and recurrent colorectal

cancer^{150,151}. The anti-neoplastic effects of NSAIDs were initially attributed to their anti-inflammatory function of inhibiting Cyclooxygenase 2 (COX-2). However, NSAIDs surprisingly slowed proliferation of COX-2-deficient colorectal cancer cells, including SW480 cells, suggesting an additional mechanism^{152,153}. A subset of NSAIDs also has significant γ -secretase inhibitory (GSI) activity¹⁵⁴, and we correspondingly found that ibuprofen induced a dose-dependent decrease of canonical Notch transcriptional activity, determined by Notch/RBP-J-dependent luciferase activity in SW480 cells (**Fig. 4f**). Ibuprofen treatment also lowered levels of active β -Catenin transcriptional activity and protein (**Fig. 4g, h**). Importantly, the reduction of β -Catenin protein levels upon Ibuprofen treatment of cancer cells was not observed after knockdown of *Notch1-4* (**Fig. 4i**). This suggests that NSAIDs act, at least in part, through Notch to decrease active β -Catenin protein levels, and this regulation may contribute to the overall protective effects of NSAIDs on colorectal cancers. This result is consistent with the observation that GSI treatment in APC mutant mice reduces proliferating adenomas in the intestine^{155,156}.

Discussion

In the present study, we show that Notch negatively regulates protein levels of active β -Catenin in a post-translational manner and thereby serves to titrate Wnt/ β -Catenin signaling in stem and progenitor cells (**Fig. 5**). Our finding of a physical interaction between Notch and β -Catenin provides a potential explanation for some aspects of non-canonical Notch effects described by our group and others¹⁵⁷. In our experiments, the interaction between these two critical regulatory proteins did not require ligand-dependent cleavage of Notch, and membrane-bound Notch could form a complex with the active form of β -Catenin. This was observed in cells with active Wnt signaling, where inactivation of the destruction complex resulted in higher levels of active β -Catenin. Thus, in the presence of Wnt signaling, Notch might serve to titrate active β -Catenin levels to temper the proliferative state of expanding cells and affect cellular decisions. Indeed, expression of Notch1 in CPCs of mice rescued the β -Catenin-induced expansion of CPCs, demonstrating the potency of this titration effect on a cellular outcome in vivo. Furthermore, it is interesting to speculate that Notch may also serve to clear low levels of active β -Catenin that escape destruction complex-mediated degradation.

The bulk of our findings indicate that membrane-bound Notch can interact with and lower levels of β -Catenin, however, we also found that overexpression of the NICD could also inhibit β -Catenin in a similar manner. While NICD can interact with β -Catenin in the cytosol and co-localizes with the lysosomal marker upon overexpression, this is unlikely to be its normal function given its low cytoplasmic levels under physiologic conditions. Instead, it may be the membrane-bound Notch that serves to titrate the active form of β -

Catenin in cells responding to Wnt signaling. The evolutionary conservation of this process is striking, as Notch also interacts with Armadillo in endocytic vesicles in *Drosophila* and negatively regulates Wnt signaling¹⁵⁸.

Remarkably, stabilizing Notch at the membrane with GSIs in human colon cancer cells reduced β -Catenin levels sufficiently to overcome the accumulation of β -Catenin due to mutations in APC. Generally, GSIs, such as DAPT, mimic canonical Notch loss-of-function mutations. However, our findings suggest that GSI treatment paradoxically decreases Wnt/ β -Catenin signals through membrane-bound Notch, which effectively reduces active β -Catenin levels and activity. Biochemical approaches to purify the Notch- β -Catenin complex may reveal the more precise mechanism by which Notch affects active β -Catenin accumulation/degradation and provide more specific approaches to disrupt or promote the Notch- β -Catenin interaction.

Materials and Methods

Mouse Genetics and Cell Culture

The *Isl1^{Cre}*; *RBP-J^{lox/lox}* or *Isl1^{Cre}*; *Notch1^{lox/lox}* embryos were obtained by crossing *Isl^{Cre}*; *RBP-J^{lox/+}* mice with *RBP-J^{lox/lox}* or *Notch1^{tm2Rko}* mice, respectively^{107,127}. *Isl1^{Cre}*; *β-Catenin(ex3)^{loxP/+}* or *Isl1^{Cre}*; *β-Catenin(ex3)^{loxP/+}*; *Gt(ROSA)26Sor^{tm1(Notch1)Dam}/J* embryos were obtained by crossing *Isl^{Cre}* mice with *β-Catenin(ex3)^{loxP/+}*, *Gt(ROSA)26Sor^{tm1(Notch1)Dam}/J* mice¹³⁴. Mouse ESCs (E14) were cultured on gelatin-coated tissue culture dishes with standard maintenance media (GMEM with 10% FBS with 1xESGRO (Chemicon), Glutamax, sodium pyruvate, MEM Non-Essential amino acid). Human ESCs were cultured on matrigel-coated dishes in mTesR (STEMCELL Technologies). SW480, HT-29, NE4C were cultured as suggested by ATCC.

Constructs, siRNA, Transfection, Gene Expression and Luciferase Assays

For *Notch*, *RBP-J*, *MAML* or *Numb/Numbl* knockdown experiments, Notch1-4, RBPSUH, MAML or Numb/Numbl On-TARGETplus SMARTpool (Dharmacon L-041110, L-044202, L-047867, L-046498, L-059179, L-007772 or L-046935/L-046983) or Block-iT Alexa Fluor Red (46-5, 318, Invitrogen) was used at concentrations of 50, 100, or 150 nM for cell transfection. Tethered and truncated forms of *Notch1* constructs were kindly provided by Drs. R. Kopan (Washington University, St. Louis, MO) and M. Nakafuku (Cincinnati Children's Hospital, Cincinnati, OH), respectively. Active β -Catenin construct (S33Y) was obtained from Addgene. We used 75–100ng of the constructs to transfect 3×10^5 cells. Cells were transfected with Lipofectamine LTX

(Invitrogen) or Lipofectamine 2000 (Invitrogen) in single-cell suspensions. For gene expression analysis, qPCR was performed with the ABI Prism system (7900HT, Applied Biosystems) with the following primers: *β-Catenin* (Mm01350394_m1), *Cyclin D1* (Mm00432359_m1), *Axin2* (00443610_m1), or *Gapdh* (Mm99999915_g1). All samples were run at least in triplicate. Real-time quantitative PCR data were normalized and standardized with SDS2.2 software. The constructs to measure Notch/RBP-J (JH23A) were kindly provided by Dr. N. Gaiano (Johns Hopkins University). For luciferase assays, Renilla was used as an internal normalization control.

Co-Immunoprecipitation, Western, and Immunocytochemistry Analyses

Cells were transfected with indicated constructs and cultured for 24 hours (with/without BIO, 2 μM). Cells were scraped off the 100-mm dish and lysed in 1 ml of lysis buffer (1 mM PMSF, 1 mM EDTA, 10 mM Tris-HCl, 0.1% Triton X100, 1x Complete Protease Inhibitor Cocktail (Roche) in PBS). The lysates were spun down, and 1 μg of anti-c-Myc antibody (Sigma, M4439) or anti-Flag antibody (Sigma, F1804) was added to 500 μl of the supernatant. A 50-50 mixture of protein A Sepharose (Amersham) and protein G Sepharose (Amersham) was added to the lysate/antibody mixture for immunoprecipitation for 1 hour. The resulting outputs were washed with lysis buffer and subjected to western blot analysis. For western blotting/immunocytochemistry, samples were analyzed using primary antibodies against active-β-Catenin (anti-ABC, Millipore), phospho-β-Catenin (Ser33/37/Thr41), Axin1 (C7B12), GSK3β (27C10), APC, Rab7 (Cell Signaling), Lamp1 (ab24170, Abcam), Isl1 (DSHB), Numb (ab14140), Rab7 β-

Catenin (sc-1496), TrCP (C-18), Gapdh (Santa Cruz Biotechnology). Alexa 488 and 568 (Invitrogen) were used for secondary antibodies. Densitometry was carried out in Photoshop.

DAPT, Ibuprofen, Batimastat, Ilomastat, Bafilomycin A and BIO Treatment

Cells were treated with DAPT (CALBIOCHEM Cat#565784), ibuprofen (99% pure, Sigma), Batimastata (TOCRIS Cat#2961), Ilomastat (SIGMA Cat # M5939), Bafilomycin A1(TOCRIS Cat#1334), or BIO (CALBIOCHEM Cat#361550) at the indicated concentrations.

ESC Differentiation and Flow Cytometry

ESCs were trypsinized into single cells, and differentiated as standard embryoid bodies in 75% IMDM, 25% F12 supplemented with N2, and B27 supplements. The Becton Dickinson FACS Calibur flow cytometer was used for quantifying Bry-GFP⁺ cells.

Statistical Analyses

The two-tailed Student's *t*-test, type II, was used for data analyses. $P < 0.05$ was considered significant.

ACKNOWLEDGEMENTS

We thank Drs. R. Kopan (Washington University, St. Louis, MO), M. Nakafuku (Cincinnati Children's Hospital, Cincinnati, OH), T. Honjo (Kyoto University, Kyoto, Japan) and Dr. P. Stanley for providing tethered Notch constructs, Notch deletion constructs, *RBP-J^{flox}* mice and *Notch1^{lbd/lbd}* ES cells (Albert Einstein College of Medicine), respectively. The authors thank G. Howard and S. Ordway for editorial assistance, Srivastava lab members for helpful discussions, B. Taylor for assistance with manuscript and figure preparation, and B. Bruneau for critical reading of the manuscript. We also thank J. Fish and C. Miller in the Gladstone Histology core.

Figure Legends

Figure 1: Notch Negatively Regulates Active β -Catenin in Stem Cells Independently of RBP-J. **a**, Western analysis of ESCs transfected with control or *Notch1* (*NI*) siRNA with active (Act), Phospho (Ser37), or total β -Catenin antibodies that detect N-terminal-dephosphorylated β -Catenin. **b, c**, Relative β -Catenin/TCF-directed luciferase activity in ESCs (**b**) or neural stem cells (NSCs) (**c**) transfected with control *siRNA* or *siRNA* against *Notch1* or *Notch1-4*. β -Catenin/TCF activity was measured by co-transfecting cells with a luciferase reporter downstream of multiple TCF binding sites (Topflash). A mutant reporter (Fopflash) exhibited negligible activity in all luciferase assays done in this study. **d**, Relative *RBP-J* expression levels by qPCR in ESCs after transfection with control or *RBP-J siRNA*, determined by qPCR. **e**, Western analysis of ESCs transfected with control or *RBP-J siRNA* (50 or 100 nM) with Act β -Cat antibodies. **f**, Transverse sections of control, *Notch1* knockout (KO) (*Isl^{Cre}, Notch1^{tm2Rko(ex3)^{loxP}}*) or *RBP-J* KO (*Isl^{Cre}, RBP-J^{flox/flox}*) embryos stained with H&E (top) or Isl1 antibody (green, bottom) at embryonic day 9.5, at level of outflow tract (ot). Asterisks indicate precardiac mesoderm containing cardiac progenitor cells. Dapi (blue) was used to counterstain the nuclei. The cutting plane is indicated by a dotted line (left). All luciferase values were normalized to Renilla activity and represent n=4. *, $P < 0.01$. Gapdh antibody was used as a loading control. Numbers on Western blots correspond to relative quantification. h, head; ht, heart tube; Con, control; N1KD, *Notch1 siRNA*; N1-4KD, *Notch 1-4 siRNA*.

Figure 2: Notch1 Negatively Regulates Active β -Catenin in ESCs and Physically Interacts with β -Catenin. **a**, Relative expression of *β -Catenin* and *Cyclin D1* mRNA in ESCs transfected with control or *Notch1* siRNA (100 nM), determined by qPCR. **b**, Western analysis of ESCs transfected with control or Notch1 intracellular domain (N1ICD) (100 or 300 ng) and cultured with BIO. GAPDH antibody was used as a loading control. **c**, Relative β -Catenin/TCF luciferase activity of BIO-treated ESCs transfected with control or N1ICD +/- *MAML* or *RBP-J* siRNA. **d**, Relative β -Catenin/TCF luciferase activity of ESCs transfected with control or *Notch1* siRNA and cultured with or without BIO. **e, f**, Transverse sections of control, *Isl^{Cre}; β -Catenin(ex3)^{loxP}* (Act- β -Cat) or *Isl^{Cre}; Gt(ROSA)26Sor^{tm1(Notch1)Dam/J}* (Act- β -Cat; N1ICD overexpression) embryos at embryonic day 9.5, stained with H&E (**e**) or β -Catenin antibody (red, **f**). Asterisks indicate precardiac mesoderm containing cardiac progenitor cells (**e**). DAPI (blue) was used to counterstain the nuclei (**f**). nt, neural tube; ot, outflow tract; pe, pharyngeal endoderm; ec pharyngeal ectoderm; pm, precardiac mesoderm. **g, h**, ESCs treated with or without BIO (**g**) or SW480 (human colon cancer) cells (**g, h**) were transfected with expression constructs for Myc (-) or N1ICD-Myc (+), immunoprecipitated (IP) with anti-Myc antibody and immunoblotted (IB) with β -Catenin antibody recognizing its C-terminus (**g**), dephosphorylated (active) form, or the phosphorylated N-terminus (**h**). Notch expression was detected with anti-Myc antibody (**g**). **i**, Schematic representation of Notch1 deletion constructs and their interactions with β -Catenin. **j**, Co-IP of BIO-treated ESCs with Notch1 deletion constructs shown in (**i**) using antibodies indicated. Arrowheads indicate Notch1 expression. **k**, Relative β -Catenin/TCF activity of BIO-treated ESCs transfected with Notch constructs shown in (**i**). TM (transmembrane

domain), R (RAM domain), ANK (Ankyrin repeats), TA (transactivation domain), P (PEST domain). BIO was used at 2 μ M. All luciferase values were normalized to Renilla activity and represent n=4. *, $P < 0.01$. Numbers on Western blots correspond to relative quantification. Con, control; N1KD, *Notch1* siRNA.

Figure 3: Membrane-Bound Notch1 Negatively Regulates Active β -Catenin Levels through Numb and Numb-like in Stem Cells. **a**, Schematic representation of a cleavage site–mutated tethered form of Notch1 (V1774L, top) and Western analysis of ESCs transfected with Myc-tagged wild type Notch1 or tethered Notch1 (V1774L) and blotted with anti-myc antibody (bottom), showing lack of cleaved protein band. **b**, Relative RBP-J responsive luciferase activity of mESCs transfected with control, tethered Notch1 or N1ICD. **c**, Relative β -Catenin/TCF luciferase activity of ESCs transfected with control or tethered Notch1 (V1774L) construct shown in (a) or treated with Dkk1 (50 ng/ml). **d**, BIO-treated ESCs transfected with control or tethered Notch1-myc constructs immunoprecipitated (IP) with anti-Myc antibody and immunoblotted (IB) with β -Catenin antibody. Notch1 expression was detected with anti-Myc antibody. **e**, Western analysis of active or total β -Catenin in BIO-treated ESCs transfected with control or tethered Notch1. **f**, Percent of *Brachyury*-GFP positive cells after 3 days of differentiation of mouse ESCs with tethered Notch (V1774L) or control in the presence or absence of BIO (0.5 μ M). **g**, Relative β -Catenin/TCF luciferase activity of ESCs or NSCs treated with increasing doses of DAPT, a γ -secretase inhibitor, for 72–96 h. **h**, Western analysis of active β -Catenin in mouse or human ESCs, NSCs, or bone marrow mesenchymal stem cells (MSCs) treated with increasing doses (0, 25, 50 or 100 μ M) of DAPT for 72–96 h. **i**,

Percent of *Brachyury*-GFP positive cells after 3.5 days of differentiation of mouse ESCs with control or DAPT. **j**, Relative β -Catenin/TCF luciferase activity of ESCs treated with control or Batimastat, an γ -secretase inhibitor. **k**, Relative β -Catenin/TCF luciferase activity of wild type ESCs (control) or ESCs with ligand-binding site-deleted Notch1 (*Notch1^{lbd/lbd}*) treated with Wnt3a. **l**, Human colon cancer cells (SW480) transfected with pcDNA-Myc or tethered Notch (V1774L)-Myc constructs, immunoprecipitated (IP) with anti-Myc antibody and immunoblotted (IB) with anti-Numb antibody. Expression of tethered Notch was detected with anti-Myc antibody; expression of pcDNA-myc was confirmed by PCR. **m**, Relative β -Catenin/TCF luciferase activity of ESCs transfected with control, N1ICD or tethered Notch (V1774L) in the presence or absence of *Numb/Numbl* siRNA and cultured in BIO for 72 h. **n**, Western analysis of active β -Catenin in ESCs transfected with control or tethered Notch (V1774L) in the presence or absence of *Numb/Numbl* siRNA. **o**, Western analysis of active β -Catenin in ESCs treated with control or DAPT in the presence or absence of Bafilomycin A1, which inhibits lysosomal activity. All luciferase values were normalized to Renilla activity and represent n=4. Gapdh antibody was used as a loading control. Numbers on Western blots correspond to relative quantification. *, $P < 0.01$; NS, not significant. BIO was used at 2 μ M. Con, control.

Figure 4: γ -Secretase Inhibitors (GSIs) Suppress Expansion of Human Colon Cancer Cells by Blocking Notch Cleavage. **a**, Western analysis of active β -Catenin in SW480 human colon cancer cells transfected with control or siRNA against *Notch1-4* (N1-4KD, 100 nM each). **b**, Relative β -Catenin/TCF luciferase activity of SW480 cells treated with

increasing doses of DAPT for 96 h. **c**, Western analysis of β -Catenin levels in SW480 and a second colon cancer cell line, HT-29, treated with increasing doses (0, 25, 50 or 100 μ M) of DAPT for 96 h. **d**, Relative number of SW480 cells treated with DAPT (50 or 100 μ M for 72 h. **e**, Western analysis of active β -Catenin levels in SW480 cells with increasing DAPT in the presence or absence of proteasome inhibitor (PI) MG-132 (5 nM) for 72 h. Fewer PI-treated cells were loaded in the right panel since they exhibit higher levels of β -Catenin. **f**, Notch/RBP-J luciferase reporter activity (multimerized RBP-J binding sites) of SW480 cells treated with increasing doses of ibuprofen. **g**, Relative β -Catenin/TCF luciferase activity of SW480 cells treated with Ibuprofen for 72 h. **h**, Western analysis of active β -Catenin in SW480 cells treated with Ibuprofen for 72 h. **i**, Western analysis of active β -Catenin in SW480 cells treated with control or Ibuprofen and transfected with *Notch1-4* (100 nM each) siRNA. GAPDH antibody was used as a loading control. All luciferase values were normalized to Renilla activity and represent $n=4$. *, $P<0.01$. Numbers on Western blots correspond to relative quantification. Con, control; N1-4KD, *Notch 1-4* siRNA.

Figure 5: Model for Post-Translational Regulation of β -Catenin Protein by Notch. In the absence of Wnt, the destruction complex of Axin, APC and GSK3 β phosphorylates β -Catenin, leading to its proteasomal degradation (left). When the destruction complex is inactivated by Wnts, dephosphorylated (active) β -Catenin functions as a transcriptional activator with TCF/LEF. We show that active β -Catenin protein levels can be negatively regulated by interaction with Notch in a Numb-dependent manner, involving the

lysosome. Notch-mediated degradation of β -Catenin is independent of the APC-dependent destruction complex.

Supplementary Materials

Figure s1. Knockdown efficiency of *Notch 1–4* and *Numb/Numbl* siRNA by qPCR.

Figure s2. Western analysis of active (Act) β -Catenin in embryonic stem cells (ESCs) treated with or without BIO (1 μ M). GAPDH antibody was used as a loading control.

Figure s3. qPCR quantification of pcDNA-Myc, N1ICD-Myc or tethered Notch1-Myc (V1774L-Myc) constructs introduced in ESCs for immunoprecipitation. PCR primers to amplicon were used to quantify the constructs.

Figure s4. Immunoprecipitation assay. ESCs treated with BIO were transfected with expression constructs for pcDNA-Myc or NICD-myc, immunoprecipitated (IP) with anti-Myc antibody and immunoblotted (IB) with indicated antibodies.

Figure s5. Confocal microscopy analysis of SW480 cells transfected with NICD-Myc construct. Cells were immunostained with Myc primary antibody and Alexa 488 secondary antibody. Arrows indicate cytoplasmic localization of NICD. Dapi (blue) was used to counterstain the nuclei.

Figure s6. Relative β -Catenin/TCF luciferase activity of NSCs transfected with tethered Notch1 (V1774L) and *RBP-J* siRNA.

Figure s7. Confocal microscopy analysis of SW480 cells transfected with tethered Notch1-Myc (T-Notch-Myc) and active β -Catenin-Flag (S33Y) constructs. Cells were immunostained with primary antibodies (Myc, Flag, Lamp1) detecting indicated proteins and fluorescent secondary antibodies (Alexa 488, 568). Arrows indicate co-localization. Dapi (blue) was used to counterstain the nuclei.

Figure 1

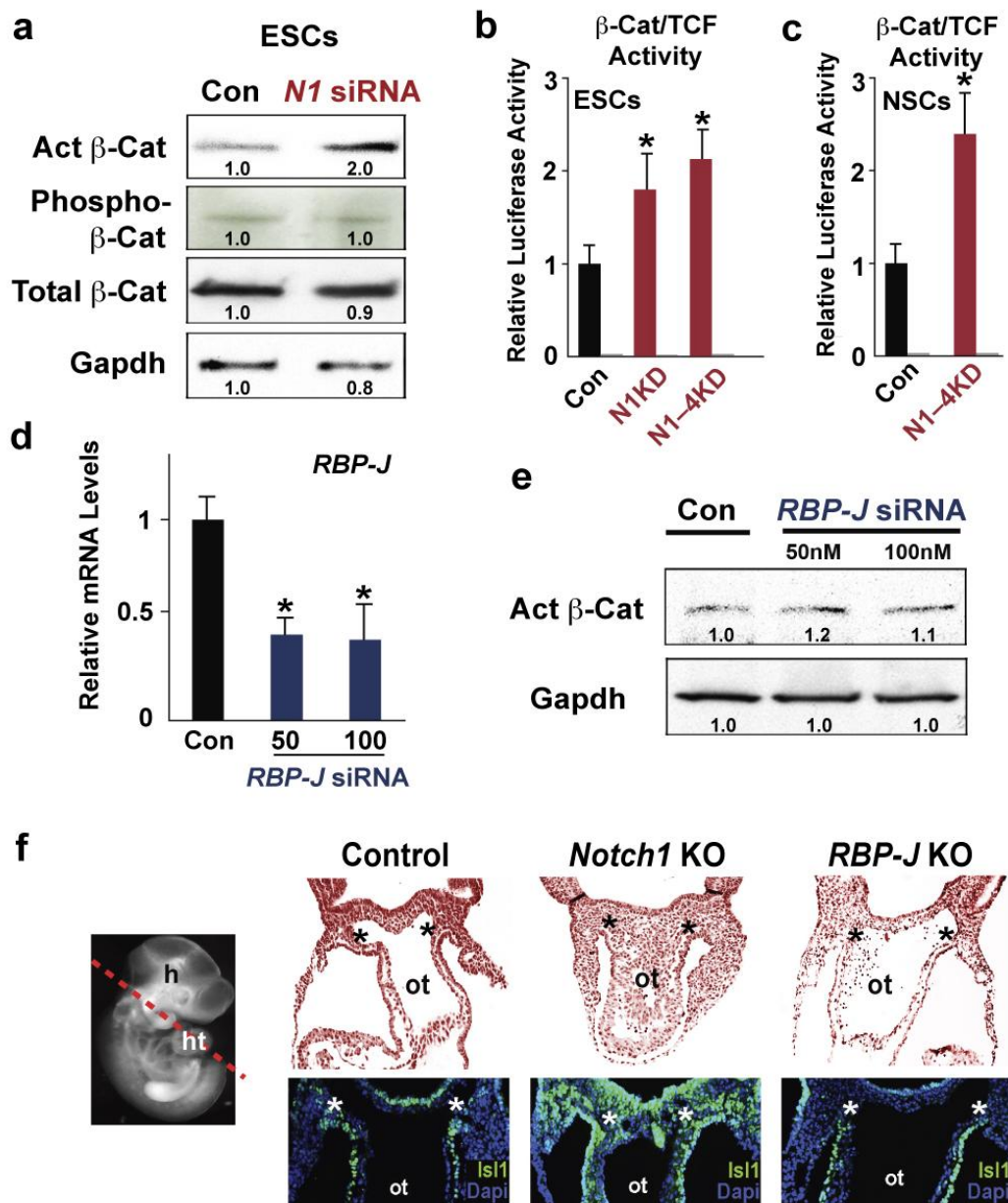


Figure 2

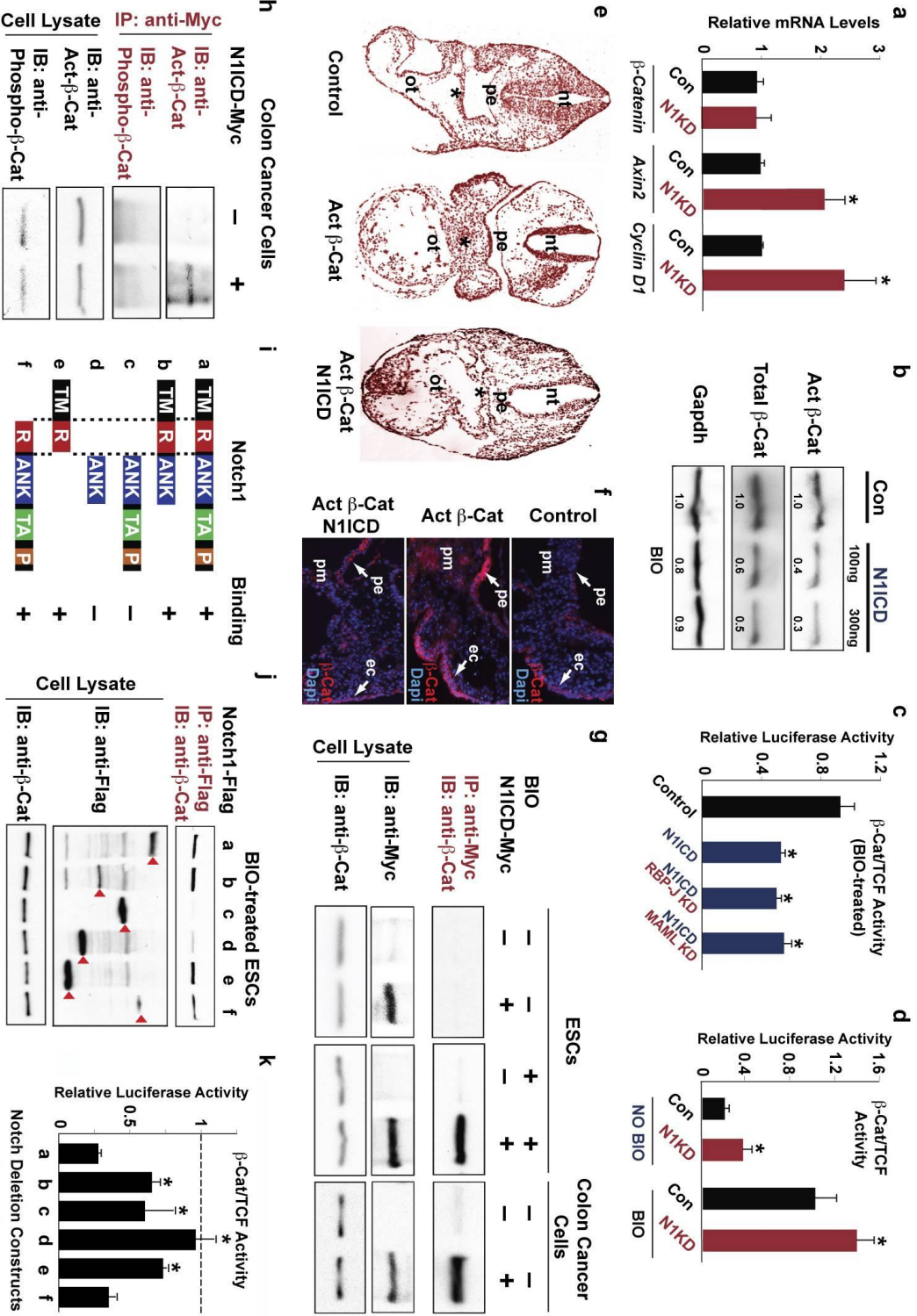


Figure 3

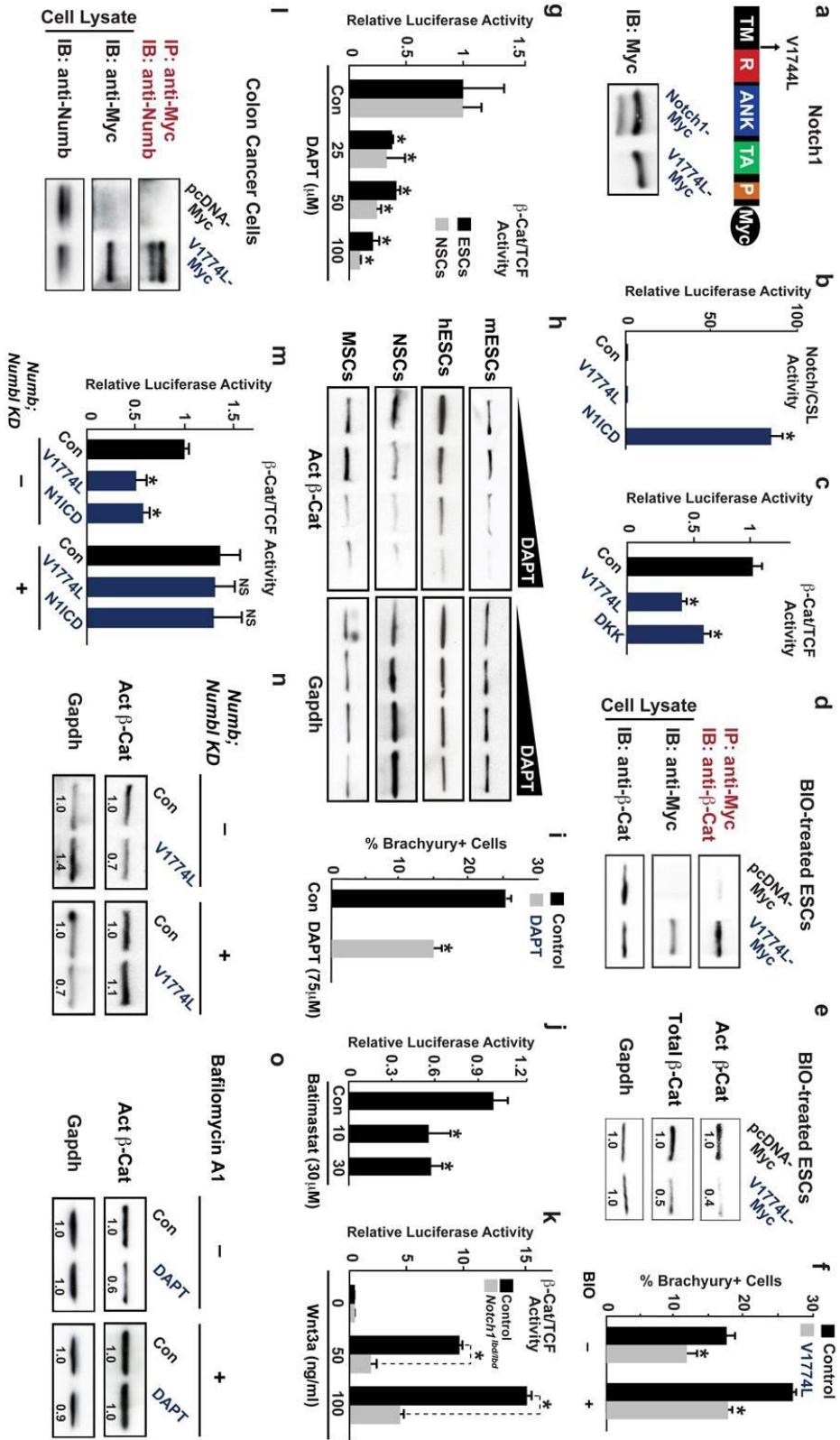


Figure 4

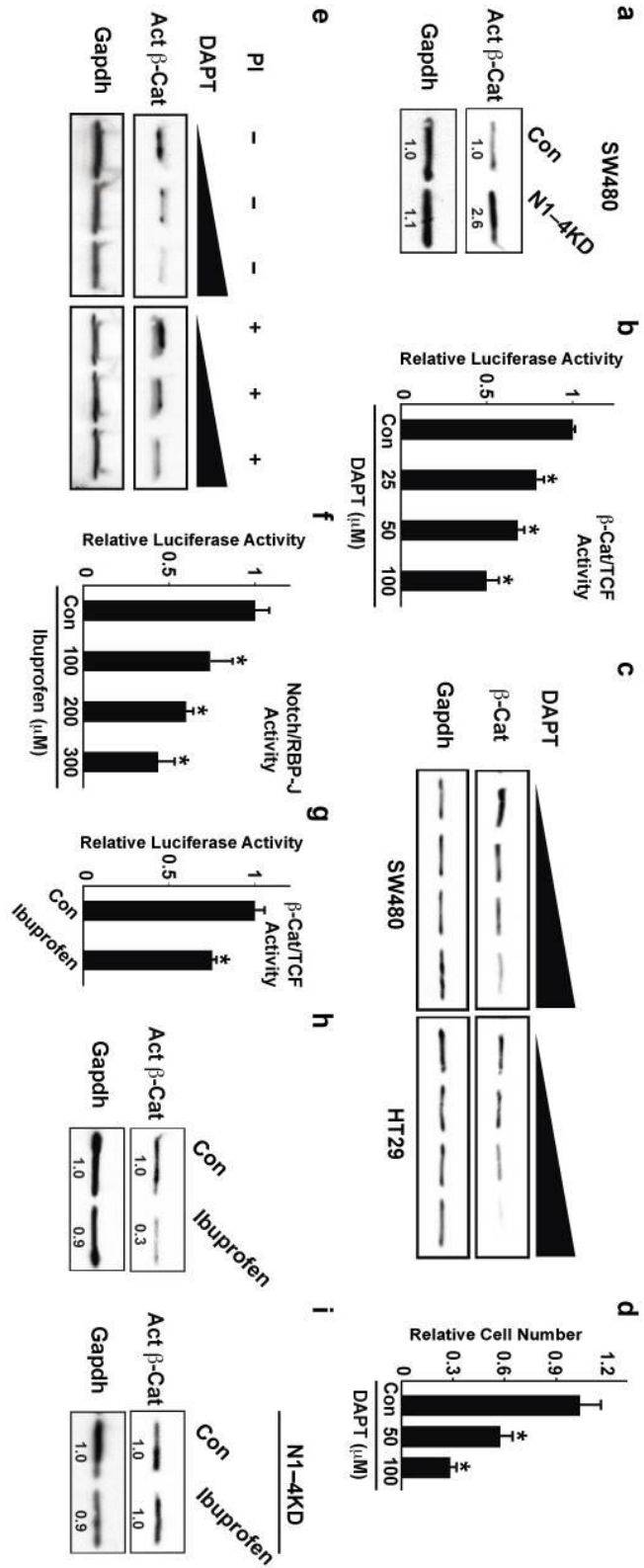


Figure 5

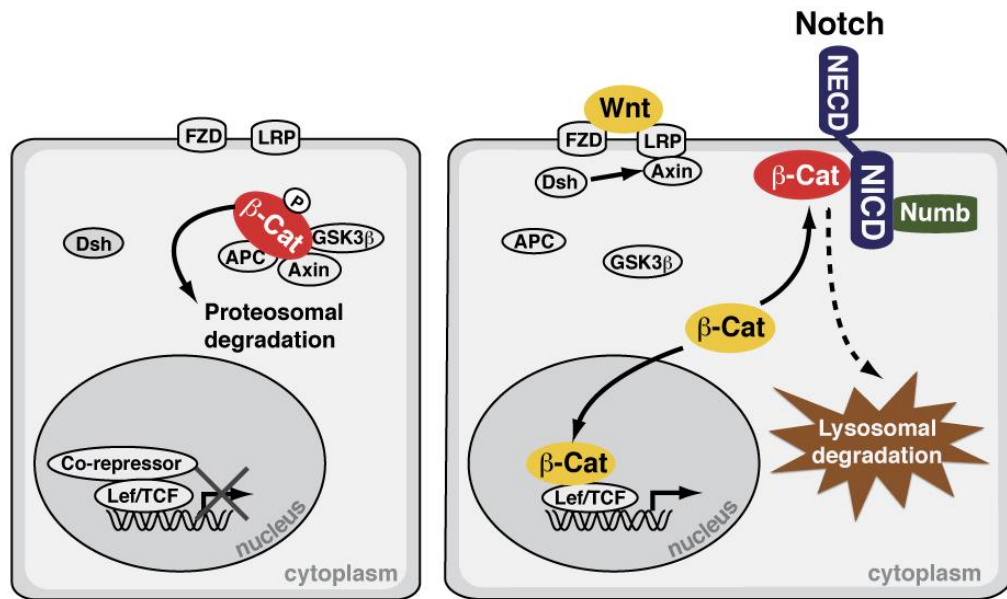


Figure S1

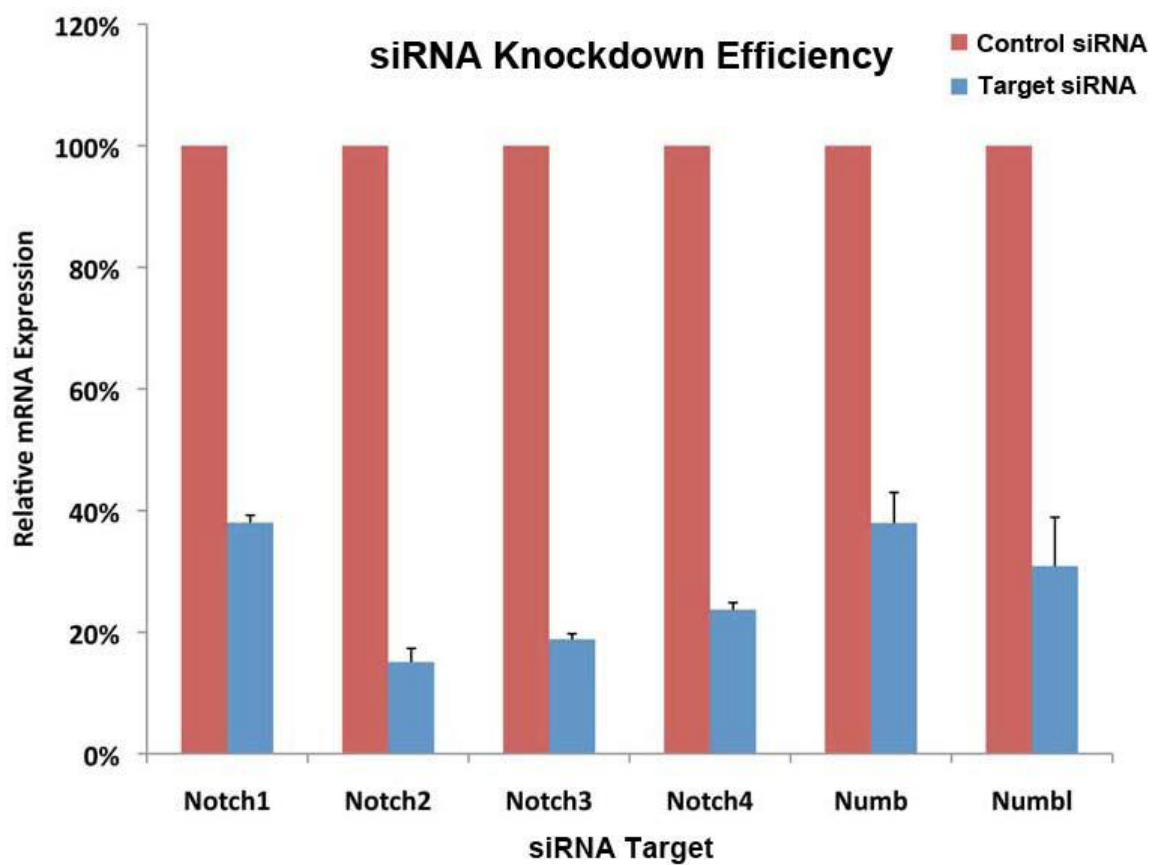


Figure S2

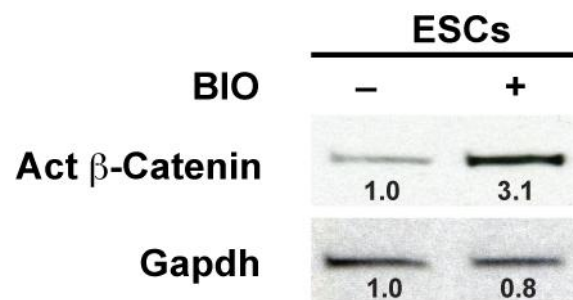


Figure S3

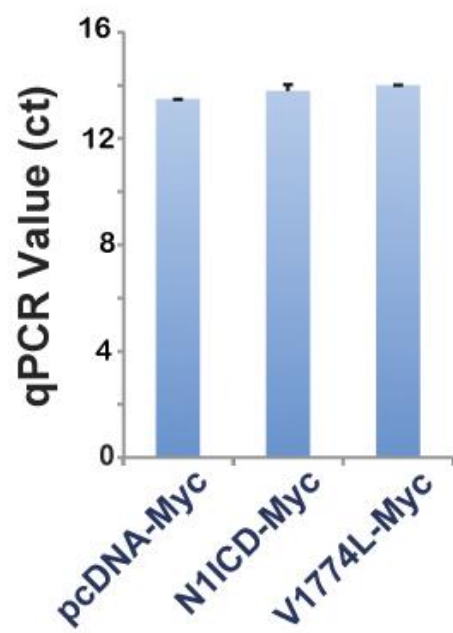


Figure S4

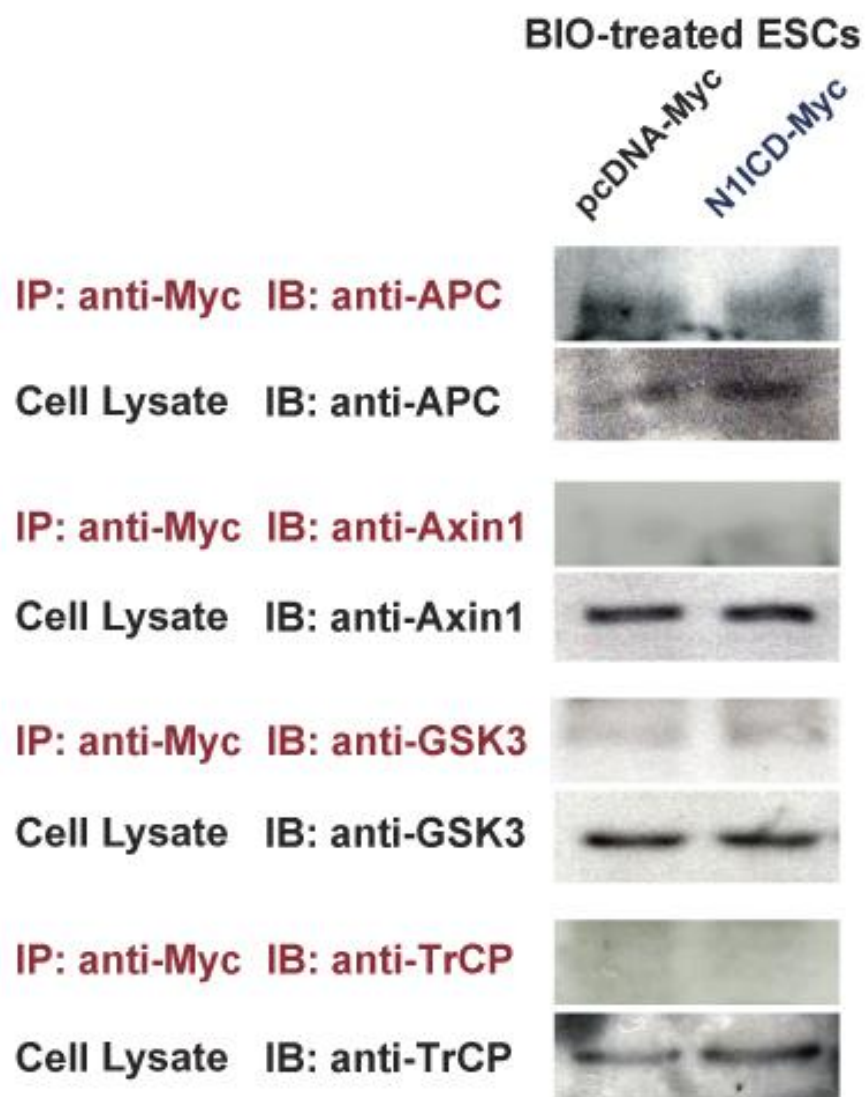


Figure S5

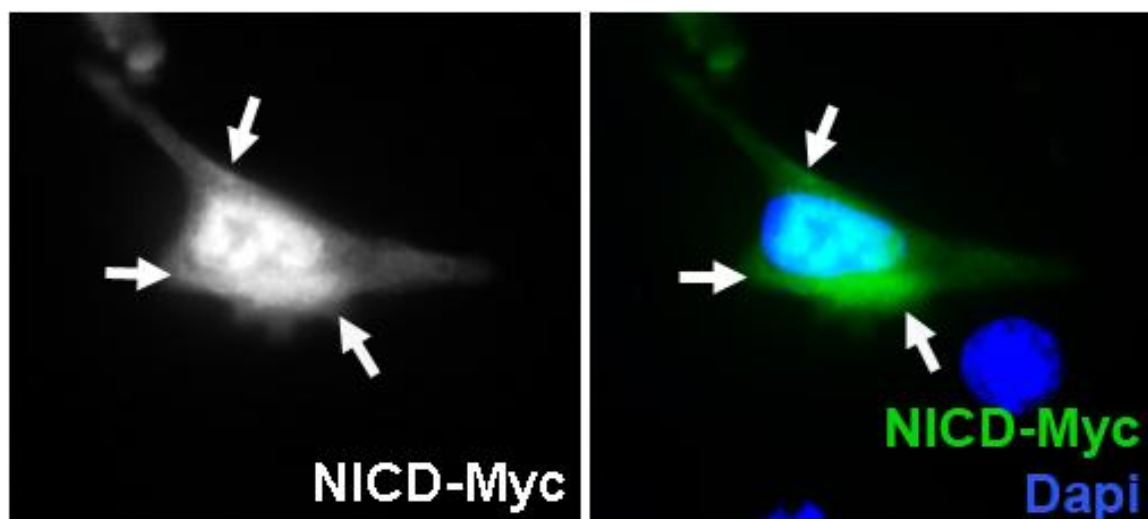


Figure S6

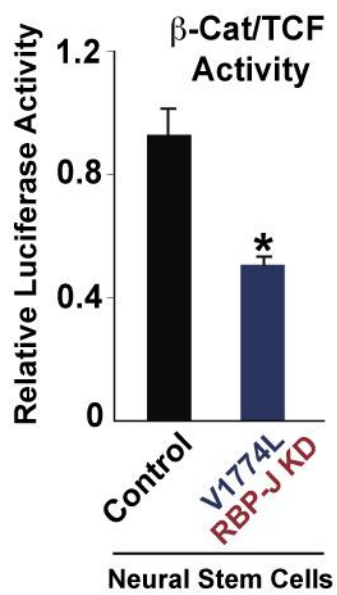
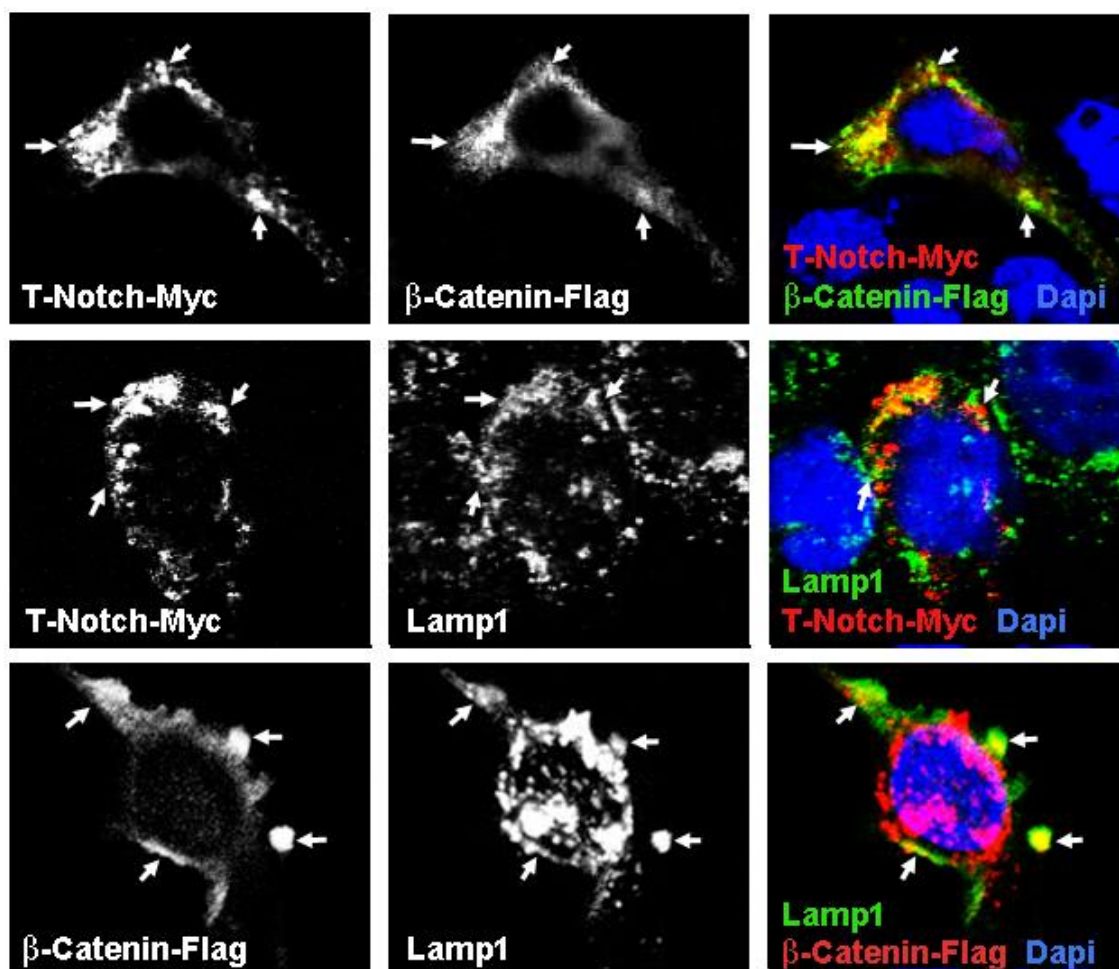


Figure S7



6. Conclusion and Future Directions

Over the past four years, the scientific field has made significant progress in understanding the signals that regulate the biology of cardiac progenitors. We have contributed to this pool of knowledge by elucidating a network of signaling that regulates the induction and maintenance of cardiac progenitors involving the extracellular matrix and Notch/Wnt signaling. The novel crosstalk between Notch and Wnt signaling discovered in our system is generalizable to many populations of stem cells and has therapeutic potential in human cancers. We are confident that our insight into the morphogenic roles of the extracellular matrix will prove to be important in numerous subsequent developmental studies. In the process, our studies also uncovered new questions that need to be answered.

Results from our serum-free differentiation and fibronectin studies reveal previously unrecognized intricacies in the process of lineage commitment. The polarizing lineage decisions based on small changes in the cytokine concentration cannot be fully explained by our current understanding of signal transduction and transcriptional control. Luckily, we already know the identities and timing of the important transcription factors involved. The molecular mechanism of lineage determination may be elucidated through genome-wide study of the occupancy and function of these transcription factors alongside bioinformatics approaches to identify novel regulatory elements.

Our fibronectin study described detailed mechanisms regarding how fibronectin promotes mesoderm formation. Left unexplained, however, is the particular sensitivity of pre-cardiac mesoderm to the loss of fibronectin. It is likely that the cardiac-specific sensitivity may be due to the influence of fibronectin on a later signal after the cells commit to a mesodermal fate. Works in Ciona have implicated the role of an integrin-dependent activation of FgF signaling in biasing *Mesp1* positive cells towards the cardiac lineage. It is quite possible that this is the same system at play, and is worth further investigation.

While we showed that Wnt signaling, through inhibition of pro-differentiation signals, is critical for the expansion of cardiac progenitors during development, we found that exogenous wnt can only temporarily expand the progenitor population and is insufficient to promote long-term self-renewal. Whether or not cardiac progenitors can be coaxed, through other cytokines, to take on stem cell-like abilities of self-renewal remains to be seen. A better understanding of the minimal requirements for maintenance of these cells is required to expand this population for tissue engineering purposes.

Our study on the reciprocal interaction between notch and wnt signaling reveals a Numb-mediated mechanism for post-translational modification. However, we have yet to identify other players that are involved. Furthermore, except for cardiac progenitors, most of our studies have been performed on stem cells in vitro. While circumstantial evidence suggests functional significance of this interaction in vivo, the importance of the endogenous role of this interaction remains to be elucidated. To get at that question, the

important players involved in this regulation need to be identified, potentially through immuno-precipitation followed by mass spectrometry, and then knocked out *in vivo*.

On the tissue engineering front, many questions remain to be tackled. First and foremost is the question of cardiomyocyte maturation. While we are approaching adequate levels of directed differentiation, it is clear that the resultant cardiomyocytes are immature compared to adult or even neonatal cardiomyocytes. Aging the cells in culture promotes a more mature phenotype, but these cardiomyocytes are still far from primary cardiomyocytes. Little is known about the signals necessary for the maturation of these cardiomyocytes *in vitro* and *in vivo*. Given that mouse knockouts of mechano-sensing components often result in poor myocyte maturation *in vivo*, it is likely that maturing these cells *in vitro* will require mechanical loading of these cells. This is a field primed for utilizing the wide-variety of synthetic matrices that are amenable to stiffness modification.

Lastly, we need to address the issue of delivery. The post-infarct environment is hypoxic, highly inflammatory, and generally considered hostile for injected cells. A delivery method that can shield the cell from the hostile environment while promoting blood supply to the graft is most likely required. This can be accomplished through a variety of methods such as cytokine-embedded synthetic matrices or micro-fabricated graft architecture. A better understanding of the post-infarct scar, including factors that influence pathological modification as well as graft-scar interaction, will be critical to achieve optimal graft-host integration. Tailoring different therapeutic approaches to different infarcts and cardiomyopathies based on geometry and mechanical properties is

most likely necessary. Much research needs to be done before cardiac cell therapy can become a reality. Regardless, initial results from cardiac cell-therapy trials have been promising, assuring us that each incremental gain on the bench may be rapidly translated to the bedside. With the combined efforts of biology and engineering, we may one day successfully reduce mortality and alleviate human suffering associated with cardiovascular diseases.

REFERENCES

- 1 Roger, V. L. *et al.* Executive summary: heart disease and stroke statistics--2012 update: a report from the American Heart Association. *Circulation* 125, 188-197, doi:125/1/188 [pii]
10.1161/CIR.0b013e3182456d46 (2012).
- 2 Thomsett- Scott, B. C. National Center for Health Statistics. *Choice: Current Reviews for Academic Libraries* 49, 544-544 (2011).
- 3 Hunt, S. A. *et al.* ACC/AHA 2005 Guideline Update for the Diagnosis and Management of Chronic Heart Failure in the Adult: a report of the American College of Cardiology/American Heart Association Task Force on Practice Guidelines (Writing Committee to Update the 2001 Guidelines for the Evaluation and Management of Heart Failure): developed in collaboration with the American College of Chest Physicians and the International Society for Heart and Lung Transplantation: endorsed by the Heart Rhythm Society. *Circulation* 112, e154-235, doi:CIRCULATIONAHA.105.167586 [pii]
10.1161/CIRCULATIONAHA.105.167586 (2005).
- 4 Taylor, C. J., Roalfe, A. K., Iles, R. & Hobbs, F. D. Ten-year prognosis of heart failure in the community: follow-up data from the Echocardiographic Heart of England Screening (ECHOES) study. *Eur J Heart Fail* 14, 176-184, doi:hfr170 [pii]
10.1093/eurjhf/hfr170 (2012).
- 5 Roger, V. L. *et al.* Heart disease and stroke statistics--2011 update: a report from the American Heart Association. *Circulation* 123, e18-e209, doi:CIR.0b013e3182009701 [pii]
10.1161/CIR.0b013e3182009701 (2011).
- 6 Levy, D. *et al.* Long-term trends in the incidence of and survival with heart failure. *N Engl J Med* 347, 1397-1402, doi:10.1056/NEJMoa020265
347/18/1397 [pii] (2002).
- 7 Marian, A. J. Pathogenesis of diverse clinical and pathological phenotypes in hypertrophic cardiomyopathy. *Lancet* 355, 58-60, doi:S0140673699061875 [pii] (2000).
- 8 Murry, C. E., Reinecke, H. & Pabon, L. M. Regeneration gaps: observations on stem cells and cardiac repair. *J Am Coll Cardiol* 47, 1777-1785, doi:S0735-1097(06)00350-0 [pii]
10.1016/j.jacc.2006.02.002 (2006).
- 9 Whelan, R. S., Kaplinskiy, V. & Kitsis, R. N. Cell death in the pathogenesis of heart disease: mechanisms and significance. *Annu Rev Physiol* 72, 19-44, doi:10.1146/annurev.physiol.010908.163111 (2010).
- 10 Hsieh, P. C. *et al.* Evidence from a genetic fate-mapping study that stem cells refresh adult mammalian cardiomyocytes after injury. *Nat Med* 13, 970-974, doi:nm1618 [pii]
10.1038/nm1618 (2007).
- 11 Anversa, P. & Nadal-Ginard, B. Myocyte renewal and ventricular remodelling. *Nature* 415, 240-243, doi:10.1038/415240a
415240a [pii] (2002).
- 12 Bergmann, O. *et al.* Evidence for cardiomyocyte renewal in humans. *Science* 324, 98-102, doi:324/5923/98 [pii]
10.1126/science.1164680 (2009).

- 13 Beltrami, A. P. *et al.* Adult cardiac stem cells are multipotent and support myocardial regeneration. *Cell* 114, 763-776, doi:S0092867403006871 [pii] (2003).
- 14 Messina, E. *et al.* Isolation and expansion of adult cardiac stem cells from human and murine heart. *Circ Res* 95, 911-921, doi:01.RES.0000147315.71699.51 [pii]
10.1161/01.RES.0000147315.71699.51 (2004).
- 15 Johnston, P. V. *et al.* Engraftment, differentiation, and functional benefits of autologous cardiosphere-derived cells in porcine ischemic cardiomyopathy. *Circulation* 120, 1075-1083, 1077 p following 1083, doi:CIRCULATIONAHA.108.816058 [pii]
10.1161/CIRCULATIONAHA.108.816058 (2009).
- 16 Chimenti, I. *et al.* Relative roles of direct regeneration versus paracrine effects of human cardiosphere-derived cells transplanted into infarcted mice. *Circ Res* 106, 971-980, doi:CIRCRESAHA.109.210682 [pii]
10.1161/CIRCRESAHA.109.210682 (2010).
- 17 Oh, H. *et al.* Cardiac progenitor cells from adult myocardium: homing, differentiation, and fusion after infarction. *Proc Natl Acad Sci U S A* 100, 12313-12318, doi:10.1073/pnas.2132126100
2132126100 [pii] (2003).
- 18 Mouquet, F. *et al.* Restoration of cardiac progenitor cells after myocardial infarction by self-proliferation and selective homing of bone marrow-derived stem cells. *Circ Res* 97, 1090-1092, doi:01.RES.0000194330.66545.f5 [pii]
10.1161/01.RES.0000194330.66545.f5 (2005).
- 19 Andersen, D. C., Andersen, P., Schneider, M., Jensen, H. B. & Sheikh, S. P. Murine "cardiospheres" are not a source of stem cells with cardiomyogenic potential. *Stem Cells* 27, 1571-1581, doi:10.1002/stem.72 (2009).
- 20 Li, T. S. *et al.* Direct comparison of different stem cell types and subpopulations reveals superior paracrine potency and myocardial repair efficacy with cardiosphere-derived cells. *J Am Coll Cardiol* 59, 942-953, doi:S0735-1097(11)05271-5 [pii]
10.1016/j.jacc.2011.11.029 (2012).
- 21 Blau, H. M. & Webster, C. Isolation and characterization of human muscle cells. *Proc Natl Acad Sci U S A* 78, 5623-5627 (1981).
- 22 Jain, M. *et al.* Cell therapy attenuates deleterious ventricular remodeling and improves cardiac performance after myocardial infarction. *Circulation* 103, 1920-1927 (2001).
- 23 Hagege, A. A. *et al.* Skeletal myoblast transplantation in ischemic heart failure: long-term follow-up of the first phase I cohort of patients. *Circulation* 114, 1108-1113, doi:114/1_suppl/I-108 [pii]
10.1161/CIRCULATIONAHA.105.000521 (2006).
- 24 Duckers, H. J. *et al.* Final results of a phase IIa, randomised, open-label trial to evaluate the percutaneous intramyocardial transplantation of autologous skeletal myoblasts in congestive heart failure patients: the SEISMIC trial. *EuroIntervention* 6, 805-812, doi:EIJV6I7A139 [pii]
10.4244/EIJV6I7A139 (2011).
- 25 Cleland, J. G. *et al.* Clinical trials update from the American Heart Association 2006: OAT, SALT 1 and 2, MAGIC, ABCD, PABA-CHF, IMPROVE-CHF, and percutaneous mitral annuloplasty. *Eur J Heart Fail* 9, 92-97, doi:S1388-9842(06)00394-1 [pii]
10.1016/j.ejheart.2006.12.001 (2007).

- 26 Menasche, P. *et al.* Autologous skeletal myoblast transplantation for severe postinfarction left ventricular dysfunction. *J Am Coll Cardiol* 41, 1078-1083, doi:S0735109703000925 [pii] (2003).
- 27 Siminiak, T. *et al.* Autologous skeletal myoblast transplantation for the treatment of postinfarction myocardial injury: phase I clinical study with 12 months of follow-up. *Am Heart J* 148, 531-537, doi:10.1016/j.ahj.2004.03.043 S0002870304002017 [pii] (2004).
- 28 Quaini, F. *et al.* Chimerism of the transplanted heart. *N Engl J Med* 346, 5-15, doi:10.1056/NEJMoa012081 346/1/5 [pii] (2002).
- 29 Segers, V. F. & Lee, R. T. Stem-cell therapy for cardiac disease. *Nature* 451, 937-942, doi:nature06800 [pii] 10.1038/nature06800 (2008).
- 30 Wollert, K. C. *et al.* Intracoronary autologous bone-marrow cell transfer after myocardial infarction: the BOOST randomised controlled clinical trial. *Lancet* 364, 141-148, doi:10.1016/S0140-6736(04)16626-9 S0140673604166269 [pii] (2004).
- 31 Schachinger, V. *et al.* Intracoronary bone marrow-derived progenitor cells in acute myocardial infarction. *N Engl J Med* 355, 1210-1221, doi:355/12/1210 [pii] 10.1056/NEJMoa060186 (2006).
- 32 Janssens, S. *et al.* Autologous bone marrow-derived stem-cell transfer in patients with ST-segment elevation myocardial infarction: double-blind, randomised controlled trial. *Lancet* 367, 113-121, doi:S0140-6736(05)67861-0 [pii] 10.1016/S0140-6736(05)67861-0 (2006).
- 33 Wollert, K. C. & Drexler, H. Cell therapy for the treatment of coronary heart disease: a critical appraisal. *Nat Rev Cardiol* 7, 204-215, doi:nrcardio.2010.1 [pii] 10.1038/nrcardio.2010.1 (2010).
- 34 Murry, C. E. *et al.* Haematopoietic stem cells do not transdifferentiate into cardiac myocytes in myocardial infarcts. *Nature* 428, 664-668, doi:10.1038/nature02446 nature02446 [pii] (2004).
- 35 Balsam, L. B. *et al.* Haematopoietic stem cells adopt mature haematopoietic fates in ischaemic myocardium. *Nature* 428, 668-673, doi:10.1038/nature02460 nature02460 [pii] (2004).
- 36 Abdel-Latif, A. *et al.* Adult bone marrow-derived cells for cardiac repair: a systematic review and meta-analysis. *Arch Intern Med* 167, 989-997, doi:167/10/989 [pii] 10.1001/archinte.167.10.989 (2007).
- 37 Wang, X. *et al.* Donor myocardial infarction impairs the therapeutic potential of bone marrow cells by an interleukin-1-mediated inflammatory response. *Sci Transl Med* 3, 100ra190, doi:3/100/100ra90 [pii] 10.1126/scitranslmed.3002814 (2011).
- 38 Nakatsuji, N., Nakajima, F. & Tokunaga, K. HLA-haplotype banking and iPS cells. *Nat Biotechnol* 26, 739-740, doi:nbt0708-739 [pii] 10.1038/nbt0708-739 (2008).
- 39 Jiang, X., Rowitch, D. H., Soriano, P., McMahon, A. P. & Sucov, H. M. Fate of the mammalian cardiac neural crest. *Development* 127, 1607-1616 (2000).
- 40 Sater, A. K. & Jacobson, A. G. The specification of heart mesoderm occurs during gastrulation in *Xenopus laevis*. *Development* 105, 821-830 (1989).

- 41 Artinger, M., Blitz, I., Inoue, K., Tran, U. & Cho, K. W. Interaction of goosecoid and brachyury in *Xenopus* mesoderm patterning. *Mech Dev* 65, 187-196 (1997).
- 42 Kitajima, S., Takagi, A., Inoue, T. & Saga, Y. MesP1 and MesP2 are essential for the development of cardiac mesoderm. *Development* 127, 3215-3226 (2000).
- 43 Saga, Y. *et al.* MesP1: a novel basic helix-loop-helix protein expressed in the nascent mesodermal cells during mouse gastrulation. *Development* 122, 2769-2778 (1996).
- 44 Saga, Y., Kitajima, S. & Miyagawa-Tomita, S. Mesp1 expression is the earliest sign of cardiovascular development. *Trends Cardiovasc Med* 10, 345-352, doi:S105017380100069X [pii] (2000).
- 45 Prall, O. W. *et al.* An Nkx2-5/Bmp2/Smad1 negative feedback loop controls heart progenitor specification and proliferation. *Cell* 128, 947-959, doi:S0092-8674(07)00243-7 [pii] 10.1016/j.cell.2007.01.042 (2007).
- 46 Wu, S. M. *et al.* Developmental origin of a bipotential myocardial and smooth muscle cell precursor in the mammalian heart. *Cell* 127, 1137-1150 (2006).
- 47 Bu, L. *et al.* Human ISL1 heart progenitors generate diverse multipotent cardiovascular cell lineages. *Nature* 460, 113-117 (2009).
- 48 Kattman, S. J. *et al.* Stage-specific optimization of activin/nodal and BMP signaling promotes cardiac differentiation of mouse and human pluripotent stem cell lines. *Cell Stem Cell* 8, 228-240, doi:S1934-5909(10)00703-4 [pii] 10.1016/j.stem.2010.12.008 (2011).
- 49 Mima, T., Ueno, H., Fischman, D. A., Williams, L. T. & Mikawa, T. Fibroblast growth factor receptor is required for in vivo cardiac myocyte proliferation at early embryonic stages of heart development. *Proc Natl Acad Sci U S A* 92, 467-471 (1995).
- 50 Ueno, S. *et al.* Biphasic role for Wnt/beta-catenin signaling in cardiac specification in zebrafish and embryonic stem cells. *Proc Natl Acad Sci U S A* 104, 9685-9690, doi:0702859104 [pii] 10.1073/pnas.0702859104 (2007).
- 51 Kwon, C. *et al.* Canonical Wnt signaling is a positive regulator of mammalian cardiac progenitors. *Proc Natl Acad Sci U S A* 104, 10894-10899 (2007).
- 52 Takahashi, K. & Yamanaka, S. Induction of pluripotent stem cells from mouse embryonic and adult fibroblast cultures by defined factors. *Cell* 126, 663-676, doi:S0092-8674(06)00976-7 [pii] 10.1016/j.cell.2006.07.024 (2006).
- 53 Taylor, C. J. *et al.* Banking on human embryonic stem cells: estimating the number of donor cell lines needed for HLA matching. *Lancet* 366, 2019-2025, doi:S0140-6736(05)67813-0 [pii] 10.1016/S0140-6736(05)67813-0 (2005).
- 54 Srivastava, D. Making or breaking the heart: from lineage determination to morphogenesis. *Cell* 126, 1037-1048 (2006).
- 55 Buckingham, M., Meilhac, S. & Zaffran, S. Building the mammalian heart from two sources of myocardial cells. *Nat Rev Genet* 6, 826-835 (2005).
- 56 Murry, C. E. & Keller, G. Differentiation of embryonic stem cells to clinically relevant populations: lessons from embryonic development. *Cell* 132, 661-680, doi:S0092-8674(08)00216-X [pii] 10.1016/j.cell.2008.02.008 (2008).
- 57 Mercola, M., Ruiz-Lozano, P. & Schneider, M. D. Cardiac muscle regeneration: lessons from development. *Genes Dev* 25, 299-309, doi:25/4/299 [pii]

- 10.1101/gad.2018411 (2011).
- 58 Schultheiss, T. M., Xydas, S. & Lassar, A. B. Induction of avian cardiac myogenesis by anterior endoderm. *Development* 121, 4203-4214 (1995).
- 59 Schultheiss, T. M. & Lassar, A. B. Induction of chick cardiac myogenesis by bone morphogenetic proteins. *Cold Spring Harb Symp Quant Biol* 62, 413-419 (1997).
- 60 Marvin, M. J., Di Rocco, G., Gardiner, A., Bush, S. M. & Lassar, A. B. Inhibition of Wnt activity induces heart formation from posterior mesoderm. *Genes Dev* 15, 316-327, doi:10.1101/gad.855501 (2001).
- 61 Holtzinger, A., Rosenfeld, G. E. & Evans, T. Gata4 directs development of cardiac-inducing endoderm from ES cells. *Dev Biol* 337, 63-73, doi:S0012-1606(09)01246-9 [pii] 10.1016/j.ydbio.2009.10.003 (2010).
- 62 Liu, Y. *et al.* Sox17 is essential for the specification of cardiac mesoderm in embryonic stem cells. *Proc Natl Acad Sci U S A* 104, 3859-3864, doi:0609100104 [pii] 10.1073/pnas.0609100104 (2007).
- 63 Rudy-Reil, D. & Lough, J. Avian precardiac endoderm/mesoderm induces cardiac myocyte differentiation in murine embryonic stem cells. *Circ Res* 94, e107-116, doi:10.1161/01.RES.0000134852.12783.6e 01.RES.0000134852.12783.6e [pii] (2004).
- 64 Mummery, C. *et al.* Differentiation of human embryonic stem cells to cardiomyocytes: role of coculture with visceral endoderm-like cells. *Circulation* 107, 2733-2740, doi:10.1161/01.CIR.0000068356.38592.68 01.CIR.0000068356.38592.68 [pii] (2003).
- 65 Nijmeijer, R. M., Leeuwis, J. W., DeLisio, A., Mummery, C. L. & Chuva de Sousa Lopes, S. M. Visceral endoderm induces specification of cardiomyocytes in mice. *Stem Cell Res* 3, 170-178, doi:S1873-5061(09)00081-6 [pii] 10.1016/j.scr.2009.06.003 (2009).
- 66 Inman, K. E. & Downs, K. M. Localization of Brachyury (T) in embryonic and extraembryonic tissues during mouse gastrulation. *Gene Expr Patterns* 6, 783-793, doi:S1567-133X(06)00014-7 [pii] 10.1016/j.modgep.2006.01.010 (2006).
- 67 Wilkinson, D. G., Bhatt, S. & Herrmann, B. G. Expression pattern of the mouse T gene and its role in mesoderm formation. *Nature* 343, 657-659, doi:10.1038/343657a0 (1990).
- 68 Kispert, A. & Herrmann, B. G. Immunohistochemical analysis of the Brachyury protein in wild-type and mutant mouse embryos. *Dev Biol* 161, 179-193, doi:10.1006/dbio.1994.1019 S0012-1606(84)71019-0 [pii] (1994).
- 69 Fehling, H. J. *et al.* Tracking mesoderm induction and its specification to the hemangioblast during embryonic stem cell differentiation. *Development* 130, 4217-4227 (2003).
- 70 Hansson, M. *et al.* A late requirement for Wnt and FGF signaling during activin-induced formation of foregut endoderm from mouse embryonic stem cells. *Dev Biol* 330, 286-304, doi:S0012-1606(09)00230-9 [pii] 10.1016/j.ydbio.2009.03.026 (2009).
- 71 Kattman, S. J., Huber, T. L. & Keller, G. M. Multipotent flk-1+ cardiovascular progenitor cells give rise to the cardiomyocyte, endothelial, and vascular smooth muscle lineages. *Dev Cell* 11, 723-732 (2006).

- 72 Yang, L. *et al.* Human cardiovascular progenitor cells develop from a KDR+ embryonic-stem-cell-derived population. *Nature* 453, 524-528 (2008).
- 73 Hsiao, E. C. *et al.* Marking embryonic stem cells with a 2A self-cleaving peptide: a NKX2-5 emerald GFP BAC reporter. *PLoS One* 3, e2532, doi:10.1371/journal.pone.0002532 (2008).
- 74 Julich, D., Geisler, R. & Holley, S. A. Integrin α 5 and delta/notch signaling have complementary spatiotemporal requirements during zebrafish somitogenesis. *Dev Cell* 8, 575-586, doi:S1534-5807(05)00020-1 [pii] 10.1016/j.devcel.2005.01.016 (2005).
- 75 Trinh, L. A. & Stainier, D. Y. Fibronectin regulates epithelial organization during myocardial migration in zebrafish. *Dev Cell* 6, 371-382, doi:S1534580704000632 [pii] (2004).
- 76 Rodaway, A. & Patient, R. Mesendoderm. an ancient germ layer? *Cell* 105, 169-172, doi:S0092-8674(01)00307-5 [pii] (2001).
- 77 Sakaguchi, T., Kikuchi, Y., Kuroiwa, A., Takeda, H. & Stainier, D. Y. The yolk syncytial layer regulates myocardial migration by influencing extracellular matrix assembly in zebrafish. *Development* 133, 4063-4072, doi:133/20/4063 [pii] 10.1242/dev.02581 (2006).
- 78 George, E. L., Georges-Labouesse, E. N., Patel-King, R. S., Rayburn, H. & Hynes, R. O. Defects in mesoderm, neural tube and vascular development in mouse embryos lacking fibronectin. *Development* 119, 1079-1091 (1993).
- 79 Ieda, M. *et al.* Cardiac fibroblasts regulate myocardial proliferation through beta1 integrin signaling. *Dev Cell* 16, 233-244, doi:S1534-5807(08)00517-0 [pii] 10.1016/j.devcel.2008.12.007 (2009).
- 80 Vuori, K. & Ruoslahti, E. Activation of protein kinase C precedes alpha 5 beta 1 integrin-mediated cell spreading on fibronectin. *J Biol Chem* 268, 21459-21462 (1993).
- 81 Ross, R. S. *et al.* Beta1 integrins participate in the hypertrophic response of rat ventricular myocytes. *Circ Res* 82, 1160-1172 (1998).
- 82 Rallis, C., Pinchin, S. M. & Ish-Horowicz, D. Cell-autonomous integrin control of Wnt and Notch signalling during somitogenesis. *Development* 137, 3591-3601, doi:dev.050070 [pii] 10.1242/dev.050070 (2010).
- 83 Veeman, M. T., Slusarski, D. C., Kaykas, A., Louie, S. H. & Moon, R. T. Zebrafish prickle, a modulator of noncanonical Wnt/Fz signaling, regulates gastrulation movements. *Curr Biol* 13, 680-685, doi:S0960982203002409 [pii] (2003).
- 84 Plusa, B., Piliszek, A., Frankenberg, S., Artus, J. & Hadjantonakis, A. K. Distinct sequential cell behaviours direct primitive endoderm formation in the mouse blastocyst. *Development* 135, 3081-3091, doi:135/18/3081 [pii] 10.1242/dev.021519 (2008).
- 85 Kimelman, D., Christian, J. L. & Moon, R. T. Synergistic principles of development: overlapping patterning systems in *Xenopus* mesoderm induction. *Development* 116, 1-9 (1992).
- 86 Spiegel, E., Burger, M. & Spiegel, M. Fibronectin in the developing sea urchin embryo. *J Cell Biol* 87, 309-313 (1980).
- 87 Yang, J. T., Rayburn, H. & Hynes, R. O. Embryonic mesodermal defects in alpha 5 integrin-deficient mice. *Development* 119, 1093-1105 (1993).
- 88 Chen, H. *et al.* In vivo beta1 integrin function requires phosphorylation-independent regulation by cytoplasmic tyrosines. *Genes Dev* 20, 927-932, doi:20/8/927 [pii]

- 10.1101/gad.1408306 (2006).
- 89 Yamaguchi, T. P., Takada, S., Yoshikawa, Y., Wu, N. & McMahon, A. P. T (Brachyury) is a direct target of Wnt3a during paraxial mesoderm specification. *Genes Dev* 13, 3185-3190 (1999).
- 90 Kwon, C. *et al.* A regulatory pathway involving Notch1/beta-catenin/Isl1 determines cardiac progenitor cell fate. *Nat Cell Biol* 11, 951-957 (2009).
- 91 Gradl, D., Kuhl, M. & Wedlich, D. The Wnt/Wg signal transducer beta-catenin controls fibronectin expression. *Mol Cell Biol* 19, 5576-5587 (1999).
- 92 Westerfield, M. *The Zebrafish Book. A Guide for the Laboratory Use of Zebrafish (Danio rerio)*. 3rd Edition edn, (University of Oregon Press, 1995).
- 93 Fish, J. E. *et al.* miR-126 regulates angiogenic signaling and vascular integrity. *Dev Cell* 15, 272-284, doi:S1534-5807(08)00287-6 [pii]
- 10.1016/j.devcel.2008.07.008 (2008).
- 94 Kimmel, C. B., Ballard, W. W., Kimmel, S. R., Ullmann, B. & Schilling, T. F. Stages of embryonic development of the zebrafish. *Dev Dyn* 203, 253-310, doi:10.1002/aja.1002030302 (1995).
- 95 Cohen, E. D. *et al.* Wnt/beta-catenin signaling promotes expansion of Isl-1-positive cardiac progenitor cells through regulation of FGF signaling. *J Clin Invest* 117, 1794-1804 (2007).
- 96 Qyang, Y. *et al.* The renewal and differentiation of Isl1+ cardiovascular progenitors are controlled by a Wnt/beta-catenin pathway. *Cell Stem Cell* 1, 165-179 (2007).
- 97 Cai, C. L. *et al.* Isl1 identifies a cardiac progenitor population that proliferates prior to differentiation and contributes a majority of cells to the heart. *Dev Cell* 5, 877-889 (2003).
- 98 Moretti, A. *et al.* Multipotent embryonic isl1+ progenitor cells lead to cardiac, smooth muscle, and endothelial cell diversification. *Cell* 127, 1151-1165 (2006).
- 99 Laugwitz, K. L. *et al.* Postnatal isl1+ cardioblasts enter fully differentiated cardiomyocyte lineages. *Nature* 433, 647-653 (2005).
- 100 Christoforou, N. *et al.* Mouse ES cell-derived cardiac precursor cells are multipotent and facilitate identification of novel cardiac genes. *J Clin Invest* 118, 894-903 (2008).
- 101 Lyons, I. *et al.* Myogenic and morphogenetic defects in the heart tubes of murine embryos lacking the homeo box gene Nkx2-5. *Genes Dev* 9, 1654-1666 (1995).
- 102 Stanley, E. G. *et al.* Efficient Cre-mediated deletion in cardiac progenitor cells conferred by a 3'UTR-ires-Cre allele of the homeobox gene Nkx2-5. *Int J Dev Biol* 46, 431-439 (2002).
- 103 Hayward, P., Kalmar, T. & Arias, A. M. Wnt/Notch signalling and information processing during development. *Development* 135, 411-424 (2008).
- 104 Ronces, M. S., McLaughlin, K. A., Raffin, M. & Mercola, M. Serrate and Notch specify cell fates in the heart field by suppressing cardiomyogenesis. *Development* 127, 3865-3876 (2000).
- 105 Nemir, M., Croquelois, A., Pedrazzini, T. & Radtke, F. Induction of cardiogenesis in embryonic stem cells via downregulation of Notch1 signaling. *Circ Res* 98, 1471-1478 (2006).
- 106 Radtke, F. *et al.* Deficient T cell fate specification in mice with an induced inactivation of Notch1. *Immunity* 10, 547-558 (1999).
- 107 Srinivas, S. *et al.* Cre reporter strains produced by targeted insertion of EYFP and ECFP into the ROSA26 locus. *BMC Dev Biol* 1, 4 (2001).

- 108 Votin, V., Nelson, W. J. & Barth, A. I. Neurite outgrowth involves adenomatous polyposis coli protein and beta-catenin. *J Cell Sci* 118, 5699-5708 (2005).
- 109 Gottlieb, P. D. *et al.* Bop encodes a muscle-restricted protein containing MYND and SET domains and is essential for cardiac differentiation and morphogenesis. *Nat Genet* 31, 25-32 (2002).
- 110 Li, S., Wang, D. Z., Wang, Z., Richardson, J. A. & Olson, E. N. The serum response factor coactivator myocardin is required for vascular smooth muscle development. *Proc Natl Acad Sci U S A* 100, 9366-9370 (2003).
- 111 Tan, X., Rotllant, J., Li, H., De Deyne, P. & Du, S. J. SmyD1, a histone methyltransferase, is required for myofibril organization and muscle contraction in zebrafish embryos. *Proc Natl Acad Sci U S A* 103, 2713-2718 (2006).
- 112 Ueyama, T., Kasahara, H., Ishiwata, T., Nie, Q. & Izumo, S. Myocardin expression is regulated by Nkx2.5, and its function is required for cardiomyogenesis. *Mol Cell Biol* 23, 9222-9232 (2003).
- 113 Wang, D. *et al.* Activation of cardiac gene expression by myocardin, a transcriptional cofactor for serum response factor. *Cell* 105, 851-862 (2001).
- 114 Zawel, L. *et al.* DEC1 is a downstream target of TGF-beta with sequence-specific transcriptional repressor activities. *Proc Natl Acad Sci U S A* 99, 2848-2853 (2002).
- 115 Shen, M. *et al.* Basic helix-loop-helix protein DEC1 promotes chondrocyte differentiation at the early and terminal stages. *J Biol Chem* 277, 50112-50120 (2002).
- 116 Honma, S. *et al.* Dec1 and Dec2 are regulators of the mammalian molecular clock. *Nature* 419, 841-844 (2002).
- 117 Harada, N. *et al.* Intestinal polyposis in mice with a dominant stable mutation of the beta-catenin gene. *Embo J* 18, 5931-5942 (1999).
- 118 Kwon, C., Hays, R., Fetting, J. & Orenic, T. V. Opposing inputs by Hedgehog and Brinker define a stripe of hairy expression in the Drosophila leg imaginal disc. *Development* 131, 2681-2692 (2004).
- 119 Kwon, C., Han, Z., Olson, E. N. & Srivastava, D. MicroRNA1 influences cardiac differentiation in Drosophila and regulates Notch signaling. *Proc Natl Acad Sci U S A* 102, 18986-18991 (2005).
- 120 Dodou, E., Verzi, M. P., Anderson, J. P., Xu, S. M. & Black, B. L. Mef2c is a direct transcriptional target of ISL1 and GATA factors in the anterior heart field during mouse embryonic development. *Development* 131, 3931-3942 (2004).
- 121 Logan, C. Y. & Nusse, R. The Wnt signaling pathway in development and disease. *Annu Rev Cell Dev Biol* 20, 781-810 (2004).
- 122 Peifer, M. & Polakis, P. Wnt signaling in oncogenesis and embryogenesis--a look outside the nucleus. *Science* 287, 1606-1609 (2000).
- 123 Radtke, F. & Clevers, H. Self-renewal and cancer of the gut: two sides of a coin. *Science* 307, 1904-1909 (2005).
- 124 Brack, A. S., Conboy, I. M., Conboy, M. J., Shen, J. & Rando, T. A. A temporal switch from notch to Wnt signaling in muscle stem cells is necessary for normal adult myogenesis. *Cell Stem Cell* 2, 50-59, doi:S1934-5909(07)00223-8 [pii] 10.1016/j.stem.2007.10.006 (2008).
- 125 Artavanis-Tsakonas, S., Rand, M. D. & Lake, R. J. Notch signaling: cell fate control and signal integration in development. *Science* 284, 770-776 (1999).
- 126 van Noort, M., Weerkamp, F., Clevers, H. C. & Staal, F. J. Wnt signaling and phosphorylation status of beta-catenin: importance of the correct antibody tools. *Blood* 110, 2778-2779, doi:110/7/2778 [pii]

- 10.1182/blood-2007-05-092445 (2007).
- 127 Yang, X. *et al.* Notch activation induces apoptosis in neural progenitor cells through a p53-dependent pathway. *Dev Biol* 269, 81-94 (2004).
- 128 Tanigaki, K. *et al.* Notch-RBP-J signaling is involved in cell fate determination of marginal zone B cells. *Nat Immunol* 3, 443-450 (2002).
- 129 Martinez Arias, A., Zecchini, V. & Brennan, K. CSL-independent Notch signalling: a checkpoint in cell fate decisions during development? *Curr Opin Genet Dev* 12, 524-533 (2002).
- 130 Yan, D. *et al.* Elevated expression of axin2 and hnk2 mRNA provides evidence that Wnt/beta-catenin signaling is activated in human colon tumors. *Proc Natl Acad Sci U S A* 98, 14973-14978, doi:10.1073/pnas.261574498
98/26/14973 [pii] (2001).
- 131 Tetsu, O. & McCormick, F. Beta-catenin regulates expression of cyclin D1 in colon carcinoma cells. *Nature* 398, 422-426, doi:10.1038/18884 (1999).
- 132 Meijer, L. *et al.* GSK-3-selective inhibitors derived from Tyrian purple indirubins. *Chem Biol* 10, 1255-1266 (2003).
- 133 McElhinny, A. S., Li, J. L. & Wu, L. Mastermind-like transcriptional co-activators: emerging roles in regulating cross talk among multiple signaling pathways. *Oncogene* 27, 5138-5147, doi:onc2008228 [pii]
10.1038/onc.2008.228 (2008).
- 134 Murtaugh, L. C., Stanger, B. Z., Kwan, K. M. & Melton, D. A. Notch signaling controls multiple steps of pancreatic differentiation. *Proc Natl Acad Sci U S A* 100, 14920-14925 (2003).
- 135 Korinek, V. *et al.* Constitutive transcriptional activation by a beta-catenin-Tcf complex in APC-/- colon carcinoma. *Science* 275, 1784-1787 (1997).
- 136 Yamamoto, N. *et al.* Role of Deltex-1 as a transcriptional regulator downstream of the Notch receptor. *J Biol Chem* 276, 45031-45040 (2001).
- 137 Tamura, K. *et al.* Physical interaction between a novel domain of the receptor Notch and the transcription factor RBP-J kappa/Su(H). *Curr Biol* 5, 1416-1423 (1995).
- 138 Schroeter, E. H., Kisslinger, J. A. & Kopan, R. Notch-1 signalling requires ligand-induced proteolytic release of intracellular domain. *Nature* 393, 382-386 (1998).
- 139 Haegel, H. *et al.* Lack of beta-catenin affects mouse development at gastrulation. *Development* 121, 3529-3537 (1995).
- 140 Lindsley, R. C., Gill, J. G., Kyba, M., Murphy, T. L. & Murphy, K. M. Canonical Wnt signaling is required for development of embryonic stem cell-derived mesoderm. *Development* 133, 3787-3796, doi:dev.02551 [pii]
10.1242/dev.02551 (2006).
- 141 De Strooper, B. *et al.* A presenilin-1-dependent gamma-secretase-like protease mediates release of Notch intracellular domain. *Nature* 398, 518-522 (1999).
- 142 Sastre, M. *et al.* Presenilin-dependent gamma-secretase processing of beta-amyloid precursor protein at a site corresponding to the S3 cleavage of Notch. *EMBO Rep* 2, 835-841 (2001).
- 143 Ge, C. & Stanley, P. Effects of varying Notch1 signal strength on embryogenesis and vasculogenesis in compound mutant heterozygotes. *BMC Dev Biol* 10, 36, doi:1471-213X-10-36 [pii]
10.1186/1471-213X-10-36 (2010).
- 144 Lu, H. & Bilder, D. Endocytic control of epithelial polarity and proliferation in *Drosophila*. *Nat Cell Biol* 7, 1232-1239 (2005).

- 145 Kanwar, R. & Fortini, M. E. Notch signaling: a different sort makes the cut. *Curr Biol* 14, R1043-1045 (2004).
- 146 Guo, M., Jan, L. Y. & Jan, Y. N. Control of daughter cell fates during asymmetric division: interaction of Numb and Notch. *Neuron* 17, 27-41 (1996).
- 147 Zhong, W., Jiang, M. M., Weinmaster, G., Jan, L. Y. & Jan, Y. N. Differential expression of mammalian Numb, Numbl-like and Notch1 suggests distinct roles during mouse cortical neurogenesis. *Development* 124, 1887-1897 (1997).
- 148 McGill, M. A., Dho, S. E., Weinmaster, G. & McGlade, C. J. Numb regulates post-endocytic trafficking and degradation of Notch1. *J Biol Chem* 284, 26427-26438 (2009).
- 149 Tapper, H. & Sundler, R. Bafilomycin A1 inhibits lysosomal, phagosomal, and plasma membrane H(+)-ATPase and induces lysosomal enzyme secretion in macrophages. *J Cell Physiol* 163, 137-144, doi:10.1002/jcp.1041630116 (1995).
- 150 Chan, A. T. *et al.* Long-term use of aspirin and nonsteroidal anti-inflammatory drugs and risk of colorectal cancer. *Jama* 294, 914-923 (2005).
- 151 Rostom, A. *et al.* Nonsteroidal anti-inflammatory drugs and cyclooxygenase-2 inhibitors for primary prevention of colorectal cancer: a systematic review prepared for the U.S. Preventive Services Task Force. *Ann Intern Med* 146, 376-389, doi:10.1136/annintmed.2006.06.535 [pii] (2007).
- 152 Bottone, F. G., Jr., Martinez, J. M., Collins, J. B., Afshari, C. A. & Eling, T. E. Gene modulation by the cyclooxygenase inhibitor, sulindac sulfide, in human colorectal carcinoma cells: possible link to apoptosis. *J Biol Chem* 278, 25790-25801, doi:10.1074/jbc.M301002200 M301002200 [pii] (2003).
- 153 Shiff, S. J., Qiao, L., Tsai, L. L. & Rigas, B. Sulindac sulfide, an aspirin-like compound, inhibits proliferation, causes cell cycle quiescence, and induces apoptosis in HT-29 colon adenocarcinoma cells. *J Clin Invest* 96, 491-503, doi:10.1172/JCI118060 (1995).
- 154 Eriksen, J. L. *et al.* NSAIDs and enantiomers of flurbiprofen target gamma-secretase and lower Abeta 42 in vivo. *J Clin Invest* 112, 440-449, doi:10.1172/JCI18162 112/3/440 [pii] (2003).
- 155 Koch, U. & Radtke, F. Notch and cancer: a double-edged sword. *Cell Mol Life Sci* 64, 2746-2762, doi:10.1007/s00018-007-7164-1 (2007).
- 156 van Es, J. H. *et al.* Notch/gamma-secretase inhibition turns proliferative cells in intestinal crypts and adenomas into goblet cells. *Nature* 435, 959-963, doi:nature03659 [pii] 10.1038/nature03659 (2005).
- 157 Heitzler, P. Biodiversity and noncanonical Notch signaling. *Curr Top Dev Biol* 92, 457-481, doi:S0070-2153(10)92014-0 [pii] 10.1016/S0070-2153(10)92014-0 (2010).
- 158 Sanders, P. G. *et al.* Ligand-independent traffic of Notch buffers activated Armadillo in *Drosophila*. *PLoS Biol* 7, e1000169 (2009).

Appendix

Serum-Free Differentiation Protocol (Adapted from Keller Lab)

Day 0 (From Serum Free mESC Culture)

1. Aspirate medium from ES cells.
2. Add 1 mL trypsin to each 6 well. Incubate for 2 minutes in 37°C incubator.
3. Pipette up and down to remove all cells and mix thoroughly.
4. Transfer to 15 mL conical.
5. Add 10 mL of IMDM w/ 10% FBS.
6. Centrifuge at 1500 RPM for 3 minutes. Aspirate supernatant.
7. Wash 2X with IMDM.
8. Perform cell count.
9. Supplement SFD with ascorbic acid (100x stock) and MTG (300x)
10. Prepare cell suspension so that there are 75,000 cells per mL of SFD. Culture in 10 mLs per 10 cm² dish.

Day 2-Induction

1. Check cultures. Note morphology and characteristics of EBs to help in troubleshooting if differentiation fails.
2. Harvest EBs by mixing plates well and transferring all 10 mLs to a conical tube.
3. Centrifuge at 800 RPM for 3 minutes. Gently aspirate supernatant.
4. Add 1 mL trypsin. Incubate in 37°C water bath for ~ 2 minutes. Flick tube routinely, stop as soon as EBs can no longer be seen.

5. Quench with 10ml of IMDM with 10% FBS.
6. Centrifuge at 1500 RPM for 3 minutes. Aspirate supernatant.
7. Wash 2X in IMDM.
8. Perform cell count.
9. Supplement SFD with ascorbic acid (100x stock), MTG (300x), VEGF (final concentration of 5ng/ml), and Activin A (desirable concentration can vary, for E14: 5 ng/ml)
10. Prepare cell suspension so that there are 75,000 cells per mL of SFD. Culture in 10 mLs per 10 cm² dish.
11. Add BMP to individual plates to desirable concentrations (0.3ng/ml for E14)

Optimization for induction needs to be done with each new cell line. It is best done with a grid of activin A and BMP4. The intervals between different concentrations of BMP4 should be no more than 2x.

Day 3 + (8-24hr)- Replating

1. Check cultures. Note morphology and characteristics of EBs to help in troubleshooting if differentiation fails.
2. Harvest EBs by mixing plates well and transferring all 10 mLs to a 15ml conical tube
3. Centrifuge at 800 RPM for 3 minutes.
4. Gently aspirate supernatant.

5. Add 1 mL trypsin. Incubate in 37°C water bath for ~ 2 minutes. Flick tube intermittently.
6. Add 10 mL of IMDM + 10% FBS.
7. Centrifuge at 1500 RPM for 3 minutes. Aspirate supernatant.
8. Wash 1X in IMDM.
9. Resuspend cells in 10ml IMDM
10. Perform cell count.
11. Centrifuge at 1500 RPM for 3 minutes. Aspirate supernatant.
12. Resuspend cells in Stem Pro 34 with cytokines at 125,000 cells/200µL.
13. Gelatinize appropriate number of 96-well wells.
14. Add 200µL to each well of a 96 well plate

Instead of replating, cells can also be replated in an ultra-low attachment dish at 300,000cells/ml

Day 4-6-Maintaining Monolayers

Aspirate media from each well.

Add 200 µL of fresh Stem Pro 34 medium without DKK1.

Reagents

- IMDM → (Cellgro Cat#. 15-016-CV)
- Ham's F12 → (Cellgro Cat#. 10-080-CV)
- N2-SUPPLEMENT → (Gibco Cat#. 17502-048)
- B27(No retinoic acid) → (Gibco Cat#. 12587-010)
- 10% BSA (in PBS) → (TC Grade)
- 100X Glutamax (Gibco Cat.# 25030-081)
- 100X Pen/Strep (Gibco Cat#. 15070-063)
- Stem Pro 34 (Gibco Cat#. 10639-011)-Combo

Stem Pro supplement comes in 13ml bottle, can be divided into 10 aliquots and stored at -20.

- hVEGF → (R & D Systems Cat#. 293-VE)
- hFGFb → (R & D Systems Cat#. 233-FB)
- hFGF10 → (R & D Systems Cat#. 345-FG)
- Activin A → (R & D Systems Cat #. 338-AC)
- MTG → (Sigma Cat #. M-6145)

Stock of 13 μ l in 1ml of IMDM can be stored at 4°C

- Ascorbic Acid → (Sigma Cat #. A-4544)

Ascorbic acid stock 5 μ g/ μ L can be made and store at -20°C. Each aliquot can be used up to a week while stored at 4°C.

- BMP4 → (R & D Systems Cat # 314-BP)
- DKK-1 → (R & D Systems Cat#. 1096-DK/CP)

In general, consult datasheet for resuspending cytokines. If a carrier is needed, use PBS w/ 0.1% BSA (TC Grade)

SFD Medium

IMDM (3/4 volume) → 750 mL
Ham's F12 (1/4 volume) → 250 mL
N2-Supplement (.5% v/v) → 5 mL
B27-retinoic acid (1% v/v) → 10 mL
10% BSA (in PBS) (.5% v/v) → 5 mL
Glutamax (100x) → 10 mL
Pen-Strep (100x) → 10 mL

Stem Pro34 Medium

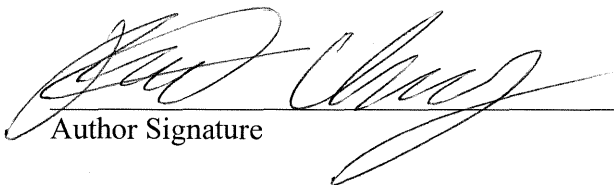
Glutamax 1x
Ascorbic Acid 2x
5ng/ml VEGF
10ng/ml hFGFb
25ng/mL hFGF10
150ng/mL DKK1 (not always necessary)
Cytokine should be added fresh

Publishing Agreement

It is the policy of the University to encourage the distribution of all theses, dissertations, and manuscripts. Copies of all UCSF theses, dissertations, and manuscripts will be routed to the library via the Graduate Division. The library will make all theses, dissertations, and manuscripts accessible to the public and will preserve these to the best of their abilities, in perpetuity.

Please sign the following statement:

I hereby grant permission to the Graduate Division of the University of California, San Francisco to release copies of my thesis, dissertation, or manuscript to the Campus Library to provide access and preservation, in whole or in part, in perpetuity.



Author Signature

3/23/12

Date